ALSO PUBLISHED ONLINE:
www.highfrequencyelectronics.com

JANUARY 2009

HIGH FREQUENCY ELECTRONICS

TUTORIAL: BROADBAND IMPEDANCE MATCHING FOR RF POWER AMPLIFIERS

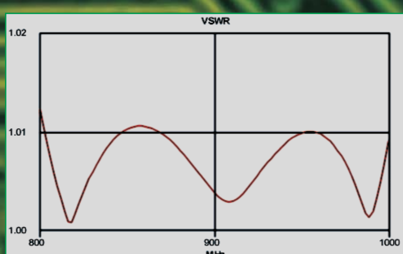

INSIDE THIS ISSUE:

Is the 5th Harmonic Still Useful for Digital Signal Bandwidth?

An Improved Method for Design of Stepped Line Microwave Filters

Technology Report—Recent Developments in Component Modeling

Featured Products—RF/Microwave Connectors & EDA Tools

Special Product Supplement—Test Equipment

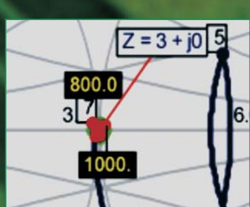

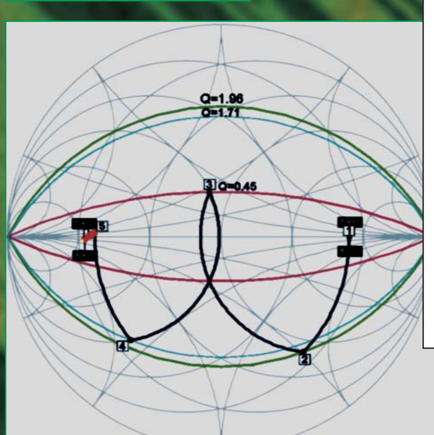

Online Edition

JUMP DIRECTLY TO THE TABLE OF CONTENTS

JUMP DIRECTLY TO THE ADVERTISER INDEX

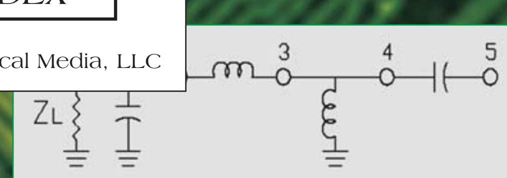

Ideas for today's engineers: Analog · Digital · RF · Microwave · mm-wave · Lightwave

MILLIMETER WAVE

MIXER ASSEMBLIES

From Stock

MIXERS

Model Number	Frequency (GHz) RF	LO	IF	LO Power (dBm)	Conversion Loss (dB Typ.)	LO-RF Isolation (dB, Typ.)
TB0440LW1	4–40	4–42	.5–20	10–15	10	20
DB0440LW1	4–40	4–40	DC–2	10–15	9	25
SBE0440LW1	4–40	2–20**	DC–1.5	10–15	10	20
IR2640L17*	26–40	26–40	Note 1	15	10	15
M2640W1	26–40	26–40	DC–12	10–12	10	20
TB2640LW1	26–40	26–40	.5–20	10–15	10	20

* Image Rejection typically 15 dB. ** Sub Harmonic
Note 1: IF Option A: 20–40 MHz, B: 40–80 MHz, C: 100–200 MHz, Q: DC–1000 MHz

MULTIPLIERS

Model Number	Frequency (GHz) Input	Output	Input Power (dBm)	Output Power (dBm, Typ.)	Fundamental Leakage (dBc, Typ.)
SYS2X1428	14	28	+12	+12	-50
SYS2X1734	16–17.5	32–35	+12	+12	-50
SYS3X1442	14	42	+12	+12	-50
SYS4X1146	11	46	+12	+15	-60
SYS2X2040	10–20	20–40	+12	+15	-15
TD0040LA2	2–20	4–40	+10	-5	-20

MIXER/MULTIPLIER ASSEMBLIES

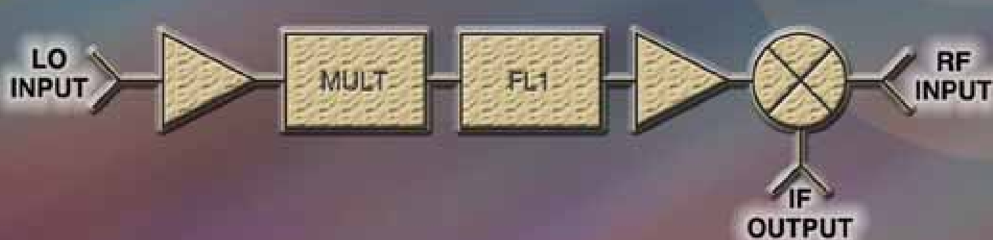

Model Number	Frequency (GHz) RF	LO	IF	LO Power (dBm)	Conversion Loss (dB, Typ.)	Input IP^3 (dBm, Typ.)	Fundamental LO-RF Isolation (dB, Typ.)
SYSMM2X2335	23.67–35.33	11.385–17.665	.04–.230	13–15	12	+15	50
SYSMM3X2640	26.5–40	8.8–13.3	DC–.5	10	10	+15	40

MITEQ also offers custom designs to meet your specific requirements. For further information, please contact Mary Becker at (631) 439-9423 or e-mail mbecker@miteq.com

Stock items may be depleted without notice, contact factory for availability.

MITEQ

100 Davids Drive, Hauppauge, NY 11788
TEL.: (631) 436-7400 • FAX: (631) 436-7430
www.miteq.com

MCL B 744
ADP-2-10

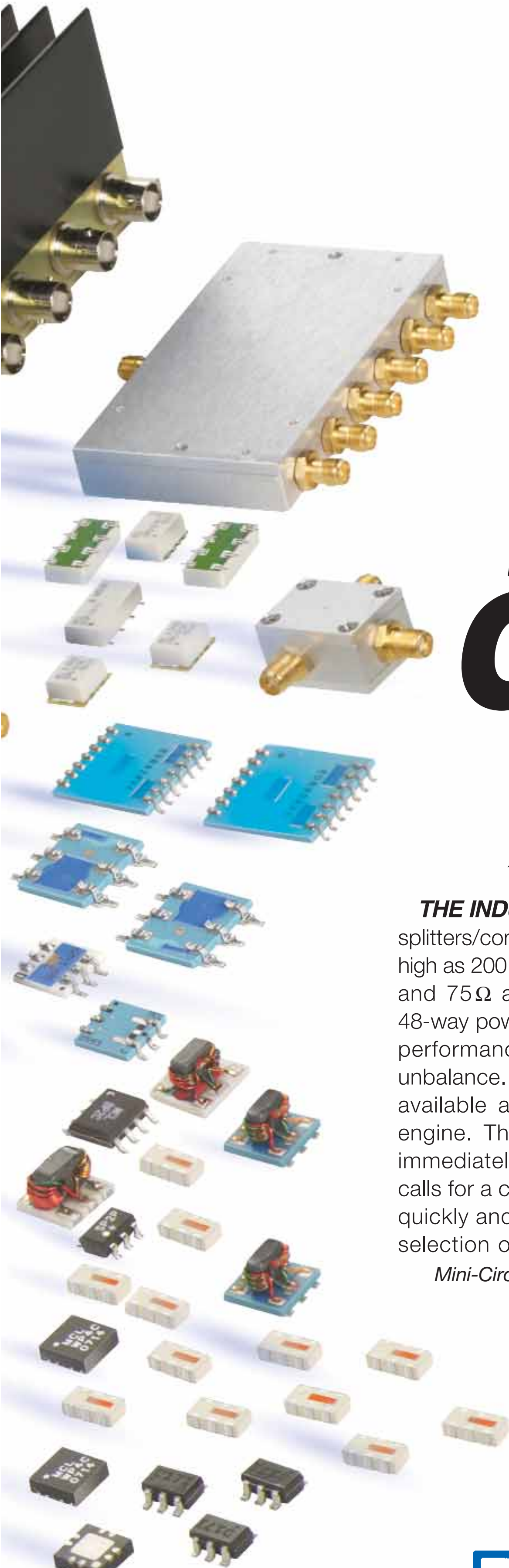

ALSO PUBLISHED ONLINE AT:
www.highfrequencyelectronics.com

JANUARY 2009
Vol. 8 No. 1

HIGH FREQUENCY ELECTRONICS

You can view this issue page-by-page, or click on any of the articles or columns in the Table of Contents below

Regular Columns

HIGH FREQUENCY
ELECTRONICS

Editorial Director
Gary Breed
gary@highfrequencyelectronics.com
Tel: 608-437-9800
Fax: 608-437-9801

Publisher
Scott Spencer
scott@highfrequencyelectronics.com
Tel: 603-472-8261
Fax: 603-471-0716

Associate Publisher
Tim Burkhard
tim@highfrequencyelectronics.com
Tel: 707-544-9977
Fax: 707-544-9375

Associate Editor
Katie Landmark
katie@highfrequencyelectronics.com
Tel: 608-437-9800
Fax: 608-437-9801

Business Office
High Frequency Electronics
7 Colby Court, Suite 7-436
Bedford, NH 03110

Editorial and Production Office
High Frequency Electronics
104 S. Grove Street
Mount Horeb, WI 53572

Also Published Online at
www.highfrequencyelectronics.com

Subscriptions
Sue Ackerman
Tel: 651-292-0629
Fax: 651-292-1517
circulation@highfrequencyelectronics.com

High Frequency Electronics (USPS 024-316) is published monthly by Summit Technical Media, LLC, 3 Hawk Dr., Bedford, NH 03110. Vol. 8 No. 1, January 2009. Periodicals Postage Paid at Manchester, NH and at additional mailing offices.

POSTMASTER: Send address corrections to *High Frequency Electronics*, PO Box 10621, Bedford, NH 03110-0621.

Subscriptions are free to qualified technical and management personnel involved in the design, manufacture and distribution of electronic equipment and systems at high frequencies.

2009 New Year's Resolution: Get Back to Basics

Gary Breed
Editorial Director

It's always good to review the fundamental principles that guide our personal and professional lives. In these difficult economic times, many people are emphasizing the personal approach, remembering which things are essential, which things are useful additions, and which things are optional for our daily living. A recession is a wake up call, a time to assess our responsibilities to ourselves, families, communities and countries.

In the financial community, where our current woes are centered, I sure hope a review of the basics is underway. 233 years ago, Adam Smith published the first thorough economic analysis in *An Inquiry Into the Nature and Causes of the Wealth of Nations*. Our bankers and brokers should all go back to the things they learned from this book in Economics 101. Smith had insights into labor, banking, trade and national monetary policy that still have value. They should not be forgotten, since they are the earliest foundation on which modern complex theories of economics and market behavior are based.

In high frequency engineering, many younger engineers have been educated and entered the workplace completely reliant on the knowledge of others, as embodied in the software of today's advanced EDA tools. They made it through their classwork, but did not work as many problems "by hand" as their predecessors had done. Sometimes I think all great new ideas should start with a sketch on a napkin or the back of an envelope! Then they can be developed, analyzed and refined using the latest tools.

All engineers benefit from the basics, and I recommend that all my colleagues stay in touch with the past foundations of their work. In the past ten years or so, I have casually gathered a number of classic (and less well-known) engineering books. I am amazed and inspired by the insights that were made in the 1920s and 1930s, making the very first connections between the practical application of the original "wireless" and a growing understanding of circuit theory and electromagnetics.

A trip back to the basics can be surprisingly valuable, as I often recall from my own experience. After receiving a degree and working for a few years, I returned to the classroom for some undergraduate and graduate classes in Physics, starting with the typical sophomore sequence of Classical Mechanics. In the process of working on the same problems addressed by Isaac Newton, I eventually realized that Calculus now made sense in a way that had eluded me. Sure, I could work the problems, but the core understanding did not come until I followed Newton's path. A similar realization came later when I took the Physics version of Electromagnetics, deriving the same equations that had been simply memorized before as an EE undergrad.

I hope many of you will make an effort to develop a better perspective of "how we got here" — connecting history with today's engineering and tomorrow's new ideas.

Clarification on DTV

Last month's column on Digital Television generated quite a few e-mail responses! One reader pointed out an error — not all TV stations will vacate the Low Band VHF spectrum (Channels 2-6). After a little research, I found that the original intent was to move all TV stations to the High Band VHF and UHF channels, but a small number (less than 20 out of the 1700 total stations) have Low Band DTV assignments. A quick check showed that some of them (maybe all?) had successfully appealed to the FCC to change their original DTV assignment, citing both coverage area and economic reasons.

As a side note, I recently obtained converter boxes for my old CRT TV sets and am quite pleased with the results from these low-cost devices, mainly the improved picture quality on those old, cheap TVs. I can't offer any observations about coverage issues, since I am in an area of good signal strength, with little multipath.

2009 in HFE

Every year, we review how *High Frequency Electronics* operates, and whether there are things that need to be changed.

For 2009, very few changes are planned in the printed magazine, which continues to get good reviews from our readers.

The primary area of attention is our Web site and other online information pathways to our readers. Although we are not making any sudden changes, we are constantly reviewing which content and service additions will make our efforts useful for even more high frequency engineers.

CONFERENCES

January 18-22, 2009
Radio Wireless Week
San Diego, CA
Information: Conference Web site
http://www.radiowirelessweek.org

January 19-21, 2009
9th Topical Meeting on Silicon Monolithic Integrated Circuits in RF Systems (SiRF 2009)
San Diego, CA
Information: Conference Web site
http://www.eng.auburn.edu/~niuguof/sirf

February 8-13, 2009
4th Intl. Waveform Diversity & Design Conference
Orlando, FL
Information: Conference Web site
http://www.waveformdiversity.org

February 23-26 2009
IDGA 7th Annual Software Radio Summit
Vienna, VA
Information: Conference Web site
http://www.softwareradiosummit.com

March 23-27, 2009
EuCAP2009—3rd European Conference on Antennas and Propagation
Berlin, Germany
Information: Conference Web site
http://www.eucap2009.org

March 30 - April 1, 2009
IEEE 2009 Sarnoff Symposium
Princeton, NJ
Information: Conference Web site
http://ewh.ieee.org/r1/princeton-centraljersey/2009_Sarnoff_Symposium/

April 1-3, 2009
CTIA Wireless 2009
Las Vegas, NV
Information: Conference Web site
http://www.ctiawireless.com

April 5-8, 2009
WCNC 2009—IEEE Wireless Communications and Networking Conference
Budapest, Hungary
Information: Conference Web site
http://www.ieee-wcnc.org/2009

April 15, 2009
CST North American User Group Meeting 2009
Dallas/Ft. Worth, TX
Information: Conference Web site
http://www.cst.com

April 18-23, 2009
2009 NAB Show
Las Vegas, NV
Information: Conference Web site
http://www.nabshow.com

April 20-21, 2009
WAMICON 2009—IEEE Wireless and Microwave Technology Conference
Clearwater, FL
Information: Conference Web site
http://www.wamicon.org

April 27-28, 2009
IEEE RFID 2009
Orlando, FL
Information: Conference Web site
http://www.ieee-rfid.org/2009/

May 4-8, 2009
RadarCon09—2009 IEEE Radar Conference
Pasadena, CA
Information: Conference Web site
http://www.radarcon09.org

June 1-5, 2009
2009 International Symposium on Antennas and Propagation and the 2009 USNC/URSI National Radio Science Meeting
North Charleston, SC
Information: Conference Web site
http://www.apsursi2009.org

June 7-12, 2009
2009 IEEE MTT-S International Microwave Symposium
Boston, MA
Information: Conference Web site
http://www.ims2009.org

SHORT COURSES

Besser Associates
201 San Antonio Circle, Suite 115
Mountain View, CA 94040
Tel: 650-949-3300
Fax: 650-949-4400
E-mail: info@besserassociates.com
http://www.besserassociates.com
Applied RF Techniques I
February 23-27, 2009, San Diego, CA
Signal Processing for Wireless Communications
February 23-26, 2009, San Diego, CA
RF Transceiver Architecture, Design and Evaluation
February 23-27, 2009, San Diego, CA
Advanced Wireless and Microwave Techniques
February 23-27, 2009, San Diego, CA
WiMAX Broadband Wireless Access
February 23-25, 2009, San Diego, CA
Engineering UHF RFID Systems


Speed is Nothing without accuracy!
I'm a Microwaver

February 23-24, 2009, San Diego, CA
LTE
February 23-27, 2009, San Diego, CA
RF and Wireless Made Simple
February 25-27, 2009, San Diego, CA
DSP Made Simple for Engineers
February 25-27, 2009, San Diego, CA
RF and High Speed PC Board Design Fundamentals
February 25-27, 2009, San Diego, CA
Wideband/HF Amplifier Design Techniques
February 25-27, 2009, San Diego, CA
Wireless Circuits, Systems and Test Fundamentals
March 23-27, 2009, San Jose, CA
RF Measurements:Principles & Demonstration
March 23-27, 2009, San Jose, CA
Semiconductor Device Physics for RF Design
March 23-25, 2009, San Jose, CA
Wireless Systems Operations
March 23-27, 2009, San Jose, CA
EMI/EMC Fundamentals with Emphasis on Successful Shielding Strategies
March 26-27, 2009, San Jose, CA

The Technology Academy
37-39 Southgate Street
Winchester, SO23 9EH, UK
Tel: 0044 1962 855 730
Fax: 0044 1962 854 400
E-mail: enquiries@thetechnologyacademy.com
http://www.thetechnologyacademy.com
Practical Design of Wireless Digital Communications Systems
January 20-22, 2009, Weybridge, UK

Kimmel Gerke Associates, Ltd., with Tektronix
628 LeVander Way
South St. Paul, MN 55075
Tel: 1-888-EMI-GURU (364-4878)
http://www.emiguru.com/seminartek.htm
Winter Getaway Seminars—Two days of grounding and shielding and circuit board design followed by an optional one-day EMI troubleshooting workshop.
February 3-5, 2009, Orlando, FL
February 10-12, 2009, San Diego, CA

Times Microwave Systems
358 Hall Avenue
PO Box 5039
Wallingford, CT 06492-5039
Tel: 800-TMS-COAX (867-2629)
Tel: 203-949-8400; FAX: 203-949-8423
http://www.timesmicrowave.com

Times Microwave Systems now offers an LMR® Certified Installer Training Program (part number CITP) covering all installation aspects of LMR coaxial transmission line cables, connectors and components including grounding. The one-day program is available to groups of 10 or more and can be held at a location convenient to the group, at Times Microwave in Wallingford, CT or at a participating Times distribution partner location. The program is $300.00 per person and can be arranged through any Times distributor.

University of Wisconsin—Madison
Department of Engineering
Professional Development
432 N. Lake St.
Madison, WI 53706
Tel: 800-462-0876
Fax: 608-263-3160
E-mail: danbeck@engr.wisc.edu
http://epd.engr.wisc.edu
The Engineer in Transition to Management
January 26-28, 2009, Las Vegas, NV
Introduction to Planning and Designing Fiber to the Premises
January 27-28, 2009, Las Vegas, NV
Electrical Grounding of Communication Systems
March 2-4, 2009, Las Vegas, NV

Call for Papers

IEEE 59th Annual Broadcast Symposium
Alexandria, VA
Conference Dates: October 14-16, 2009
Abstract Submission Deadline: May 15, 2009

Topics:

Proposals are solicited for panels on technology, applications, business, and policy-related issues and opportunities for the broadcasting industry. Potential topic areas may include: technical issues associated with the termination of analog television broadcasting; repurposing of analog television broadcast transmitters; digital radio and television systems: terrestrial, cable, satellite, Internet, wireless; streaming, IPTV, VoIP, VoD, mobile TV, wireless multimedia; wirelesss broadband networks, e.g., IEEE 802.22 wireless regional area networks (“WRANS”); transmission, propagation, reception, redistribution of broadcast signals.

Information:

Abstract submissions are due 15 May 2009. Full papers will be due 28 August 2009. Abstracts should clearly explain the subject, originality and relevance. All papers that are selected must be presented at the Symposium by the authors or their designated presenters. Submit your 500-1000 word abstract via email to: bts@ieee.org. Include author’s name and contact information.

We are pleased to publish your conferences, short courses and calls for papers. If you would like to see your announcements in our Meetings & Events section, please e-mail editor@highfrequencyelectronics.com

Technology News

Agilent Technologies Inc. announced a breakthrough nonlinear modeling technique for components such as amplifiers and transistors that are commonly used in the wireless and aerospace defense industries. The X-parameters can be generated either from simulation with the company's Advanced Design System (ADS) EDA software or from Agilent's test and measurement instruments, for faster communications-product development.

TT electronics BI Technologies has added a new deposition chamber to its thin film manufacturing capabilities. The new deposition chamber enables the uniform application of thin film resistor materials in layers as thin as 1000 Angstroms onto silicon or ceramic substrates. The new deposition chamber also reduces resistor network lead times by doubling the substrate capacity of the previous system, as well as quicker pump downs allowing for shorter cycle times. Increased stability of the devices also provides higher resistor network reliability.

Business News

California Eastern Laboratories (CEL) has partnered with **Synapse Wireless, Inc** to collaborate on IEEE 802.15.4 wireless mesh network technology. Synapse is a leader in easy-to-use control and monitoring software for 802.15.4 networks. Its SNAP and Portal technology will help enable CEL's low-cost, high-performance transceiver components to instantly form wireless mesh networks. CEL's radio modules and System-on-Chip transceivers serve a broad range of 802.15.4 applications, including communications, home and building automation, medical, and industrial controls.

Ducommun Incorporated announced that it has acquired DynaBil Industries, Inc., a privately held company based in Coxsackie, NY. DynaBil is a leading provider of titanium and aluminum structural components and assemblies for commercial and military aerospace applications. DynaBil's sales in calendar year 2008 are expected to be approximately $43 million.

LPKF Laser & Electronics AG has received the Cathay Pacific China Trader Awards for Innovation & Technology. The award recognizes German corporations that demonstrate innovative technology and design. The award was presented in Frankfurt, Germany on November 18, 2008.

Aeroflex announced it has secured a series of sales for the recently launched TD-LTE version of its market-leading TM500 test mobile from various leading suppliers of cellular mobile infrastructure equipment in China.

TriQuint Semiconductor, Inc. announced its North Carolina design center has moved into a new facility to accommodate its growing handset business. The North Carolina design center opened two years ago with one person and now hosts a team of highly advanced RF engineers. The team, with a dozen patents and more than 300 years collective experience in electrical engineering and technical support, develops TriQuint's latest advanced module solutions for mobile phone manufacturers. The new facility is double the size of the first location and will accommodate future growth.

Raytheon Missile Systems Tucson presented supplier awards to companies that routinely demonstrated excellence in product quality and on-time delivery, over the last 12 months with a 95% rating. **SV Microwave** is proud to be one of the eighteen companies that received the Raytheon Missile System's Excellence Award out of over 500 suppliers.

AWR® and **Rohde & Schwarz Japan K.K.,** the Japanese subsidiary of **Rohde & Schwarz,** announced a partnership in Japan to deliver customized hardware/software solutions. AWR software and Rohde & Schwarz test equipment will be combined to produce solutions ranging from component characterization through sub-system and system verification. Under the terms of this partnership, which took effect December 1, 2008, the companies will provide customized platforms that combine Rohde & Schwarz test and measurement equipment with AWR's high-frequency design software to produce unique simulation and measurement solutions.

Bliley Technologies, Inc. (BTI) announces a major global sales force realignment reflecting a shift to a more customer-centric, design- and engineering-led sales model. With greater integration of microwave/RF engineering in its sales and service processes, Bliley's primary sales force realignment goal is to increase customer involvement in system definition and performance selection prior to finalizing and releasing designs for manufacturing. The company also plans to further develop product-compatibility systems to match BTI products with other frequency generation components and sub-systems, according to customer needs.

Mouser Electronics, Inc. announced it has signed a global distribution agreement with **Walsin,** a supplier of passive components. Mouser's Walsin product portfolio includes RF high-frequency components including antennas, band pass filters, baluns, balance filters, common mode filters, and diplexers.

Flex Interconnect Technologies (FIT) announced that they have received official International Traffic in Arms Regulations (ITAR) registration from the US Department of State. The registration recognizes Flex Interconnect Technologies' adherence and commitment to the regulations that control the export and import of defense related articles and services. ITAR compliance ensures that Flex Interconnect Technologies has the capabilities, expertise and regulatory oversight to properly handle the manufacturing of Military, Defense and Aerospace technology.

1.5GHz-3.8GHz Active Mixer Beats Passives

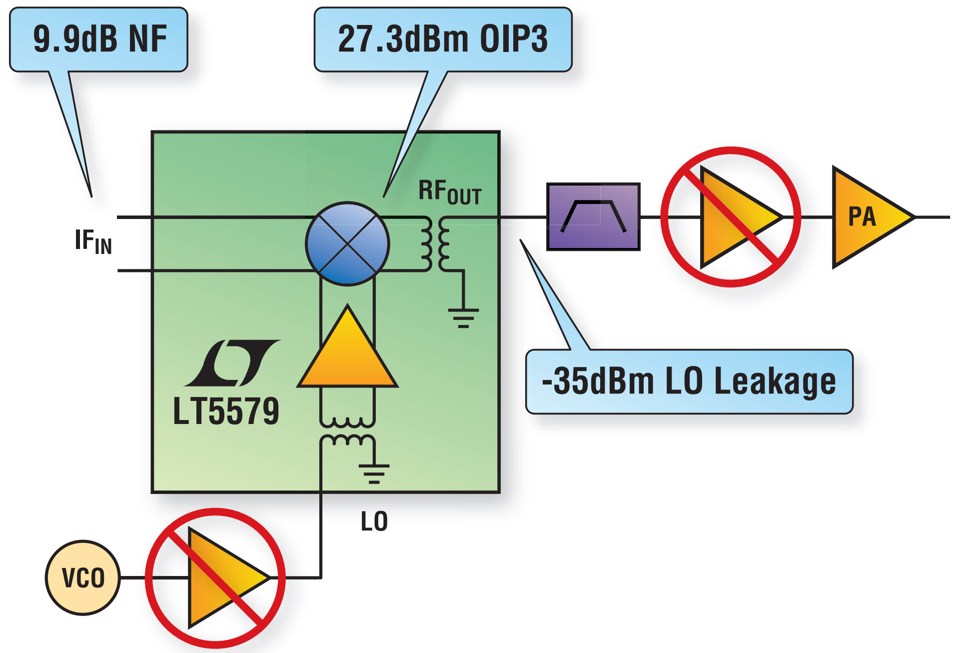

Finally, an upconverting mixer with the performance, linearity, low noise, high conversion gain and low LO leakage you demand. And its wide bandwidth capability covers the WiMAX frequency bands. The LT®5579 active mixer provides a high performance, cost-effective solution that is both compact and easy to use.

Features

- -1dBm LO Drive
- < -35dBm LO-to-RF Leakage
- 3dB Conversion Gain
- Integrated Balun Transformers

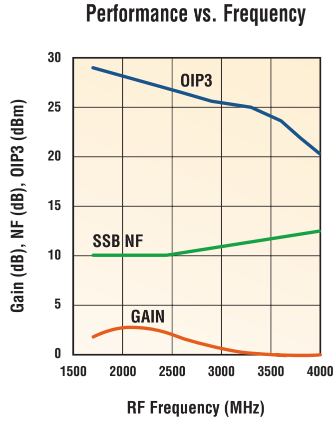

Info & Free Samples

www.linear.com/5579

1-800-4-LINEAR

Wireless Solutions Brochure

www.linear.com/wireless

LINEAR TECHNOLOGY

Raltron Electronics Corp., announced the signing of **Solid State Supplies, LTD,** as their distributor for the United Kingdom and Ireland.

EJL Wireless Research announces its third quarter 2008 China mobile handset production and shipment analysis report. Shipments of handsets into China for the third quarter increased by 8.1% when compared to the third quarter of 2007. The China mobile handset analysis reports are issued on a quarterly and annual basis and provide a unique perspective on the production and sales of GSM and CDMA mobile handsets within the Chinese market. Mobile handset vendors analyzed include: Huawei, K-Touch, Lenovo, LG, Motorola, Nokia, Samsung, and ZTE.

Spectrum Signal Processing by **Vecima**, a provider of software defined radio (SDR) technology, announced that the Danish Defence Acquisition and Logistics Organization (DALO) of the Danish Ministry of Defence has selected the flexComm™ SDR-4000 transceiver for research and development of waveform portability within the Software Communications Architecture (SCA). DALO is part of the NATO Research and Technology Organization (RTO) Task Group IST-080 that is currently studying how SDR technology can enable radio communications interoperability between nations, while reducing overall hardware costs.

The merged entity of **SkyTel** and its acquirer **Velocita Wireless** have adopted the SkyTel name as a new company and an important new participant in the machine-to-machine (M2M) wireless communications space. The company's goal is to meet the rapidly growing demand for network connectivity and services for the M2M industry.

Savi®, a **Lockheed Martin** company and provider of RFID-based supply chain products and solutions, has been selected by the **U.S. Department of Defense** (DoD) to compete for future task orders under the RFID III procurement contracting vehicle. Three other prime contractors also were selected to bid for task orders during the initial three-year ordering period that's scheduled to begin early next year.

People in the News

US experts **Donald N. Heirman** and **Scott K. Jameson** received the prestigious IEC Lord Kelvin Award for their outstanding contributions to electrotechnical standardization. The awards are given by the **International Electrotechnical Commission** (IEC), the world's leading organization that prepares and publishes International Standards for all electrical, electronic and related technologies.

Avo Photonics announces that **Mr. Todd Rixman** has joined the company as Technical Manager. Mr. Rixman has in excess of 14 years of experience in mechanical design and photonics packaging. Prior to joining Avo Photonics, Mr. Rixman led programs from concept through production and performed opto-mechanical design at Princeton Lightwave, JDSU, and Kulicke & Soffa Industries. Mr. Rixman is a graduate of Penn State with both BS and MS degrees in Mechanical Engineering.

Accellera announced that its Board of Directors elected officers for its 2008/9 membership year earlier this month. **Shrenik Mehta,** Senior Director, Frontend Technologies & OpenSPARC program, Microelectroncs, Sun Microsystems, was re-elected Chair. **Dennis Brophy,** Director of Strategic Business Development, Mentor Graphics, was re-elected Vice-Chair. **Karen Bartleson,** Senior Director, Interoperability, Synopsys, was elected Secretary, and **Yatin Trivedi,** Senior Director, Strategic Alliances, Magma Design Automation was elected Treasurer.

TREK, INC., a designer and manufacturer of high-performance electrostatic instrumentation and high-voltage power amplifiers, announces that **Tom Larson,** Sales Manager at TREK, was elected to the Board of Directors by members of the Electrostatic Discharge Association at the organization's 2008 Annual Meeting and Symposium held in Tucson, Arizona. Larson will serve a three year term as a member of the ESDA Board. This is his first time serving on the Board.

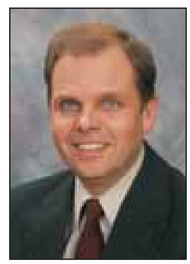

ProVision Communications has announced the establishment of its new division focused on HD video over wireless consumer products. To support the division, **Ian Walsh** has been appointed as VP of business development. Ian is an experienced business development specialist with an extensive background in electronics, telecommunications, and semiconductor products for both large companies and start-ups. He will play a key role in the new division by spearheading the introduction of the new products to the marketplace.

Sales Appointments

Peregrine Semiconductor has appointed **Clavis Company,** a division company of **Macnica, Inc.,** to market and sell Peregrine's popular line of UltraCMOS™ RFICs throughout Japan. Clavis is a market leading supplier of high-value-added electronic parts and equipment, particularly semiconductors, to the electronics, information and communications industries.

AWR expanded its relationship with **Rohde & Schwarz** to provide expanded sales channels for AWR products such as Microwave Office® in China, Taiwan, Singapore, and Malaysia. The expanded sales distribution partnership will boost AWR's presence and the use of its software in the Asia Pacific region, and takes effect immediately.


Mini-Circuits
LAVI

WIRELESS APPLICATION NEWS

Agilent Technologies Inc. (www.agilent.com) introduced a new HD Radio measurement application for its N9340B handheld RF spectrum analyzer. It supports NRSC-5 spectral emission limit masks and includes features that enable fast and easy test. It is ideal for technicians and test engineers performing measurements on HD Radio signals. HD Radio, or digital radio, and uses iBiquity Digital's proprietary IBOC technology. IBOC allows stations to simultaneously broadcast digital audio and traditional analog audio, without changing to new frequency bands. The broadcast radio industry is deploying IBOC to provide superior quality and increase content. Agilent's HD Radio application has specially-added hardware for improved phase noise performance and application measurement software for quick set up of IBOC emission measurements. This new HD Radio measurement application supports analog, digital and hybrid spectral emission limit masks for measuring radio signal emissions, including four AM signal standards (73.44 (analog), NRSC-5-B Hybrid 5k, Hybrid 8k and all digital) and three FM signal standards (73.317 (analog), NRSC-5-B Hybrid and all digital).

CommAgility (www.commagility.com) and **Axis Network Technology** (www.axisnt.com) announced that they are working together to develop solutions for WiMAX and LTE (Long Term Evolution of 3GPP) baseband processing for wireless basestations. At the LTE World Summit in London, the two companies are demonstrating the interoperability of AxisNT's Remote Radio Head (RRH) with CommAgility's AMC-3C87F signal processing board. The fully working demonstration system shows data being generated on the CommAgility board, passed to the AxisNT RRH over CPRI and then output as a OFDMA modulated RF signal. This RF signal is then displayed on a spectrum analyser to show 8W output power at 64QAM meeting the ETS 302 544 spectral mask and stringent EVM specifications. CommAgility's AMC-3C87F provides a mix of DSP and FPGA processing power together with flexible, high bandwidth I/O connectivity. AxisNT's integrated remote radio heads (RRH) are available for a complete range of WiMAX and LTE applications. Axis Radio Remote Head technology is suitable for TDD and FDD mode.

Octasic Inc. (www.octasic.com) has announced the formation of a Software Defined Radio (SDR) development group to provide wireless solutions based upon its low power, cost-effective, Opus DSP technology targeting current and emerging wireless markets. The group is headed by Emmanuel Gresset as vice president of Software Defined Radio (SDR). Gresset joined Octasic from STMicroelectronics where he managed strategic development for the Wireless Infrastructure Division. Prior to STM, Gresset worked in the U.S. and Europe for various systems and semiconductor companies focusing on the design of voice and wireless modems, digital signal processors, and System on a Chip (SoC) architectures. Octastic's DSP team, based in Montreal, is designing the industry's lowest-power DSP solutions for baseband signal processing solutions extending from femto cells to macro basestations. The Octasic wireless team will unveil its first fully soft baseband solution aimed at GSM/EDGE radio basestations next month at the GSMA Mobile World Congress in Barcelona (February 16-19, 2009).

Spectrum Signal Processing by Vecima (www.spectrumsignal.com) announces a partnership with **LiveTV LLC** (www.livetv.net) to supply next generation radios for LiveTV's connectivity system. The radios will allow passengers to send and receive email with people on the ground, while they are still in-flight. Called Kiteline, LiveTV's connectivity system uses a network of air-ground base stations to transmit data from an aircraft cabin to the ground. With Spectrum's software defined radios (SDRs), LiveTV will now be able to support current voice communications for the general aviation market as well as data services, such as email and instant messaging, for the commercial and general aviation market. Spectrum will base this new radio on a variant of its flexComm™ SDR-4800 family of embedded radio modules. Airline passengers will be able to use an on-board Wi-Fi network to connect to the in-flight system, which will in turn route the traffic over the Spectrum supplied airborne radio to LiveTV's ground network. The radio will utilize System-On-Chip (SoC) and embedded RF technologies to produce a compact, fully ruggedized solution. The radio is software reprogrammable, enabling LiveTV to roll out additional features and update the system in the future.

ARRIS (www.arrisi.com) announces that **TeleBarbados** (www.telebarbados.com) has deployed the ARRIS WiDOX 700 MHz broadband access solution at multiple locations to deliver high-speed data service to its customers throughout the island. ARRIS WiDOX technology employs DOCSIS protocols in a wireless environment to deliver high quality data experience to customers in rural environments. The ARRIS WiDOX solution provides fixed wireless solutions from a single tower to cover large geographic areas, thus eliminating the need for high infrastructure costs in rural environments. ARRIS has successfully deployed this technology in regions around the world since 2004, with several operators supporting as many as 20,000 subscribers per installation. The topography of Barbados lends itself well to this technology by virtue of its terrain and population density.

NEC RFIC Switches

Looking for a switch that's tailored to meet the specific needs of your design? *Think NEC.*

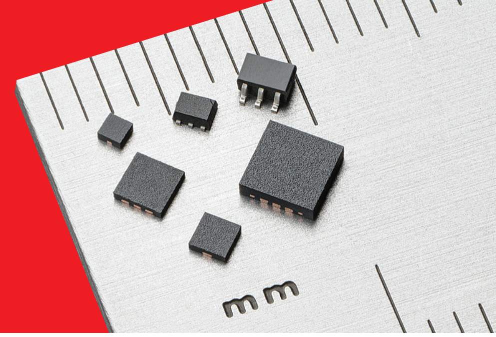

NEC's commitment to GaAs and CMOS RFIC Switch technologies means you get innovative new devices with industry-leading performance, in industry-standard *and* miniaturized packages. Our broad selection includes SPST, SPDT and multi-throw switches, internally terminated devices, 1.8V-controlled switches, and single control voltage models. For a complete list with specifications, visit **www.cel.com**.

	STANDARD SPDT	DESCRIPTION	MobileComm	Short Range Wireless	WLAN / WiFi	Bluetooth / ZigBee	WiMAX
	UPG2009TB	High power, high isolation, low insertion loss	●	●	●		
	UPG2155TB	High power, low harmonics, for GSM	●	●			
NEW	**UPG2157T5F**	High power, non-reflective, optimized for WiMAX			●		●
	UPG2158T5K	Medium power, miniature pkg, spec'd at 1.8 & 2.7 V	●	●	●	●	
NEW	**UPG2159T5K**	Low insertion loss, high isolation, miniature package	●	●		●	
	UPG2163T5N	2 – 6 GHz, industry's best insertion loss, compact pkg		●	●		
NEW	**UPG2176T5N**	High power, non-reflective, compact package			●		●
	UPG2179TB	Medium power, high performance, standard pin-out	●	●	●	●	
NEW	**UPG2185T5K**	2 – 6 GHz, miniature 1.0 x 1.0 x 0.37 mm package	●		●		
	UPG2214TB/TK	Low cost, performance guaranteed at 1.8 and 3 Volts	●	●		●	
	SINGLE CONTROL SPDT						
	UPG2010TB	High power, high isolation, low insertion loss	●	●	●		
	UPG2012TB/TK	Great at 2.4 GHz, industry-standard or miniature package	●	●		●	
	UPG2015TB	Medium power, great performance	●	●	●	●	
	UPG2160T5K	Miniature 1.0 x 1.0 x 0.37 mm package	●	●			
	UPD5713TK	Low cost CMOS, miniature package	●	●			
	MULTI-THROW SWITCHES						
	UPG2031TQ	**SP3T** Ideal for CDMA2000-1x dual band, GPS	●	●	●	●	
	UPG2150T5L	**SP3T** Extra isolation for WiFi & Bluetooth apps	●		●	●	
	UPG2162T5N	**DPDT** 2.4 – 6 GHz dual-band, compact, high isolation	●	●	●		
	UPG2164T5N	**DPDT** 2.4 – 6 GHz dual-band, compact, low insertion loss	●	●	●		
NEW	**UPG2181T5R**	**DP4T** High power, non-reflective					●
NEW	**UPD5731T6M**	**SP4T** CMOS, only two control lines req'd, miniature pkg	●	●			

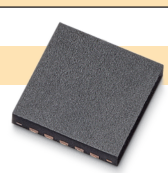

Custom Antenna Switches, too!

Let us put NEC technology to work for you in a *Custom Antenna Switch* designed to meet the needs of your specific application. Please inquire.

NEC

A Business Partner of NEC Electronics Corporation.

CEL California Eastern Laboratories

Santa Clara, California ■ 408 919-2500 ■ **www.cel.com**

DISTRIBUTORS: Arrow (800) 525-6666 **Mouser Electronics** (800) 346-6873 **Digi-Key** (800) 344-4539 **Nu Horizons** (888) 747-6846 **Future** (800) 388-8731

Is the 5th Harmonic Still Useful for Predicting Data Signal Bandwidth?

By Mark Johnson
Agilent Technologies

Rather than use the simple rule of thumb of including the 5th harmonic, we should use rise/fall time to detemine the bandwidth required to measure a high-speed digital signal

As we attempt to push data faster and faster through serial interfaces, bit rates get larger and bit periods get smaller. A common assumption made is that as the bit rate increases, the signal contains more energy at higher frequencies and, as a result, higher bandwidth is required for the test equipment such as oscilloscopes used to measure the signals. While this can be true it is not always the case, as we shall see. The 5th harmonic of a data signal (or 2.5 times the bit rate for binary, NRZ data) is often used as a guide for selecting the required bandwidth for test equipment. In reality, the 5th harmonic is a very poor predictor of essential frequency content and in fact has little relationship to critical components of a real data signal. A much better predictor of the necessary measurement bandwidth are the rise/fall times of the system.

An increase in measurement bandwidth almost always comes at a price beyond economic—but also in the form of increased noise and distortion. The increased noise not only impacts amplitude measurements but it will also impact the accuracy of timing measurements—sometimes defeating the purpose of the extra bandwidth in the first place. The best compromise is to use a measurement system with just enough bandwidth to measure the signal accurately while minimizing the extra noise introduced by the measurement system.

First of all, let's think about a perfect square wave. Imagine that we could create a clock with infinitely fast edges. As we know, a perfect square wave can be represented as the sum of an infinite number of sine waves. These sinusoids have frequencies that are at odd multiples of the fundamental frequency of the clock. For example, a perfect 1 GHz clock signal has a fundamental frequency of 1 GHz and contains an infinite series of sinusoids of frequency 3, 5, 7, 9, 11 … GHz. These are referred to as harmonics of the fundamental signal since they are located at (odd) integer multiples of the fundamental frequency. The amplitudes of the harmonics in this perfect clock are defined by the relationship: Amp = abs(sqrt(2)*SquareWaveAmp*sin(pi*harmonic.number/2)/pi*harmonic.number)

So for a perfect clock of peak-to-peak amplitude 1V, the peak-peak voltages of the fundamental and the first three harmonics would be:

Harmonic Number	1 (fundamental)	3rd	5th	7th
Amplitude	0.45V	0.15V	0.09V	0.064V

If we wanted to measure this clock with zero rise/fall times then obviously the more bandwidth our measurement instrument has, the more accurate the measurement. As we can see, the amplitude of the 5th harmonic is 9% of the amplitude of the resultant signal (0.09V/1V).

Of course, real signals have finite rise/fall times. Correspondingly they don't have an infinite number of harmonics. In Figures 1-3, we created a 0.5Vp-p 500 MHz clock with 3 different edge speeds using commonly available transition-time converters. The signals

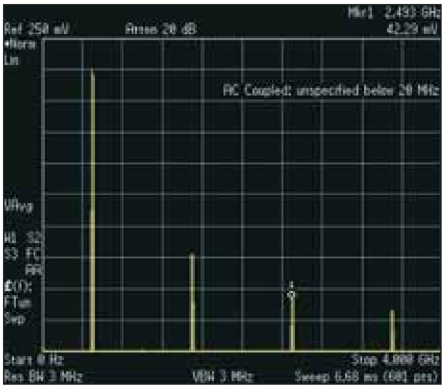

Figure 1 · 500 MHz clock with 9 ps rise/fall time (20-80%); 5th harmonic amplitude = 8.6%.

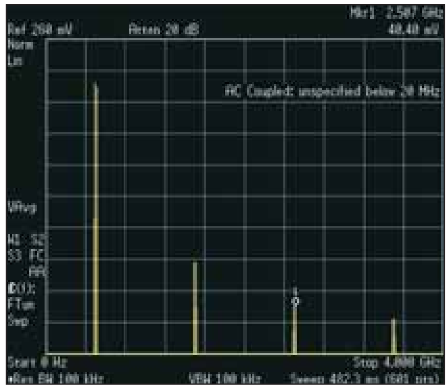

Figure 2 · 500 MHz clock with 35 ps rise/fall time (20-80%); 5th harmonic amplitude = 8.1%.

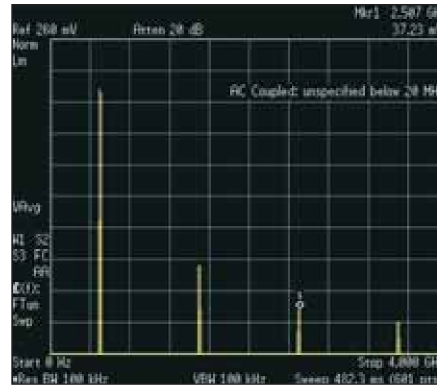

Figure 3 · 500 MHz clock with 47 ps (20-80%) rise/fall time ; 5th harmonic amplitude = 7.4%.

were measured with a 26.5 GHz RF spectrum analyzer to analyze the amplitude of the 5th harmonic.

With a perfect edge, the harmonic amplitude should have been 0.045V (9%), but as the rise/fall time increases, the amplitude of the harmonics decreases.

If we now look at a much faster bit rate of 3 GHz (still 0.5Vp-p) with the same rise/fall times we see that the 5th harmonic has a much smaller relative importance (Figures 4-6). The 5th harmonic of a 3 GHz clock pattern with 47 ps rise/fall times is only 0.3% of the amplitude of the resulting signal.

As we can see, the relative importance of the harmonics depends both on the bit rate and the edge speeds of the signal.

So far we have looked only at clock signals. Let's see what effect changing the data content of a signal has on the spectral content of signals. We took the same signal 0.5Vp-p signal source at 1 Gb/s, 9 ps edge speed, and changed the pattern to the following patterns commonly used in the testing of high speed serial interfaces:

1. PCI Express Compliance Pattern (40 bits long)
2. K28-5 (20 bit long 8b/10b encoded pattern)
3. PRBS $2^7 - 1$ (127 bits long)

in Figures 7-9, the first thing we notice is that there are no clear harmonics at multiples of the fundamental frequency of the signal (bit rate/2). There is plenty of spectral content, but it is spread out at many different frequencies. If we look at the amplitude of the content at the 5th harmonic frequency (in this case 2.5 GHz) we see that even though the edge speed is very fast (9 ps 20-80%) the amplitudes are quite small compared to the amplitude of the resultant signal. We also notice that, with more spectral content, the amplitudes of each spectral tone are lower. This is because the energy in the signal is being distributed among different frequencies. It is clearly not enough to simply look at the amplitude of the spectral content at the 5th harmonic frequency. We must take into account the energy at all frequencies to decide how much bandwidth we need in order to accurately measure a signal.

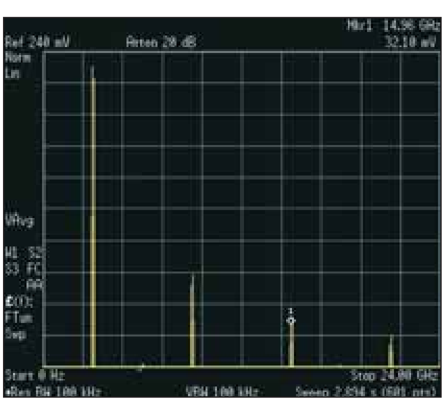

Figure 4 · 3 GHz clock with 9 ps (20-80%) rise/fall time; 5th harmonic amplitude = 6.4%.

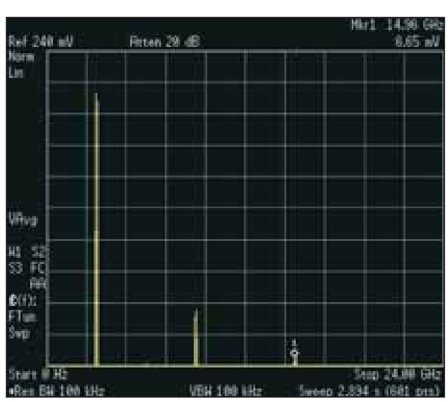

Figure 5 · 3 GHz clock with 35 ps (20-80%) rise/fall time; 5th harmonic amplitude = 1.3%.

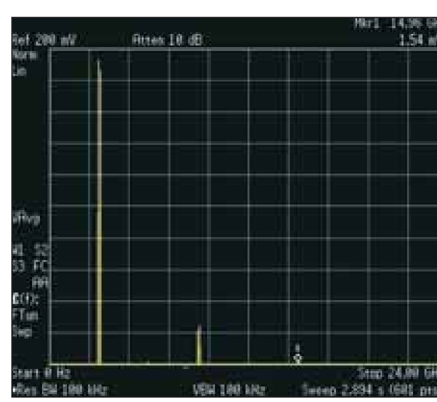

Figure 6 · 3 GHz clock with 47 ps (20-80%) rise/fall time; 5th harmonic amplitude = 0.3%.

www.awrcorp.com

Break free of infinite redesign loops.

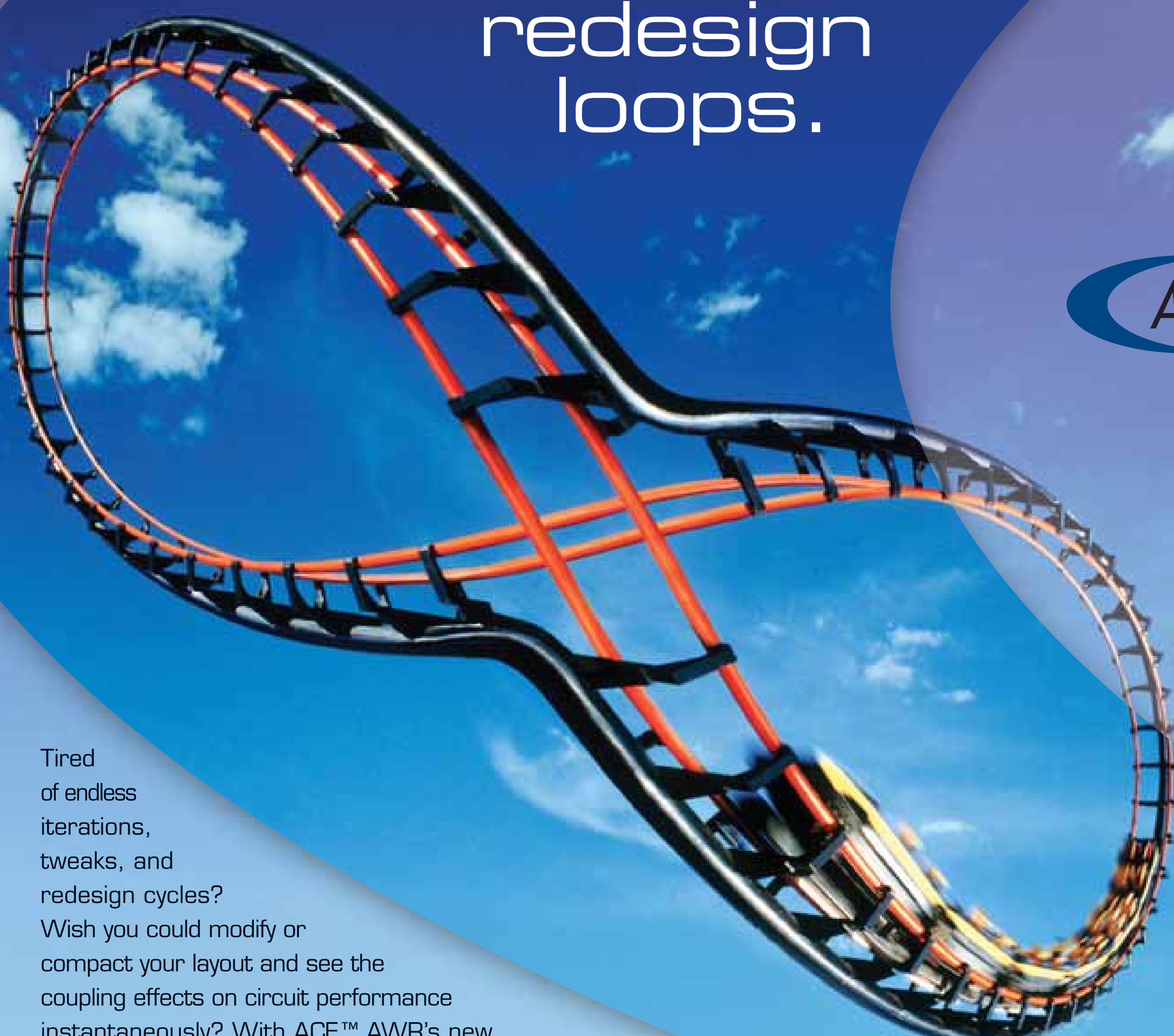

AWR

Tired of endless iterations, tweaks, and redesign cycles? Wish you could modify or compact your layout and see the coupling effects on circuit performance instantaneously? With ACE,™ AWR's new automated circuit extraction technology, you can. ACE extracts layout-driven effects — including coupling in multilayered RF modules and ICs — in seconds and stops the monotony of brute force EM analysis or schematic-driven manual fracturing techniques. Test drive it today at www.awrcorp.com/ACE.

Microwave Office

ACE. Interconnect modeling in seconds

Get info at www.HFeLink.com

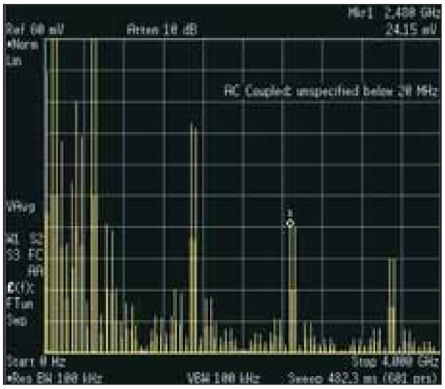

Figure 7 · PCIe Compliance Pattern; 5th harmonic amplitude = 4.8%.

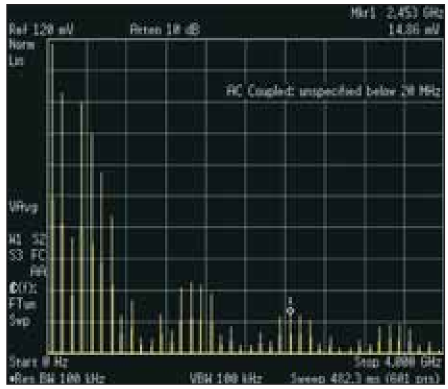

Figure 8 · K28-5 encoded pattern; 5th harmonic amplitude = 3.0%.

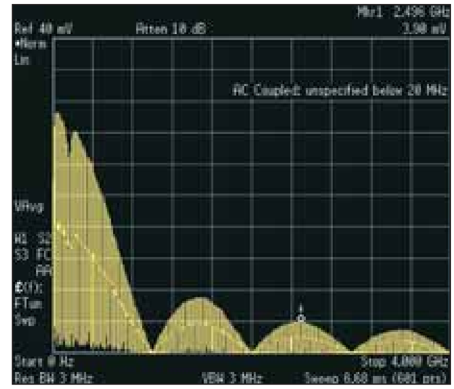

Figure 9 · PRBS $2^7 - 1$; 5th harmonic amplitude = 0.8%.

Another way to quantify how much bandwidth is required to capture the necessary frequency content of a signal is to integrate the spectral content of a signal until we reach a certain percentage of the total signal power (say 99.9%). This method ensures that we include all the spectral content that is of amplitude large enough to significantly affect the signal.

The graphs in Figures 10 and 11 compare the amount of bandwidth (in GHz) required to contain 99.9% of the signal power of a clock pattern and a $2^7 - 1$ PRBS pattern. Both simulated data and live signal measurements are compared at many different combinations of bit rate and edge speed. The edge speeds in the simulation were created using a sum of cosines filter with linear phase. Measurements of the live signal were produced with an Agilent N4903A J-BERT and cascaded Picosecond Pulse Labs transition time converters measured with a 26.5 GHz E4440A performance spectrum analyzer.

The rise time is clearly the dominant factor in determining the amount of bandwidth the signal requires. Indeed, the data even shows that in some cases a higher bit rate requires less bandwidth than a lower bit rate for a given rise time. Note that if we analyze the data closely we see that in most cases the clock pattern requires the most bandwidth for a given bit rate or rise time. Intuitively this makes sense, since the clock is switching states more often than the data pattern and thus contains more high frequency energy

In the real world it is not practical to measure each signal with a wide-band spectrum analyzer before deciding which oscilloscope to use. Although there is no easy way to predict exactly how much bandwidth is required for a given data pattern, bit-rate and rise time, we can use a conservative approximation: the bandwidth required to capture 99.9% of a signal's power is ~0.56/RiseTime. The choice of 99.9% signal power is arbitrary, but it can be shown that for a flat-response real-time oscilloscope, a measurement bandwidth equal or greater to 0.56/RiseTime will deliver rise/fall time measurement accuracy of 3% or better.

The Effect of Noise on Timing Measurements

As we discussed in the introduction, more measurement bandwidth usually means more instrument

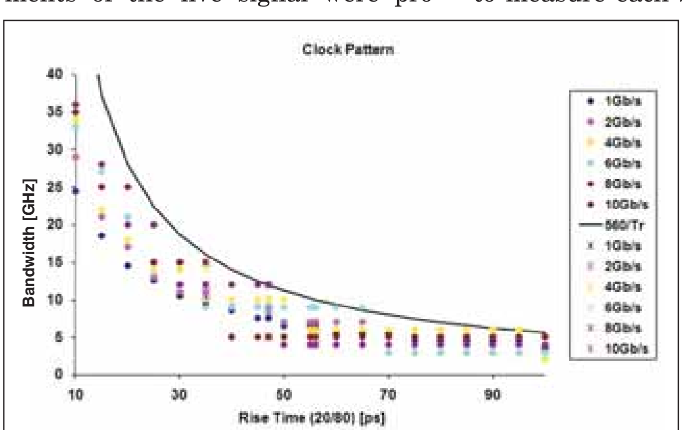

Figure 10 · Bandwidth required for a clock signal at various combinations of bit rate and edge speed.

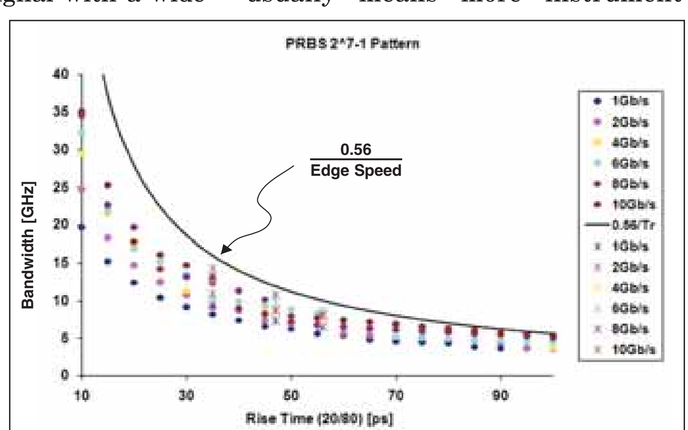

Figure 11 · Bandwidth required for a $2^7 - 1$ PRBS pattern at various combinations of bit rate and edge speed.

Figure 12 · Digital signal without added noise.

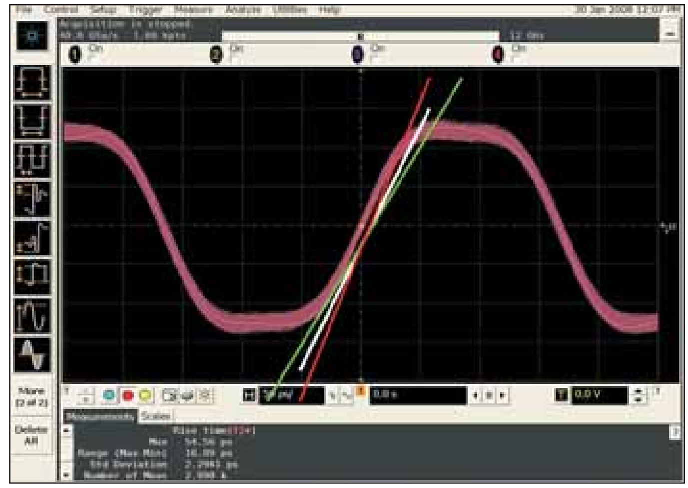

Figure 13 · Digital signal with added noise.

noise and noise impacts timing measurements.

In Figures 12 and 13 the effect of additional noise on a signal is illustrated. The signal source is the same in both cases but in Figure 13, noise has been added to the signal.

An Agilent DSO91304A real-time oscilloscope is used to measure the rise time of the signal and its standard deviation. Although the nominal rise time does not change much, the standard deviation and range of the measurement almost doubles.

The white line shows the nominal edge speed, the red line shows an apparent decrease in rise time due to noise, and the green line shows an apparent increase in rise time due to the noise. The slower the edge, the greater the impact of the noise.

If we assume that the instrument noise is mainly Gaussian, independent of signal amplitude, and the slew rate of the signal is similar at both the 20% and 80% locations on the edge, we can approximate that the standard deviation of the 20-80% rise/fall time (σ_{Tr}) is:

$$\sigma_{Tr} > \frac{\sqrt{2} * \sigma_n * Tr}{0.6 * A}$$

where σ_n is the standard deviation of the instrument noise, *Tr* is the edge speed and *A* is the nominal signal amplitude. The √2 factor comes from the fact that we are combining the noise on 2 locations on the edge, and the 0.6**A* from the choice of 20-80% signal amplitude as our rise time.

For comparison with the bandwidth requirement of 3% accuracy, a 3% standard deviation of the rise/fall time would be created purely by instrument noise when the instrument noise is:

$$\sigma_n = \frac{A}{80}$$

Thus, when measuring a 0.5V p-p signal for example, instrument rms noise of 6.25 mV would introduce a measured rms error in the rise time of approximately 3%.

The actual variation created by the instrument noise could be much higher if the instrument noise is not constant with signal amplitude.

Many other instrument effects will combine to produce measured variation of rise/fall times such as jitter, interleaving errors, etc., so it is very important to minimize the additional effect of instrument noise to avoid using up valuable measurement margin.

Conclusion

We have seen that the 5th harmonic is a very poor predictor of required measurement bandwidth. Instead, rise/fall times can predict required bandwidth much more accurately through the relationship:

$$BW = 0.56/\text{RiseTime}$$

We must also remember that it is not just bandwidth that determines the quality of a timing measurement. Instrument noise degrades the accuracy of all measurements, and so there is little benefit to high measurement bandwidth without also having low noise.

If a signal is repetitive in nature, then an equivalent time sampling oscilloscope such as the Agilent 86100C can be used. This allows for the simultaneous combination of extremely high bandwidth, low noise and ultra-low jitter.

About the Author

Mark Johnson is an Application Engineer in Austin, TX focused on High Speed Digital, Signal Integrity and Optical applications. Mark has an MPhys degree from Lancaster University in England. After working for the High Energy Magnet Research Lab at Texas A&M University for two years, Mark joined Agilent Technologies as an Optical Applications Engineer, covering fiberoptic, digital and telecomm test.

RF/MW Connectors

Snap-Lock SMA Connector Mates

Tyco Electronics introduced a new Snap-Lock SMA series plug connector that is compatible with a standard SMA jack connector. This connector series is ideal for test and instrumentation purposes, as well as mobile base station filters and cable assemblies. It is an excellent option for customers who like the quick release capability but are concerned with backwards compatibility of their existing equipment or systems. The Snap-Lock SMA Series product is offered in straight and right-angle cable plug configurations and as a SMA jack to Snap-Lock SMA plug adapter. The series has an operating temperature range of –65°C to +165°C, 50 ohms impedance, and excellent performance at frequencies up to 6 GHz.

Tyco Electronics
www.tycoelectronics.com

ZMA Bayonet Connectors

High volume cell phone manufacturers in China and throughout the world are reducing production downtime with MegaPhase ZMA connected test cables. The ZMA Series precision coaxial connectors reduce annual cable replacement rates from six per year to practically none by using bayonet coupling connectors instead of threaded connectors. MegaPhase's ZMA bayonet coupling connectors offer many critical advantages over standard threaded connectors. Since the connectors can easily be mated and de-mated by hand with a quarter turn, no torque wrenches are needed, making it ideal for applications where space is tight. The connectors are "keyed" with lugs in 2-, 3- or 4-lug styles. Since the MegaPhase ZMA connectors provide a high coupling force, they are ideal for extreme vibration applications where insufficient room is available for spring loaded blindmate panels.

MegaPhase, LLC
www.megaphase.com

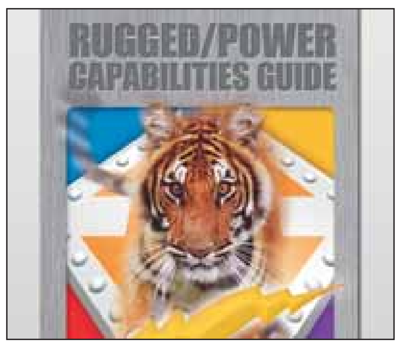

Rugged/Power Connector Capabilities Guide

Samtec's extensive line of interconnects designed specifically to address the interconnect needs of applications requiring high power and highly durable solutions is detailed in its new Rugged/Power Capabilities Guide. This includes board-to-board, cable-to-board, and panel & I/O systems. Headlined by Samtec's Edge Rate™ and Tiger Eye™ contact systems, its Rugged product line offers features such as signal integrity-optimized designs, high mating cycles, superior impedance control, as well as standard and optional "ruggedizing" features including retention pins, positive latching, friction locks, and IP68-rated sealing. In addition to Samtec's standard on-line resources and support, which include a technical library, power ratings, and testing procedures, reports and simulations, additional design, testing, and validation services specific to the needs of high power and rugged applications are readily available.

Samtec, Inc.
www.samtec.com

Miniature RF Coax Cable Assemblies

RF Connectors, a division of RF Industries, offers the MHF series coax cable jumper. These cables use the I-PEX brand MHF connector and 1.13 mm coax cable that is compatible with Hirose U.F.L. Assemblies are available with a variety of connector terminations including SMA reverse polarity, TNC female or reverse polarity female bulkhead, N female bulkhead, SMA male, N male, MMCX, MC card. Most assemblies are manufactured in standard lengths of 3, 6, 8, and 12 inches. Electrical performance is good up to 6 GHz with a VSWR rating of 1.3 maximum.

RF Industries
www.rfindustries.com

EDA Tools

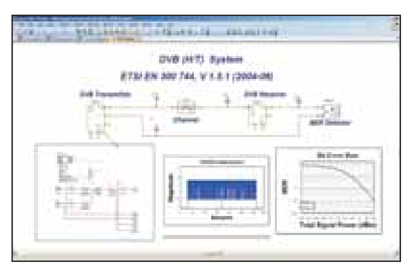

DVB Analysis Capabilities

AWR introduced the Digital Video Broadcasting (DVB) library for its Visual System Simulator (VSS) system-level design software. The library is compliant with the ETSI EN 300 744 V1.5.1 (2004-06) specifications and supports both Digital

Video Broadcast - Terrestrial (DVB-T) and Digital Video Broadcast - Handheld (DVB-H). VSS, an integral part of the AWR Design Environment™, allows the impact of “real-world” signal impairments and other factors to be evaluated early in the design cycle when their effects can be most effectively be mitigated. It gives designers the ability to create the best system architecture by optimizing each of its components from the behavioral through component levels in conjunction with AWR’s Microwave Office® software, and then use measurements to validate the final design. The DVB Library is available now.

AWR
www.awrcorp.com

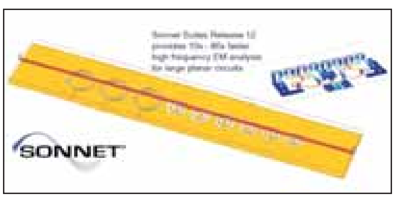

EM Software Release Enables Multicore Processing

Sonnet Software, Inc. introduces the latest SONNET® Suites Professional™ Release 12. Com-plementing Sonnet’s legendary accuracy, Sonnet now introduces dramatically faster simulations through parallel processing on multi-core CPUs. Each frequency point is computed in parallel within the same computer. Sonnet’s matrix solve algorithms have successfully achieved a speed increase of nearly seven-fold on a typical workstation with dual quad-core processors. Two new versions of Sonnet’s EM analysis engine, em™ are introduced. The Sonnet Desktop Solver engine is aimed at typical engineering desktop PCs, and utilizes 2 cores in parallel for analysis time reduction. The Sonnet High Performance Solver engine is aimed at high-end workstations with dual quad-core CPUs, and uses up to 8 cores for 8-way parallel processing on a single frequency.

Sonnet Software, Inc.
www.sonnetsoftware.com

Jivaro-for-GoldenGate

Circuit	# Parasitics	Reduction		
		Parasitics	Memory	Sim Time
VCO	115,600	82%	54%	66%
PA	252,864	58%	25%	32%
Receiver	1.7M	78%	35%	75%

Table 1: Reduction and Speed Improvement for Various RF Circuits

Parasitic Reduction Tool

Agilent Technologies Inc. announces Jivaro-for-GoldenGate, a parasitic model order-reduction tool designed for use with the company’s GoldenGate RF simulator software. Jivaro-for-GoldenGate is expected to enhance RFIC simulation speed and capacity with negligible loss in accuracy. It is designed in cooperation with edXact, a company that provides high-precision, high-performance technology for backend physical verification. edXact’s Jivaro-A netlist-reduction engine is the core of this new RFIC design software. Combining Agilent’s GoldenGate simulator with Jivaro-for-GoldenGate increases simulation capacity, reduces memory requirements and boosts simulation speed when simulating large parasitic-dominated post-layout netlists. Agilent’s Jivaro-for-GoldenGate is available now, with prices starting at approximately $30,000.

Agilent Technologies, Inc.
www.agilent.com

Emulation Technology for Mobile Wireless Networks

Scalable Network Technologies, Inc. (SNT) announced the introduction of EXata™, an advanced wireless network emulator for test and evaluation of military and commercial on-the-move wireless communication networks. EXata is breakthrough emulation technology that speeds the development and deployment of mobile wireless systems, and enables new approaches to training military and public safety personnel. EXata makes it possible to exercise both equipment-in-the-loop and humans-in-the-loop using “software virtual networks” (SVN’s). Much like the flight simulators used to train pilots, SVN’s provide a robust platform to conduct network testing and operations training with an unprecedented level of realism. SVN’s are capable of interfacing with actual networks, running actual applications, in real time—thus enabling rapid evaluation of new technologies, at much lower cost than previously possible. A free demo version of EXata is available for download on the company website, along with technical specifications and free whitepapers. The product can be ordered immediately.

Scalable Network Technologies
www.scalable-networks.com

Software Upgrade for LTE

Anritsu Company recently enhanced its LTE software and tool set. The improved software packages allow Anritsu’s MS269xA Signal Analyzer series and MG3700A Vector Signal Generator to conduct highly accurate measurements on LTE Uplink and Downlink signals. With the accuracy required for R&D and the speed needed for manufacturing, Anritsu’s test equipment facilitates efficient testing of 3GPP LTE-compliant mobile terminals, base stations, and components. The LTE Uplink and Downlink analysis packages are $18,500 each. The LTE waveform generation software for the MS269xA Signal Generator option and the MG3700A Vector Signal Generator is $5,500. Base price of the MS269xA series starts at $37,000 while the MG3700A has a base price of $29,000.

Anritsu Company
www.us.anritsu.com

Next Month’s Featured Products:
Crystals & Oscillators
Antennas
Substrates & Laminates

M/A-COM Technology Solutions

RF & Microwave Components

proven performance in demanding applications

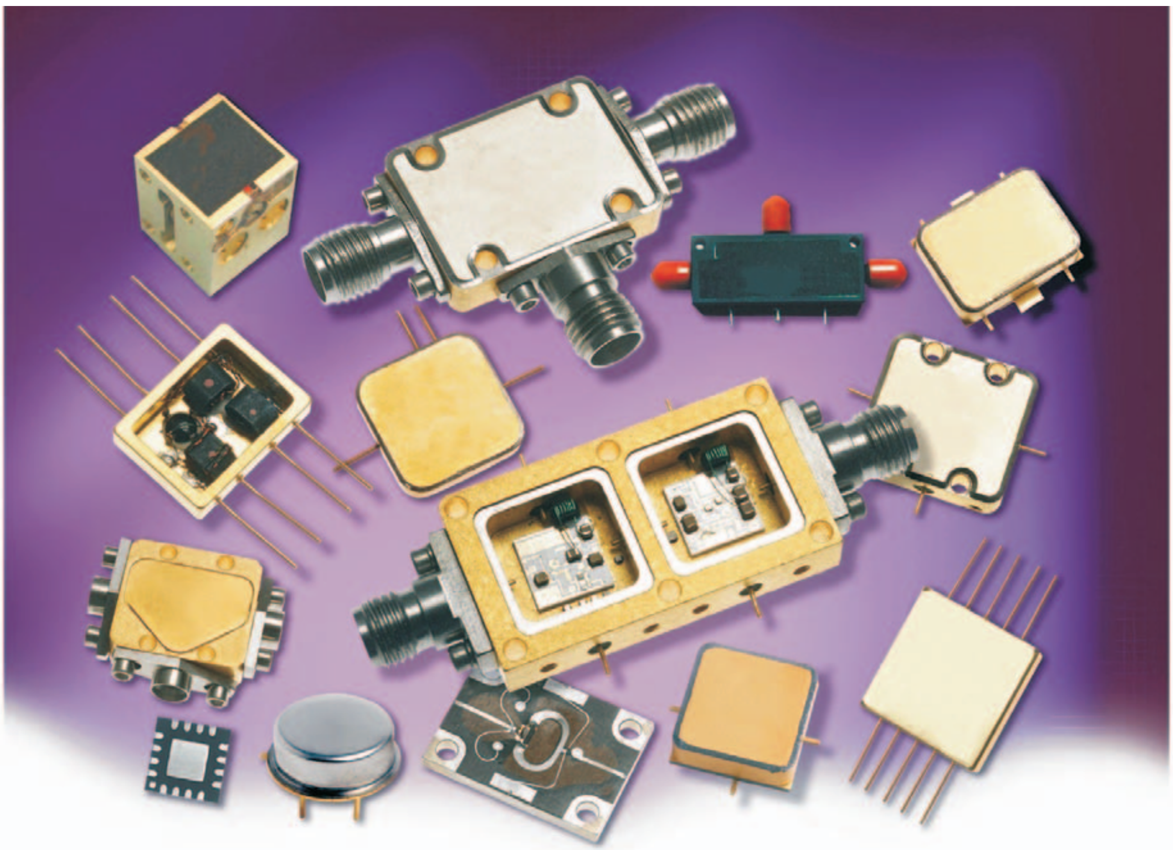

Active & Control Products

Mixers	Amplifiers
Detectors	Switches
Phase Shifters	Limiters

Attenuators (Digital/Voltage Variable)

Passive Products

Couplers
Power Dividers/Combiners
Attenuators (Digital/Voltage Variable)

Signal Generation Products

VCOs
Frequency Doublers

MMIC Devices

Amplifiers (High & Medium Power)
LNAs
Phase Shifters
Attenuators
Switches

Call us today to receive a product catalog...

VISA MasterCard AMERICAN EXPRESS

MICROWAVE COMPONENTS

Phone: (888) 591-4455 or (772) 286-4455 Fax: (772) 286-4496
E-mail: admin@microwavecomponentsinc.com
Web Site: www.microwavecomponentsinc.com

ISO 9001:2000 CERTIFIED

Get info at www.HFeLink.com

Recent Developments in High Frequency Component Modeling

The ever-growing importance of computer simulation and analysis of high frequency circuits demands high-accuracy models for the components comprising those circuits. Over the past 25 years, those models have evolved from relatively simple equivalent circuits that include only major parasitic elements, to measurement-based or electromagnetic simulation-based behavioral models that may cover a wide range of frequencies, temperature, and operating voltage (or current).

Commercial Support of EDA Tools

For many years, major component companies have supplied models of their devices, but recently, the number of components in the catalog, the accuracy of the models, and especially the frequency range of their characterization have all increased.

Passive component models from SMT vendors allow even low-cost, high-volume consumer products to have accurate simulation in the design phase. Large-scale suppliers like MuRata, Toko, Coilcraft, Taiyo Yuden, AVX and others, have joined the specialized RF/microwave suppliers that have included *S*-parameter models for many years, and now provide advanced models with greater accuracy.

Active device models have had a similar growth in the number and detail of available component models. All RF and microwave semiconductor suppliers have extensive *S*-parameter files as a minimum level of support, and many provide advanced nonlinear, frequency-dependent models as well.

Process-specific models are essential tools for RFIC and MMIC design, as well as for LTCC (low temperature co-fired ceramic) and recent SoC (system-on-chip) technologies. Foundries providing fabrication services for these devices work closely with all major EDA developers to provide compatible Process Design Kits (PDKs) that include the necessary device, interconnect and other models that will increase the chances of a first-pass design success. Major IC layout tools have recently been seamlessly integrated into RF/microwave EDA tools with joint interface development efforts.

Independent commercial model development has been pursued sporadically for many years, but recently has reached greater importance with the services offered by Modelithics, Inc. This spin-off from the University of South Florida provides measurement-based modeling services to the high frequency industry. The component models provided for major EDA tools include active devices from companies such as Avago, Eudyna, Excelics, Hexawave, Mitsubishi, MIMIX, MWT and NEC. The company also provides passive component models for devices from AVX, American Technical Ceramics, Coilcraft, MuRata, Johanson, KOA, TDK, Toko, Panasonic, and many others. Libraries of these components are offered for major EDA tools such as AWR Corp.'s Microwave Office and Agilent Corporation's Advanced Design System (ADS).

Connector companies also provide simulation and layout models for many high frequency connectors. These may include data for multiple substrates and metallization schemes. The combination of a prescribed method of installation (including mechanical assembly and soldering) with an accurate model for simulation helps designers solve the classic problem of poor prediction of interconnect performance. Samtec provides similar data for a reference layout and computer simulation for high speed digital connectors, which often have had only approximations or design rules to guide engineers.

Developing Models by Electromagnetic (EM) Simulation

EM simulation vendors such as CST, Agilent, Ansoft, AWR, Sonnet and others place great importance on using their tools to develop behavioral models, not just to simulate a specific circuit.

EM tools have evolved to a high level of accuracy, with well-defined capabilities and limitations. Although it is possible to combine circuit simulation with EM simulation, the large problem size of EM simulation makes this a slow process, relative to circuit simulation alone. Many academic papers and company application notes address the process of developing a behavioral model using EM simulation, then using that model for fast computation in

MINI-CIRCUITS

USB POWER SENSOR

Turns Your Laptop Into A Power Meter

-30 to +20 dBm 1 to 6000 MHz

POWER SENSOR PWR-6G+ Package

only $695 *ea. (qty.1-4)*

Includes:
PWR-SEN-6G+ Power Sensor Unit
Power Data Analysis Software
SMA Adaptor, USB Cable

Fully loaded software features

- *Power data analysis*
- *Power level offset*
- *Scheduled data recording*
- *Average of measurements*
- *Interface with test software*
- *Multi sensor support software* (up to 16 sensors support software)

Now, Mini-Circuits offers a USB Power Sensor and software that will reduce your equipment costs and provide new application features that will simplify your power measurements.

All you need is a personal computer (PC) or laptop computer and a Mini-Circuits PWR-6G+ USB Power Sensor. It turns any computer into a powerful power meter having a measurement range of -30 to +20 dBm at frequencies from 1 to 6000 MHz. The PWR-6G+ is supplied with easy-to-use, Windows-compatible measurement software to speed and simplify your power measurements, allowing you to set as many as 999 averages and to record results for further analysis. The PWR-6G+ USB Power Sensor provides 0.01-dB measurement resolution and impressive accuracy over temperature. Visit the Mini-Circuits' web site at www.minicircuits.com to learn more.

Mini-Circuits…we're redefining what VALUE is all about!

Get info at www.HFeLink.com

Mini-Circuits®
ISO 9001 ISO 14001 AS 9100 CERTIFIED

minicircuits.com

P.O. Box 350166, Brooklyn, New York 11235-0003 (718) 934-4500 Fax (718) 332-4661 For detailed performance specs & shopping online see Mini-Circuits web

YONI2™ Patent Pending *The Design Engineers Search Engine* Provides ACTUAL Data Instantly From MINI-CIRCUITS At: **www.minicircuits.com**

IF/RF MICROWAVE COMPONENTS

457 rev A

circuit simulation. This “modular” approach maintains the high accuracy of EM simulation while the engineer enjoys the computation speed of circuit simulation.

It should be noted that accurate EM simulation is not a trivial task. At most companies that employ this type of model development, the best minds on the engineering staff are involved.

Conventional Measured Model Extraction

Internal efforts by companies like Agilent, which has both EDA and instrument divisions, plus cooperative efforts between independent instrument and EDA vendors, have greatly simplified and sped up the process of parameter extraction. New model development tools aid the efforts of passive and active component manufacturers, as well as those OEMs that choose to develop certain models for their internal use.

Although the general methods are mature, the primary recent advances are in speed, accuracy and flexibility of operation. Productivity is constantly being address by this, and all other, forms of model development.

New Model Challenges

Advanced models for RFIC/MMIC design are powerful, but there are clear paths to greater accuracy and usability. Allowing a “classic” circuit design engineer to design his or her product as an integrated circuit is still a challenging task, still requiring an experienced chip designer’s assistance. A close interrelationship between circuit design and the physics of IC design has only recently begun to be addressed in depth.

Full-system simulation using physical, EM, circuit and thermal models also has much work yet to be done. Interfacing between combinations of tools has been successful, but like IC design, the models used in the various stages of the process may vary widely in the way they are defined. This “big picture” effort represents a major goal for EDA developers.

X-Parameters: The Next Step?

In mid-2008, Agilent Corporation began promoting a new concept, X-parameters, as a natural follow-on to well-known S-parameters for characterizing active and passive devices at RF and microwave frequencies.

According to Agilent literature, “X-parameters are the mathematically correct superset of S-parameters, applicable to both large-signal and small-signal conditions, for linear and nonlinear components.”

The X-parameters can be generated either from simulation with the company's Advanced Design System (ADS) EDA software or from measurements, particularly using Agilent’s Non-Linear Vector Network Analyzer (NVNA).

In the past, designers could not accurately measure, display and simulate the full amplitude and phase information of each spectral component in non-linear designs. As a result, they did not have access to a highly accurate non-linear behavioral model that fully characterizes the non-linear behavior of their devices. Agilent’s new patent-pending X-parameter technology allows designers to capture the non-linear behavior of active components such as amplifiers and transistors in the same manner as obtaining S-parameters, and save them for use in RF system or circuit designs in ADS.

According to Jason Horn, R&D engineer with Agilent’s High-Frequency Technology Center, and one of the inventors of X-parameter technology, “Literally in five minutes, you can generate a nonlinear X-parameter model from an off-the-shelf amplifier by measuring it with Agilent’s Non-Linear Vector Network Analyzer, and you can start doing non-linear designs with it in ADS immediately.”

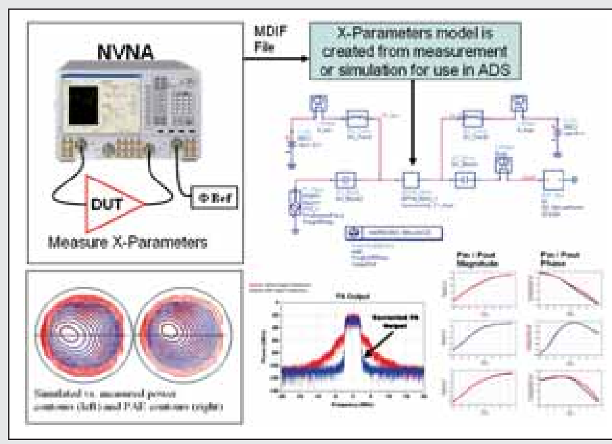

Advanced Design System from Agilent’s EEsof EDA division enables X-parameter nonlinear model generation from simulation, allowing design houses to create nonlinear X-parameter models of their RFICs and MMICs, modules and multiport devices such as mixers. X-parameter models protect the intellectual property from which they are generated while retaining the full non-linear characteristics to share with circuit and system design partners.

Users can also generate X-parameter models with load pull characteristics—for accuracy over a wide range of terminating impedances—from ADS simulation or from measurement on an Agilent NVNA using the load-pull system from Maury Microwave Corp.

Nonlinear models have been developed using other methods, but as X-parameters are studied by more engineers and companies, we will see if they become the universal solution for nonlinear device characterization.

TEST TECHNOLOGY NEWS

LXI Consortium Elects New President

The LXI Consortium Board of Directors has elected Von Campbell of Agilent Technologies as the Consortium's new president. Von Campbell holds a Bachelors in Electrical Engineering from Purdue and a Masters in Electrical Engineering from Stanford. Campbell joined Agilent Technologies (Hewlett-Packard) as a development engineer in 1982. Today, he oversees Agilent's involvement in multiple industry consortia, including LXI.

National Instruments Identifies Top Trends in Test and Measurement for 2009

National Instruments has identified three trends that will significantly improve the efficiency of test and measurement systems in 2009:

Software-Defined Instrumentation—The adoption of software-defined instrumentation is the most significant trend in test and measurement for 2009 because it helps engineers achieve new levels of measurement performance and lower test costs.

Parallel Processing Technologies—The use of parallel process technologies, such as multicore and FPGAs, are becoming more prevalent in today's automated test systems due to standard PC-based architectures, such as PXI, and higher level software abstraction tools.

New Methods for Wireless and Semiconductor Test—Software-defined instrumentation supports rapid-growth areas. This approach makes it possible for engineers to test multiple standards using common modular hardware components and implement emerging wireless protocols and algorithms.

Keithley to Develop RF WiMAX Production Test System for Fujitsu PCMCIA and USB Products

Keithley Instruments, Inc. announces that it is developing a WiMAX device production test solution for two 802.16e WiMAX devices from Fujitsu Microelectronics Limited. This WiMAX RF SISO/MIMO manufacturing test configuration features Keithley's Model 2820 RF Vector Signal Analyzer and Model 2920 RF Vector Signal Generator instruments, based on next-generation DSP-based Software-Defined Radio (SDR) architecture. The configuration will enable Fujitsu to perform a set of TX and RX test sequences quickly and efficiently. The system's easy expandability also will offer Fujitsu the ability to test its WiMAX devices in both SISO and MIMO mode.

NEW PRODUCTS

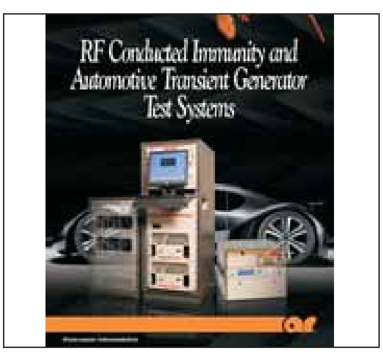

New Literature

AR RF/Microwave Instrumentation has released new literature with comprehensive information on its innovative test systems for conductive immunity and automotive transient generator testing. The new brochure includes AR's Conducted Immunity Systems, self-contained, all-in-one test systems; and the company's TGAR Systems for automotive transient generator testing. The brochure includes technical information for all the CI and TGAR models, along with a listing of all the test standards programmed into the systems.

AR RF/Microwave Instrumentation
www.ar-worldwide.com

Handover Box

JFW's Handover Test Systerms are specifically designed for proving wireless device performance at the network level. These systems are based on our multi-path attenuator networks and each system comes complete with "Handover" functionality written directly into the firmware. Created with WiMax and LTE testing in mind, many of the handover systems operate from 200 MHz up to 6 GHz. Each system can be individualized to suite your testing needs.

JFW Industries
www.jfwindustries.com

LTE Multi-Handset Test Mobile

Aeroflex announced the launch of an LTE version of its industry-standard TM500 multi-handset (multi-UE) test mobile designed to enable infrastructure equipment vendors accelerate the pace of their LTE development projects. Up to 32 LTE handset UEs are provided in one multi-UE test mobile, which simplifies complex tasks such as functional network testing with multiple UEs and performance measurement of resource scheduling algorithms. In addition to its use for functional and performance testing, TM500 Multi-UE Test Mobile can also be upgraded to support hundreds of UEs for load and stress testing in conjunction with third-party capacity test products.

Aeroflex Inc.
www.aeroflex.com

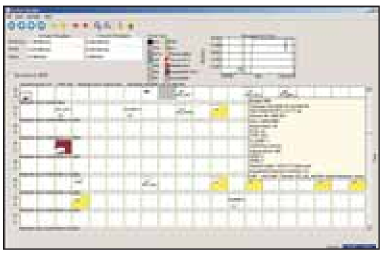

Bluetooth Testing Software

Frontline Test Equipment, Inc. is a leading provider of PC-based protocol analyzers for special-purpose data communication networks. Frontline's FTS4BT™ supports the new IEEE P11073-20601 Draft Standard for Health Informatics, Personal Health Device communication application profile and includes the Multi-Channel Adaptation Protocol. Unlike protocol analyzers that can only store data for later evaluation, Frontline's analyzers feature real-time displays to further accelerate the debugging and verification process. The effect of user actions-whether "positive path" or regressive are observed in real time on the screen.

Frontline Test Equipment, Inc.
www.fte.com

Wireless Test System

Setcom wireless introduces the S-CAT 6010 wireless protocol test system, an advanced design approach for wireless device protocol testing. It replaces a bench full of equipment with a cost-sensitive, compact test platform that tests the full device signaling protocol stack, from the radio layer all the way up to the network services, multi-media, and applications layer.

setcom wireless products Ltd.
www.setcom.eu

Battery Powered Signal Generator

Signal Forge released a new battery-powered signal generator. The SF1020 is a small, lightweight battery-powered signal generator with a frequency range of 1 Hz to 1 GHz and numerous waveform modulation functions. It is ideal for applications such as building surveys, installation and maintenance of facility-based cellular and wireless networks and a variety of other test applications that can only be conducted outside of the lab. The new portable Signal Forge 1020 Battery Powered Signal Generator is priced at $1,395 and is available now.

Signal Forge, LLC
www.signalforge.com

Auto-Calibration Design Kit

TT electronics OPTEK Technology has developed an automatic calibration design kit. The OCB100-Kit features a driver board with three different optoelectronic circuits to enable design engineers to easily calibrate optoelectronic devices, provide a consistent output signal, and shorten their design cycle. The OCB100 Series system calibrates reflective, interruptive and special opto sensors to produce a consistent output, eliminating the need to confirm either the LED drive resistance or phototransistor load resistance to provide a steady state condition. Pricing for the OCB100 auto-calibration design kit ranges from $42.59 to $31.94 each, depending on quantity. The design kits are available immediately.

TT electronics OPTEK Technology
www.optekinc.com

One-Box Test Set

Anritsu Company introduces the MS269xA Series Signal Analyzer, equipped with a vector signal generator, a DigRF interface, and measurement software. The MS269xA-based solution provides a faster, easier, and more cost-efficient method for developers and manufacturers to ensure their RF and RFIC modules used in mobile devices are in full compliance with DigRF v3.09. The software package includes a Sequence Editor feature that produces test scripts without programming or scripting languages. With only a few mouse clicks, users can set timing, modify commands, and save test scripts. The DigRF test platform fully configured is $130,000. Delivery is 6 to 8 weeks ARO.

Anritsu Company
www.us.anritsu.com

FLEX TEST™

CABLES

DC to 18 GHz from $68.95 IN STOCK ea. (qty.1-9)

Strength, ruggedness, and reliability…*supercharged!* That's what you get when you choose Mini-Circuits ultra-flexible precision test cables. Engineered to be a workhorse for your day-to-day test operations, these triple shielded cable assemblies are qualified to at least 20,000 bends, employ an advanced strain relief system, and are equipped with passivated stainless steel connectors, *so you can rely on them to* ***flex, connect and disconnect over and over and over again!*** They're so rugged, each test cable is backed by our 6 month guarantee*! With low insertion loss and very good return loss, you can also rely on getting good performance over the wide DC-18 GHz band. Visit our website to choose and view comprehensive performance curves, data sheets, and environmental specifications.

Mini-Circuits…we're redefining what VALUE is all about!

New! ***Tough Armored Cables*** *are steel triple shielded and qualified to at least 25,000 bends. They're so rugged they can even pass a crush test of a 600lb. nitrogen tank over the cable 1000 times, without any change in electrical performance.*

RoHS compliant

Frequency Range: DC-18 GHz, Impedance: 50 ohms

Models	Connector Type	Length (Ft.)	Inser. Loss (dB) Midband Typ.	Return Loss (dB) Midband Typ.	Price $ ea. Qty.(1-9)
FLEX TEST CABLES		Male to Male			
CBL-1.5FT-SMSM+	SMA	1.5	0.7	27	68.95
CBL-2FT-SMSM+	SMA	2	1.1	27	69.95
CBL-3FT-SMSM+	SMA	3	1.5	27	72.95
CBL-4FT-SMSM+	SMA	4	1.6	27	75.95
CBL-5FT-SMSM+	SMA	5	2.5	27	77.95
CBL-6FT-SMSM+	SMA	6	3.0	27	79.95
CBL-10FT-SMSM+	SMA	10	4.8	27	87.95
CBL-12FT-SMSM+	SMA	12	5.9	27	91.95
CBL-15FT-SMSM+	SMA	15	7.3	27	100.95
CBL-25FT-SMSM+	SMA	25	11.7	27	139.95
CBL-2FT-SMNM+	SMA to N-Type	2	1.1	27	99.95
CBL-3FT-SMNM+	SMA to N-Type	3	1.5	27	104.95
CBL-4FT-SMNM+	SMA to N-Type	4	1.6	27	112.95
CBL-6FT-SMNM+	SMA to N-Type	6	3.0	27	114.95
CBL-15FT-SMNM+	SMA to N-Type	15	7.3	27	156.95
CBL-2FT-NMNM+	N-Type	2	1.1	27	102.95
CBL-3FT-NMNM+	N-Type	3	1.5	27	105.95
CBL-6FT-NMNM+	N-Type	6	3.0	27	112.95
CBL-10FT-NMNM+	N-Type	10	4.7	27	156.95
CBL-15FT-NMNM+	N-Type	15	7.3	27	164.95
CBL-20FT-NMNM+	N-Type	20	9.4	27	178.95
CBL-25FT-NMNM+	N-Type	25	11.7	27	199.95
		Female to Male			
CBL-3FT-SFSM+	SMA-F to SMA-M	3	1.5	27	93.95
CBL-2FT-SFNM+	SMA-F to N-M	2	1.1	27	119.95
CBL-3FT-SFNM+	SMA-F to N-M	3	1.5	27	124.95
CBL-6FT-SFNM+	SMA-F to N-M	6	3.0	27	146.95
ARMORED CABLES		Male to Male			
APC-6FT-NM-NM+	N-Type	6	3.0	27	181.95
APC-10FT-NM-NM+	N-Type	10	4.8	27	208.95
APC-15FT-NM-NM+	N-Type	15	7.3	27	243.95

Metric Sizes Available On Our Website

6 mo. GUARANTEE **Mini-Circuits will repair or replace your test cable at its option if the connector attachment fails within* ***six*** *months of shipment. This guarantee excludes cable or connector interface damage from misuse or abuse.*

An Introduction to Broadband Impedance Transformation for RF Power Amplifiers

By Anthony J. Bichler
RF Micro Devices, Inc.

This tutorial article reviews impedance matching principles and techniques, as they are applied to power device matching in amplifier circuits

This paper discusses broadband impedance-transforming techniques specific for radio frequency power amplifiers. Single and multiple Q matching techniques are demonstrated for broadband performance; here the reader will understand the importance of a load impedance trajectory relevant to load pull contours.

Introduction

When analytically defining radio frequency circuits, a common approach incorporates admittance or impedance. Admittance, which is symbolized by Y, is defined in terms of conductance G and an imaginary susceptance component, jB. Admittance is often useful when defining parallel elements in a network and is expressed by the complex algebraic equation $Y = G + jB$.

Impedance, the mathematical inverse of admittance, is symbolized by Z and consists of a resistive component R in units of ohms and a reactive or imaginary component jX. Together in a series complex expression they define impedance as $Z = R + jX$. Impedance in this rectangular form is often used in industry to define a power device's optimal source or load.

For linear systems, the condition for maximum power transfer is obtained when the impedance of the circuit receiving a signal has an equal resistance and an opposite reactance of the circuit sending the signal. In the mathematics of complex variables, this relationship is known as the complex conjugate. The complex conjugate of a complex number is obtained by simply reversing the sign of the imaginary part. Here Z^* denotes the complex conjugate of Z; thus, for linear systems the condition for maximum power transfer is when $Z_{\text{Load}} = Z_{\text{Source}}^*$, or: $Z_L = Z_S^*$.

As the frequency of operation changes for Z_S, relative to its parasitics, the value of the resistive component can substantially change as well as the value of the imaginary component. Transforming a standard system impedance to present a driving point load impedance Z_L that maintains a complex conjugate relationship to the source impedance change over frequency is the most challenging aspect of broadband design.

Note: The linear condition for maximum power transfer is often traded for other performance parameters such as efficiency or gain. For this tradeoff the load impedance will not hold a conjugate relationship; however, the challenge of maintaining a load for this performance parameter over a broadband will generally remain the same.

A Review of Smith Chart Fundamentals

Philip H. Smith introduced the Smith Chart in *Electronics Magazine* on January 1939, revolutionizing the RF industry [1, 2]. This chart simplified complex parallel to series conversions graphically and, for the first time, provided intuitive transmission line solutions.

The Smith Chart is a graphical reflection coefficient system with normalized conformal mapping of impedance or admittance coordinates, as shown Figure 1 and 2, respectively. Reflection coefficient is often referred to as *gamma* and is symbolized by the Greek letter Γ. Gamma in its simplest form is defined as


GREAT SERVICE ISN'T EXPENSIVE...
...IT'S PRICELESS.
EXCELLENT SERVICE
EXCELLENT DELIVERY
EXCELLENT QUALITY
RELCOMM TECHNOLOGIES, INC.
RF COAXIAL RELAYS
RMS-6S3AB-I
28Vdc D/C
RDS-2S3DB-I
12 Vdc D/C
SMA, N AND PCB LAUNCH
STANDARD AND CUSTOM DESIGNS
RELCOMM TECHNOLOGIES, INC.
• Mission Critical Communications:
- Security, Safety and Intelligence
- Commercial Telecom Infrastructure
- Military Defense Fixed, Mobile & Shipboard
• Instrumentation:
-Test and Measurement
RF Relay Store.com is the answer to your urgent small quantity needs.
RF Coaxial Relays available from Stock at www.rfrelaystore.com
sales@relcommtech.com • www.relcommtech.com • 410-749-4488
EXCELLENCE BY DESIGN

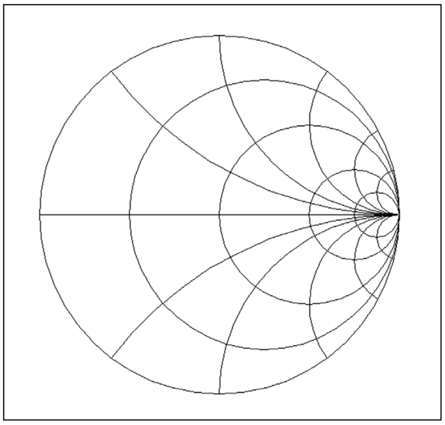

Figure 1 · The Impedance Smith Chart.

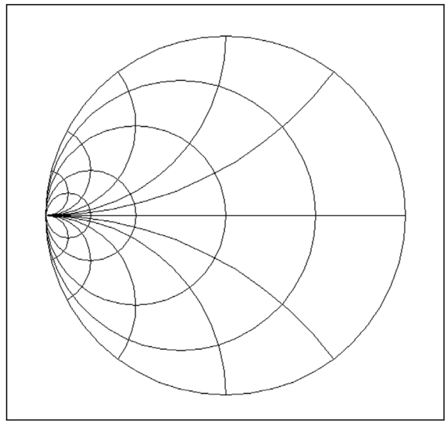

Figure 2 · The Admittance Smith Chart.

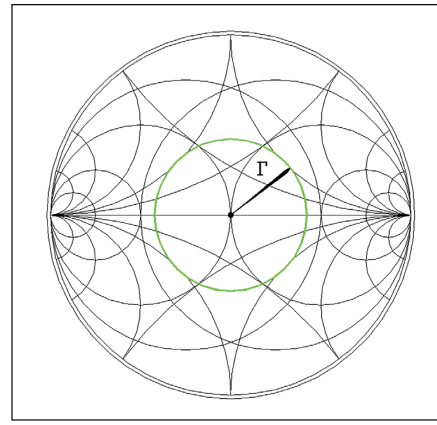

Figure 3 · The Immittance Chart with an SWR circle (green line) defined by (Γ) radius.

the ratio of the root of the incident power wave versus the root of the reflected power wave [3]:

$$\Gamma = \frac{\sqrt{W_r}}{\sqrt{W_i}}$$

where W_r is the reflected power and W_i is the incident power. Gamma can also be defined in terms of impedance where

$$\Gamma = \frac{Z_L - Z_S}{Z_L + Z_S}$$

For a large impedance mismatch Γ would approach unity, and for a near perfect match Γ would approach zero.

Impedances are often normalized when plotted on the Smith Chart. Normalizing Z_L to the center of the Smith Chart where $Z = 1$ gives one access to the chart's maximum resolution. Note that normalizing is the division of an impedance by a reference [4]. For example, normalizing with the 50-ohm system load impedance as the reference ($Z_0 = 50$), a source impedance of $Z_S = 100 + j50$ would normalize to $Z_S / Z_0 = 2 + j1 = z_s$, where the lower case z is used for normalized impedances. Most computer aided design or Smith Chart programs have simplified the normalization process. In the case of normalizing, the center of the chart will conveniently reference to 50 ohms or another value as defined by the user.

The Smith Chart's horizontal centerline is known as the *resistive line.* It is scaled left to right, zero to infinity, with the normalized impedance (Z_o) centered in the middle of the chart. On the lower half of the chart below the resistive line, are the capacitive coordinates and above the line are the inductive coordinates. The circles that are tangent to the right side of the impedance Smith Chart are the circles of constant resistance. Above and below the right side at R = infinity are the semicircles of constant reactance.

On the Admittance Smith Chart, the circles that are tangent to the left side are the circles of constant conductance and the semicircles above and below to the left where $R = 0$ are the circles of constant susceptance.

The Admittance Smith Chart is simply a mirror image of the Impedance Smith Chart where the Impedance Smith Chart can be rotated by 180 degrees to serve as an Admittance Chart. This duality of the Smith Chart is exploited for admittance to impedance conversions by simply rotating both the reflection coefficient vector by 180 degrees and then the chart itself by 180 degrees. Note that since the Smith Chart is a reflection system, 180 degrees around the circumference is equivalent to 90 degrees of wavelength rotation.

A Smith Chart that has combined the Admittance and Impedance Smith Charts for simplicity is known as the Immittance Chart [5]. With the Immittance Chart a network consisting of capacitors or inductors in shunt or in series can be easily cascaded without rotating the chart.

In Figure 3, an Immittance Chart, the Gamma vector magnitude defines the radius of a constant standing wave ratio (SWR) circle. Standing waves are a phenomenon of the voltage or current waves from the summation of an incident power wave and reflected power wave on a transmission line from a mismatched load. SWR is the ratio of the maximum versus the minimum voltage or current on a standing wave and is commonly referred to as VSWR or ISWR, for voltage or current respectively. [6, 7]

SWR can be expressed in terms of Gamma's magnitude by

$$SWR = \frac{1 + [\Gamma]}{1 - [\Gamma]}$$

or directly by the mismatch impedances

$$SWR = \frac{Z_L}{Z_S}$$

or

$$SWR = \frac{Z_S}{Z_L}$$

where the equation choice is dictated by which one provides a quantity greater than unity.

SWR circles are used throughout the following Smith Chart illustrations to quantify the mismatch over frequency.

The Importance of Quality Factors

It is important to understand the quality factors Q, as they are integral to bandwidth. Q factors are used to define the quality of a reactive element by its ability to store energy, to fundamentally define bandwidth, and to define the ability of a loaded network to store energy. To ease some of the confusion with these Q factors they have been assigned the terms unloaded Q, loaded Q, and Q of the load respectively [8].

Unloaded Q is fundamentally defined as the ratio of stored energy versus dissipated energy [10] or

$$Q_{\text{Unloaded}} = \frac{\text{reactive power}}{\text{real power}} = \frac{I^2X}{I^2R}$$

which reduces to

$$Q_{\text{Unloaded}} = \frac{X}{R}$$

For capacitors, unloaded Q is expressed as a ratio of capacitive reactance to equivalent series resistance (ESR) [9] or

$$Q_{\text{Unloaded}} = \frac{X_C}{R_{ESR}}$$

and for inductors unloaded Q is expressed by

$$Q_{\text{Unloaded}} = \frac{X_L}{R}$$

where R is the series resistance from the windings of the coil.

Loaded Q is defined by the band's center frequency (F_C) divided by the 3 dB bandwidth and is expressed as

$$Q_{\text{Unloaded}} = \frac{F_C}{BW}$$

For simple resonant tank networks, unloaded Q can be substituted with loaded Q in bandwidth calculations [11]. When the resonant frequency is equal to the center frequency, then unloaded Q can define the bandwidth by

$$BW = \frac{F_C}{Q_{\text{Unloaded}}}$$

or with substitution

$$BW = \frac{F_C}{X/R}$$

The Q of the load is often used to define a loaded network, which typically consists of ideal (lossless) matching elements. The network is not lossless since energy is propagated to and absorbed by the load. It is defined as before with the unloaded Q as a ratio of the reactance to resistance

$$Q = \frac{X}{R}$$

or in terms of vectors; the imaginary component magnitude versus the resistive component.

Plotting Q of the load as constant ratio on the Smith Chart will define a constant Q curve. These Q curves are often used as guideline boundaries for broadband transformations and will be used throughout the following illustrations to define the transforming networks. As a rule in broadband transformations, maintaining a lower Q curve for a given transformation by increasing the number of n-sections will yield a higher bandwidth.

For a single section transformation where the resistive line and a constant Q of the load curve bound the transformation, the relationship between the Q of the load and the resistive transformation ratio is given by [12]

$$1 + Q^2 = R_{ratio}$$

For increasing bandwidth by increasing the number of n-sections having equal Q the relationship becomes

$$1 + Q^2 = \left(\sqrt[n]{R_{ratio}}\right)$$

Note: Using the guideline boundaries above in this reference does not yield the optimal broadband design. Other topologies will be discussed such as the Chebyshev response transformation, which has a significant bandwidth advantage over the single Q matching technique. Single Q advantages to be considered are transformation efficiency with smaller component values and design simplicity.

In practice using more than a four-section matching network will not yield greater bandwidth.

Also, Q of the load should not be substituted with unloaded Q or loaded Q. For example, in the following multiple section illustrations, which are bounded by a Q of the load curve = 1.75 (for a 50 to 3 ohm transformation), yield more 3 dB bandwidth than defined by the loaded Q of 1.75.

Q of the load will be referred to throughout the remainder of this discussion as the single letter Q.

Computer-Aided Design (CAD) and Other Smith Chart Programs

Smith Chart programs such as the early Motorola Impedance Matching Program (MIMP) provide a useful tool by automating the repetitive graphical computations [13]. Considering the frequency point calculations required for resolution of a broadband matching network, this is a tedious task at best. Smith Chart programs quickly and accurately plot the required trajectories and circles allowing the designer to focus on the design and not the mechanics of generating a display. Other Smith Chart

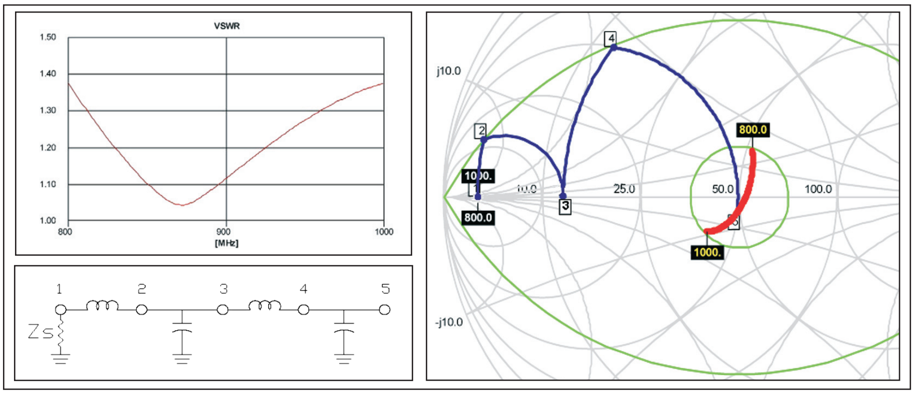

Figure 4 · Z_O = 50, Z_S = 3, Q = 1.75, SWR = 1.4; N1-2 Series L = 0.9 pH, N2-3 Shunt C = 25 pF; N3-4 Series L = 3.8 nH, N4-5 Shunt C = 6.5 pF.

programs followed MIMP such as winSmith [14], LinSmith [15], and Smith32 [16]. Although these programs leveraged an engineer's intuitive creativity with symmetrical Q matching solutions, they fall short of the sophistication that CAD systems provide. Systems such as Applied Wave Research's Microwave Office [17] and Agilent's Advanced Design System (ADS) [18] offer electromagnetic simulation of arbitrary structures, complex network synthesis, and optimizers that provide a fully automated solution. Modern CAD systems now offer a complete simulation toolset with non-linear synthesis and layout functions.

When the design challenge is more fundamental, and when the best solution is intuitively derived, Smith Chart programs are well suited for the task. The following demonstrations were plotted with the author's preference, Smith32.

Transformation and Performance

Figure 4 illustrates a 2-section (4-element) transformation from a 3-ohm driving point impedance to a 50-ohm load, a 16.7:1 transformation ratio. Confined to a constant Q = 1.75 curve and the resistive line, the Gamma from the 800 - 1000 MHz trajectory (in red) is quantified with a SWR circle of 1.4 (center green circle).

To predict the performance response from the trajectory, the transformation is reversed. Transforming from the 50-ohm system impedance the load trajectory is illustrated relative to a laterally diffused metal oxide semiconductor device (LDMOS) load pull performance contours in Figure 5.

The trajectory intersects several contours in gain and linearity; however, the contours represent performance for single frequency operation (2-tone 880 MHz). These contours will follow a trajectory of their own relative to the parasitic capacitance of an LDMOS device. Moreover and important to note, the trajectory of these contours will track opposite (counterclockwise) to the driving point load trajectory thus further degrading broadband performance.

Figure 6 illustrates a model of a LDMOS power amplifier with plotted complex conjugate load impedance points at 800 MHz, 900 MHz, and 1000 MHz. For this model, load pull contours would track counterclockwise as with the indicated conjugate trajectory points [4]. An ideal counterclockwise load trajectory would be a challenge to any broadband designer; the popular compromise is a compressed and or folded trajectory design.

The optimal output load impedance of RF transistors as generally published in manufacture data sheets includes all capacitive and package lead parasitics. In the absence of this

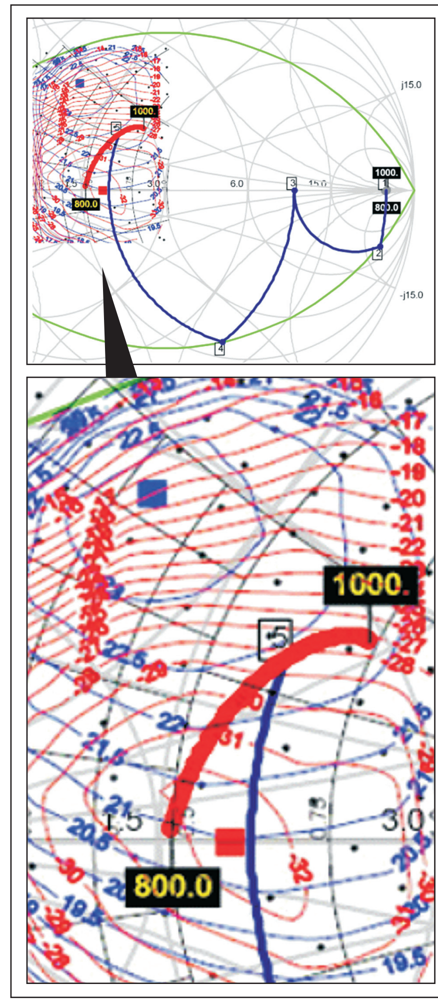

Figure 5 · Trajectory relative to 60W$_{PEP}$ LDMOS Load Pull contours (19): Z_o = 3, 28V$_{DC}$, 900 MHz; Max Gain = 23.6 dB @ Z = 1.0 + j1.3; Min IMD3 = -32.7 dBc @ Z = 1.0 + j0.0; Max Eff = 66.75% @ Z = 0.9 + j1.8.

data or when the data sheet is not applicable to the design an approximation can be derived [20].

The purely resistive component of the optimal load (RL) can be approximated from the operational RF output power and supply voltage from the equation

$$R_L = \frac{V^2}{2P_{out}}$$

With the transistor biased off the output parasitic capacitance can then be measured directly with a capaci-

DC to 8 GHz

MMIC Amplifiers

SOT-89
Actual Size

from 99¢ ea. (qty. 25)

These Tiny SOT-89 cascadable 50 ohm wideband gain blocks cover from below 10 KHz up to 8 GHz in a single model. Built to outlast the equipment it will be used in, these transient protected units are ruggedly constructed and will meet level 1 moisture sensitivity testing.
Check out our web site, over 24 models available with performance data, curves, environmental specs and easy downloading of S parameters from the web to your simulation software. Models are available to provide the performance you need from high gain, low noise, high IP3 or low DC current. Don't wait; choose the MMIC model that meets your performance/price requirements, ***Available from Stock***.

Mini-Circuits…we're redefining what VALUE is all about!

- Power output to 21 dBm
- High IP3 up to 38 dBm
- Transient and ESD protected
- Fixed voltage, GVA 84+
- Gain from 12-26 dB
- Noise figure from 2.7 dB
- InGaP HBT
- 2 year guarantee

AMPLIFIER DESIGNER'S KITS

K3-Gali_GVA+: Only $99.95
Contains 10 Ea. of Gali 24+, 74+, 84+, GVA 84+ (40 pieces total)

K4-Gali+: Only $99.95
Contains 10 Ea. of Gali 1+, 2+, 3+, 4+, 5+, 6+, 21+, 33+, 51+ (90 pieces total)

K5-Gali+: Only $64.95
Contains 10 Ea. of Gali 4F+, 5F+, 6F+, 51F+, 55+ (50 pieces total)

Evaluation Boards Available, $59.95 ea.

All models protected under U.S. patent # 6,943,629.

RoHS compliant.

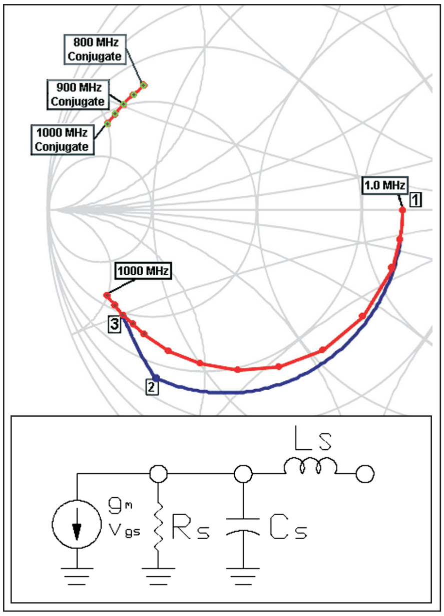

Figure 6 · A simple LDMOS model with indicated complex conjugate loads: Z_0 = 5, RL = R_S = 13, C_S = 47.5 pF, L_S = 250 pH.

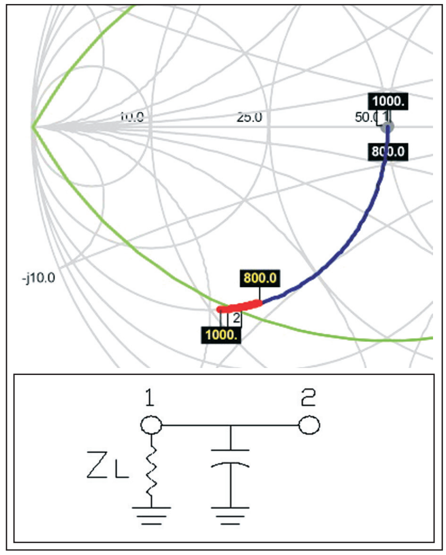

Figure 7 · Z_0 = 50, Q = 1.75; N1-2 Shunt C = 6 pF.

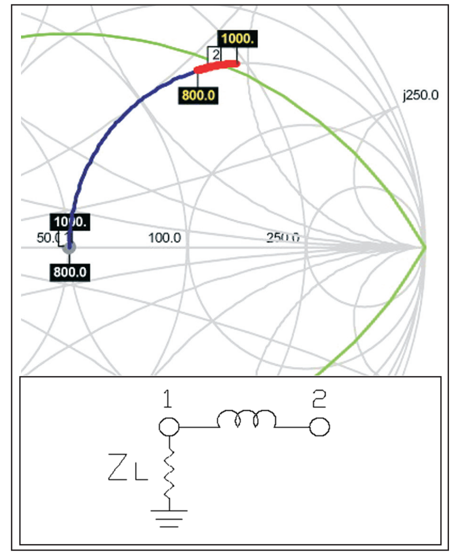

Figure 8 · Z_0 = 50, Q = 1.75; N1-2 Series L = 15nH.

tance meter. The output inductance can be derived from package and wire-bond mechanical dimensions.

In this packaged 28V, 30W, LDMOS model

$$R_{S\ Model} = R_L = 28^2/2(30) = 13\Omega$$

For 900 MHz the capacitive parasitic (C_S) and lead inductance (L_S) transform $R_{S\ \mathrm{Model}}$ to $Z_{S\ \mathrm{Model}} = 1 - 2j$

Other transistor technologies such as gallium arsenide (GaAs) and gallium nitride (GaN) have greatly reduced capacitance for broadband performance. For example RFMD's GaN1C process having higher current density is only 0.05 - 0.1 pF/W where LDMOS has roughly 0.75 pF/W of output capacitance. The bandwidth achievable is highest for the GaN followed by GaAs, and LDMOS. The tradeoff of the lower capacitance technologies is monetary with LDMOS having the best economical value.

Transformation with the Low-Pass L-Network

For standardization and uniformity, the following transformations are confined to a <25% factional bandwidth (800 MHz to 1000 MHz) with 900 MHz set as the reference.

In Figure 7 shunt capacitance rotates the trajectory clockwise from Z_L = 50 with increasing frequency or with capacitance value following the admittance equation

$$jB_C = j\omega C = \frac{1}{jX_C}$$

Note the trajectory from 800 MHz to 1000 MHz (in red) is co-angular with the shunt capacitive reactance (in blue) following the constant conductance circle.

In Figure 8, series inductance rotates the trajectory clockwise along a constant resistance circle with increasing frequency or with an increase of inductance following the reactance equation

In summary, shunt C and series L disperse a trajectory with increasing frequency. In other words when using these matching elements in a low-pass network, the higher frequencies will rotate and transform more than the lower frequencies, which spreads the trajectory relative to frequency in a clockwise direction.

In Figure 9 a two-element low-pass network is charted on a Z_0 = 25 normalized Smith Chart. The normalized impedance of 25 ohms is calculated from the geometric mean of the system load and source impedance, 50 to 12.5 ohms respectively [5].

$$Z_{Geo} = \sqrt{Z_L * Z_S}$$

The constant Q curve of 1.75 is derived from the resistive ratio of 50/12.5 from the equation

$$1 + Q^2 = R_{ratio}$$

Note that the impedance trajectory is no longer co-angular to the constant resistance arc of the series inductance reactance (nodes 2-3).

High-Pass Lumped Elements and the High-Pass L-Network

Shunt inductive reactance as demonstrated in Figure 10 rotates clockwise along a constant conductance circle with increasing frequency following the susceptance equation

$$jB_L = \frac{1}{jX_L} = \frac{1}{j\omega L}$$

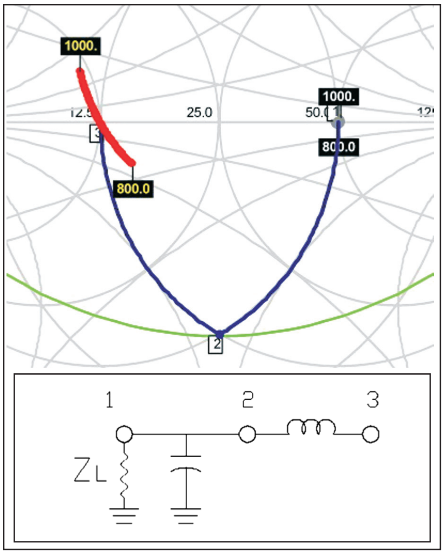

Figure 9 · Z_0 = 25, Q = 1.75; N1-2 Shunt C = 6.1 pF; N2-3 Series L = 3.8 nH.

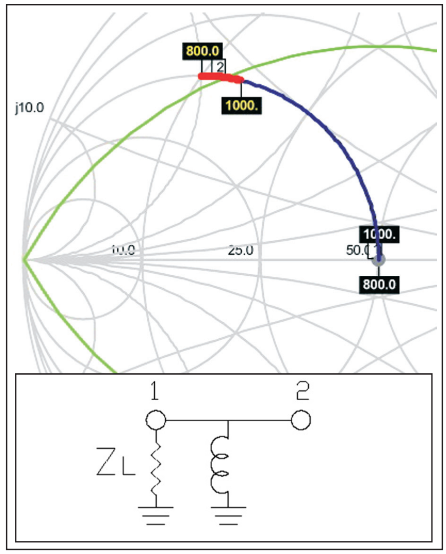

Figure 10 · Z_0 = 50, Q = 1.75; N1-2 Shunt L = 5 nH.

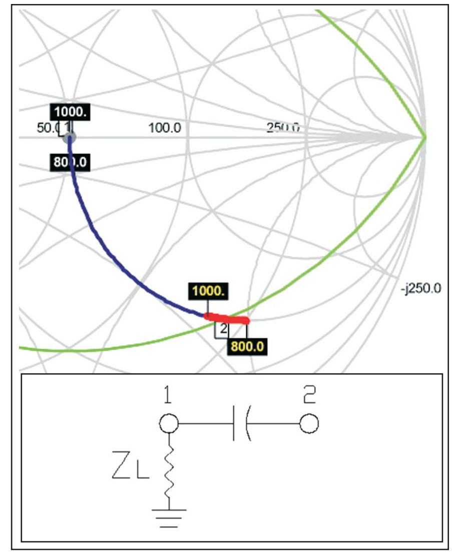

Figure 11 · Z_0 = 50, Q =1.75; N1-2 Series C = 2 pF.

This element is different than the two matching elements discussed previously such that shunt inductance susceptance decreases with increasing frequency.

Series capacitance is similar; however, its reactance is plotted on a constant resistance circle in Figure 11 following the reactance equation

$$jX_C = \frac{1}{j\omega C}$$

Series capacitive reactance rotates clockwise with increasing frequency and decreases with increasing frequency.

Shunt L and series C disperse an impedance trajectory in a clockwise direction with frequency, but the reactance will be decreasing with frequency. Hence, high-pass matching networks consisting of shunt inductors and series capacitors will transform the lower frequencies more than the higher frequencies.

In Figure 12, a two-element high-pass L-network transformation from 50 to 12.5 ohms is demonstrated on a 25-ohm normalized Smith Chart. Note that the trajectory is no longer co-angular to the constant resistance circle of (nodes 2-3) and that unlike a low-pass L-network, the higher frequencies are transformed less than the lower frequencies. If the low-pass trajectory of Figure 9 were overlaid onto Figure 12, the two trajectories would form the letter X. Exploiting this relationship by combining these dispersion effects can leverage a broadband transformation.

Compressing Trajectory Dispersion

A broadband band-pass network is illustrated in Figure 13, a 50 to 3 ohm transformation similar to the one in Figure 4. With the Smith Chart normalized to the geometric mean, it is easy to see that low pass nodes 1-2-3 are symmetrical in Q to the high pass nodes 3-4-5. Combining these two networks' halves folds and compresses the trajectory into a condensed 3-ohm driving point load.

Compare this transformation, which has a mismatch SWR of 1.08, to that of Figure 4 where the mismatch SWR is 1.4.

A Chebyshev broadbanding technique is illustrated in Figure 14. As discussed earlier, when using low-pass networks the higher frequencies transform and rotate more. Here the frequencies higher than 800 MHz are

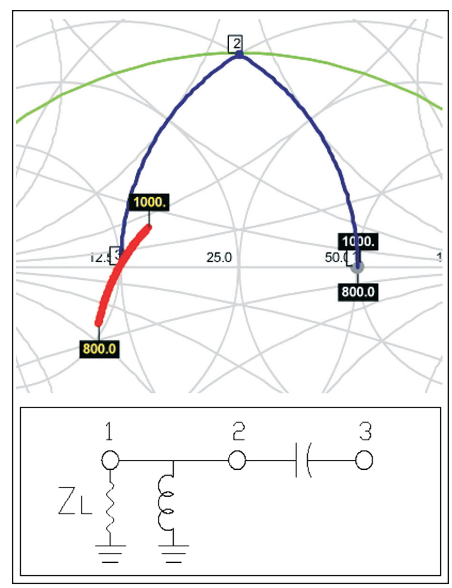

Figure 12 · Z_0 = 25 Ω, Q = 1.75; N1-2 Shunt L = 5.1 nH; N2-3 Series C = 8.2 pF.

over-rotated well beyond the resistive line at node 3, which compresses the upper frequency dispersion. Again, compare this network of Figure 14 to that of Figure 4; a 3-ohm SWR bandwidth of 1.12 versus 1.4.

The transformation is mostly symmetrical with two Q curves, an outer curve (Q_1 green) and an inner curve (Q_3 magenta). However, node 5

VCOs

10 to 6740 MHz from $11^{95} ea. (qty. 5)

Want a miniature surface mount, shielded plug-in, or rugged connectorized voltage controlled oscillator with the right stuff for your project ? Contact Mini-Circuits! From custom designs to standard catalog models ***always in stock***, we'll supply extra robust, 100% tested VCO solutions you need at a price you can afford. Choose from narrow, to broad, to octave bandwidths. Select from models with low phase noise, linear tuning, load insensitivity, dual output, wide modulation bandwidths, or 5V models optimized for PLL ICs and synthesizers. And pick from an innovative array of miniature surface mount packages as small as 0.25" square, all featuring our exclusive glue-down process on each circuit component to give you ultimate reliability during reflow soldering. You can quickly find the model you need using our online catalog or "The YONI2 Search Engine" at the Mini-Circuits web site. Just enter your specs into YONI2…click…and immediately start evaluating suggested VCO solutions using the actual measured performance data displayed. But perhaps you need a custom design. Not a problem! Contact us for our fast response, low prices, and quick turnaround. For your commercial, industrial, and military applications, choose Mini-Circuits VCOs!

Pb RoHS COMPLIANT ™

RoHS models available, consult factory.

Mini-Circuits ...we're redefining what VALUE is all about!

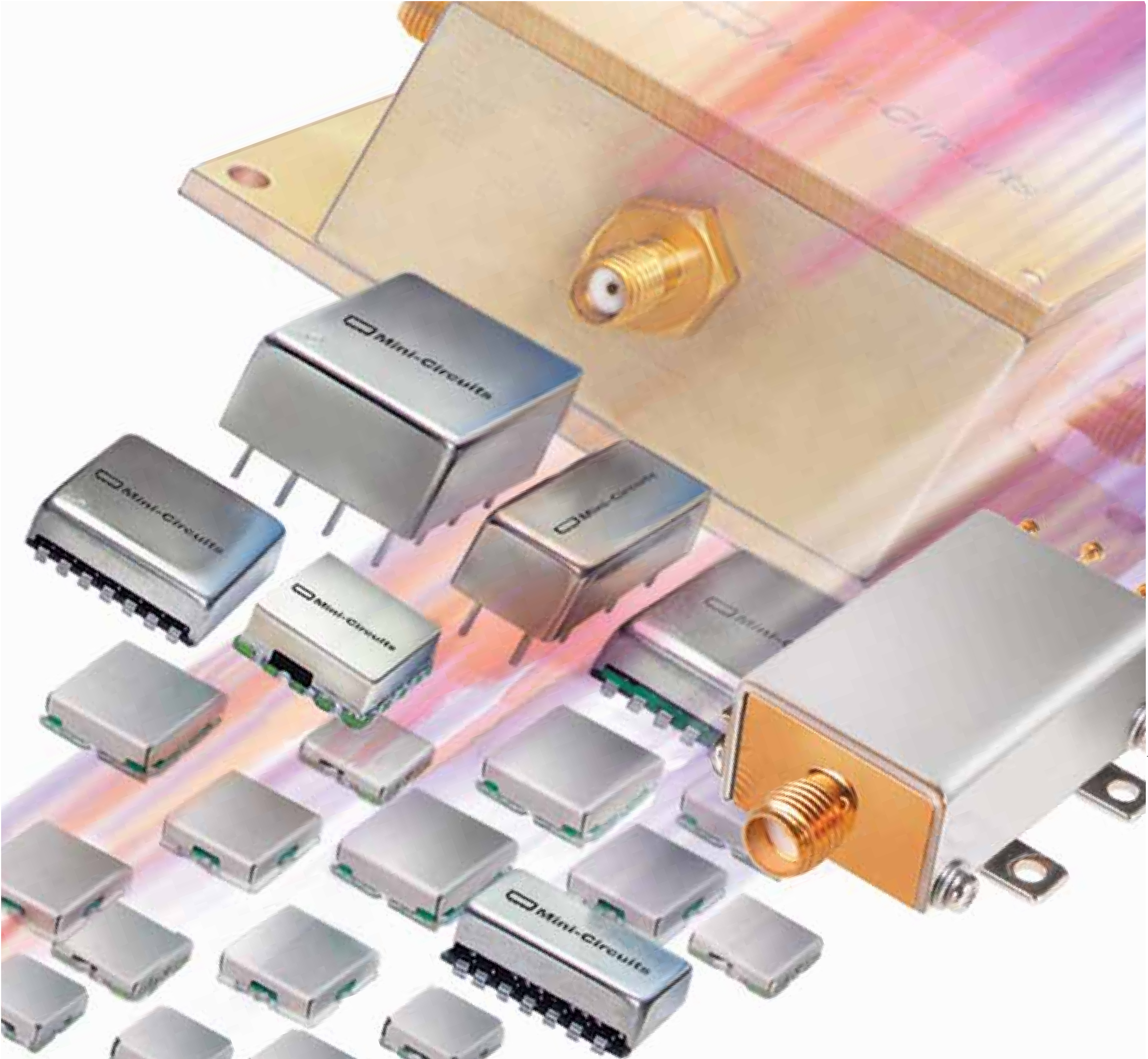

Agilent Technologies

For high reliability, all Mini-Circuits VCOs are tested with the Agilent E5052B Signal Source Analyzer.
www.agilent.com/find/ssa

Detailed Performance Data & Specs For Mini-Circuits VCOs Available Online at: ***www.minicircuits.com/oscillat.html***

Get info at www.HFeLink.com

Mini-Circuits®
ISO 9001 ISO 14001 CERTIFIED

ALL NEW minicircuits.com

P.O. Box 350166, Brooklyn, New York 11235-0003 (718) 934-4500 Fax (718) 332-4661 For detailed performance specs & shopping online see Mini-Circuits web site

YONI2™ Patent Pending *The Design Engineers Search Engine Provides ACTUAL Data Instantly From MINI-CIRCUITS At:* ***www.minicircuits.com***

IF/RF MICROWAVE COMPONENTS

402 Rev H-WDD

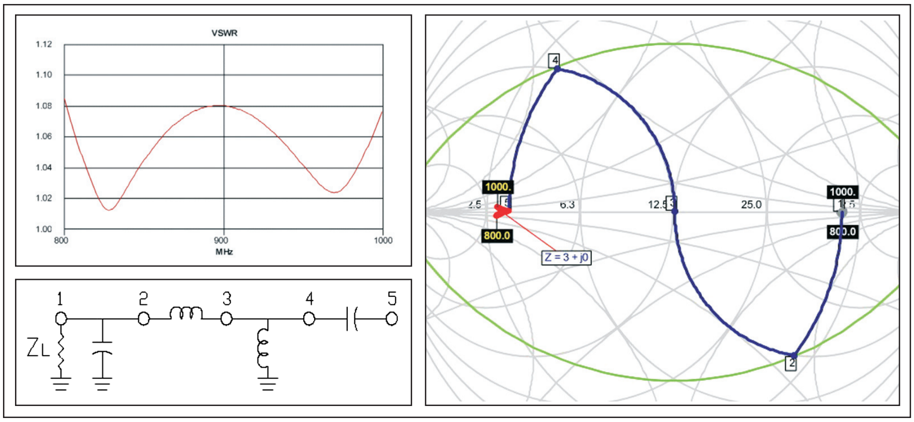

Figure 13 · 50 to 3-ohm transformation; Z_0 = 12.5, Q = 1.75; N1-2 Shunt C = 6.10 pF; N2-3 Series L = 3.85 nH; N3-4 Shunt L = 1.32 nH; N4-5 Series C = 32.3 pF.

Q_1	Q_2	Q_3	Trans Ratio
0.72	0.71	0.61	1.67
0.82	0.80	0.62	2.0
1.27	1.22	0.58	5.0
1.63	1.51	0.50	10.0
1.96	**1.71**	**0.45**	**16.67**
2.19	1.91	0.42	25.0
2.39	2.01	0.38	33.3
2.72	2.15	0.35	50
3.30	2.53	0.29	100

Table 1 · Q curves per transformation ratio (2-section network). The Q curves are numbered from the outer most Q_1 towards the inner Q_3.

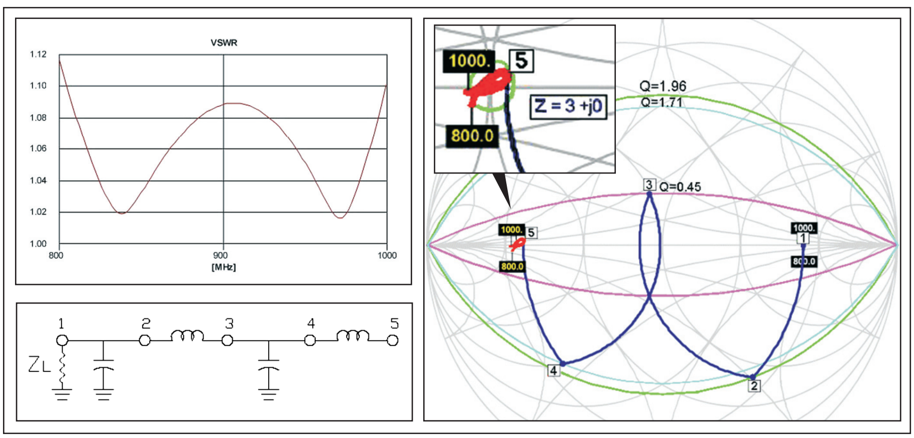

Figure 14 · Z_0 = 12.3, SWR = 1.12 @ Z_S = 3; N1-2 Shunt C = 6.9 pF; N2-3 Series L = 4.4 nH; N3-4 Shunt C = 30.4 pF; N4-5 Series L = 0.99 nH.

Q_1	Q_2	Q_3	Trans Ratio
0.92	0.60	0.65	1.67
1.37	0.90	0.61	5.00
1.53	1.00	0.60	7.14
1.68	1.08	0.58	10.00
1.89	**1.21**	**0.53**	**16.67**
2.06	1.32	0.50	25.00
2.20	1.41	0.49	33.33
2.41	1.52	0.45	50.00
2.57	1.61	0.44	66.67
2.80	1.74	0.41	100.00

Table 2 · Q curves per resistive transformation ratio (3-section network). The Q curves are numbered from the outer most Q_1 towards the inner Q_3.

falls at a higher impedance than the 3-ohm target to center the fish shaped trajectory at $Z = 3 + j0$ and so therefore a third Q curve (Q_2, cyan) is defined at node 4.

With the complexity of the multiple Q curve network, deriving a design from a Smith Chart alone would not be an intuitive process. The Q curves are in overlapping fractions of the resistive transformation and do not hold the relationship with the transformation ratio as before with single Q networks. This network and Tables 1 and 2 were derived by optimization with an ADS simulator utilizing a gradient optimizer.

Note that the inner Q curve (Q_3) as a function of the transformation ratio holds an inverse relationship to that of the other Q curves.

In Figure 15, a three-section transformation, the trajectory fits into a 3-ohm 1.01 SWR circle. Three Q curves are adquate for defining the three section network since the trajectory is small and circular in shape, unlike in Figure 14; here no impedance offset is needed at node 7.

As mentioned above, Table 2 was derived from optimization. Here Q curves are provided for resistive transformation ratios of 1.67:1 (50 ohms to 30 ohms) to 100:1 (50 ohms to 0.5 ohms).

Complex Transformations

All transformations discussed previously have been purely resistive to resistive (50-ohm to 3-ohm) transformations. Figure 16 demonstrates an immediate approach to a high Q transformation from a purely resistive impedance of Z_0 = 50, to a load impedance with where $Z_L = 20 + j50$.

A broadband match in this case is seemingly impossible to design, especially when considering the source impedance dispersion from the large corresponding parasitics. However, the transformation can be forbearing; Figure 17 includes an additional

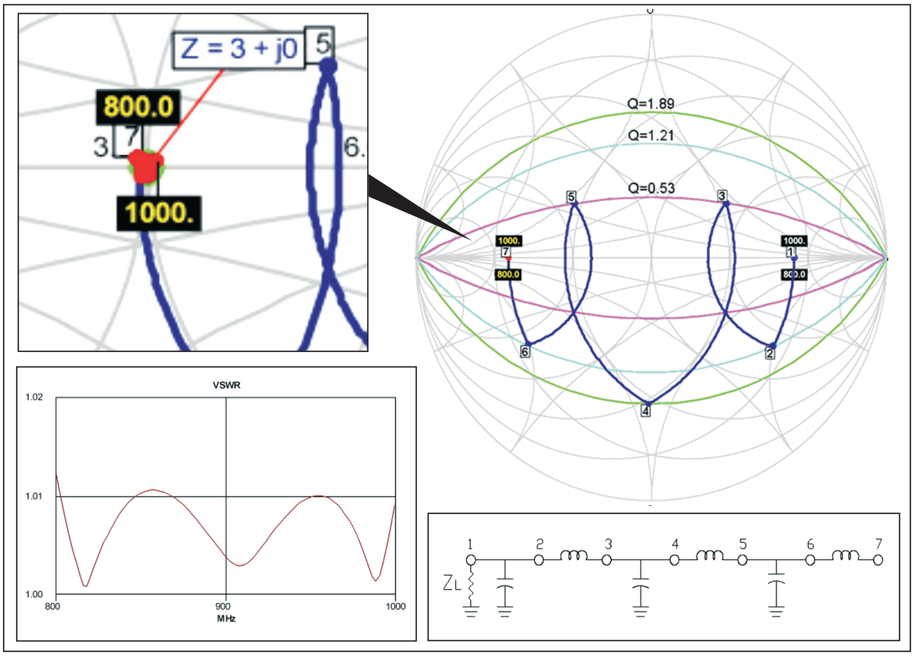

Figure 15 · Z_0 = 12.2, SWR = 1.01 @ Z_S = 3; N1-2 Shunt C = 4.30 pF, N2-3 Series L = 6.22 nH; N3-4 Shunt C = 16.57 pF, N4-5 Series L = 2.42 nH; N5-6 Shunt C = 42.05 pF, N6-7 Series L =0.63 nH.

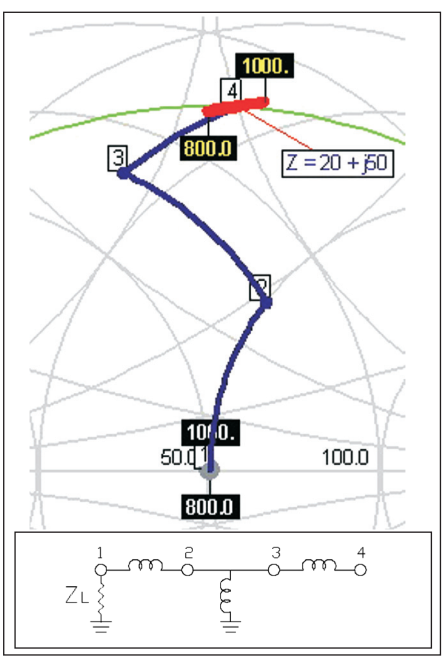

Figure 16 · Z_0 = 50 Ω, Q = 2.5.

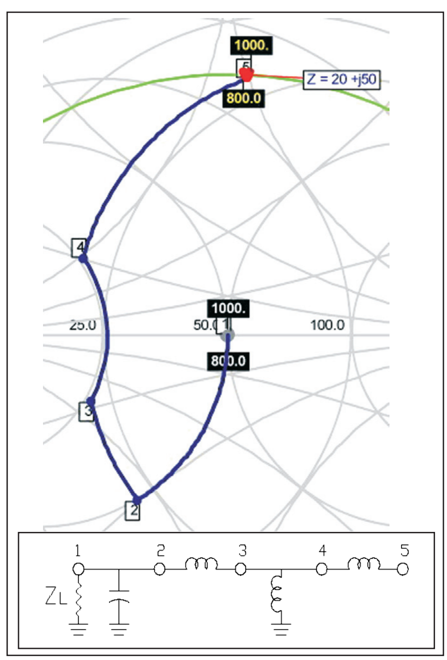

Figure 17 · Z_0 = 50 Ω, Q = 2.5; N1-2 Shunt C = 4.0 pF, N2-3 Series L = 2.8 nH; N3-4 Shunt L = 5.0 nH, N4-5 Series L = 7.0 nH.

shunt capacitor that is proportioned for the complex target impedance. This additional element re-orders the dispersion effects of the transforming network; hence improving broadband performance. It is another example of how the dispersion effects from lumped elements can be leveraged to compress and fold the trajectory.

Conclusion

Multiple frequency point load pull contours demonstrate the necessity for a compressed and/or folded impedance trajectory for optimized broadband power amplifier design. Single *Q* matching where the resistive line and *Q* curve serve as guideline boundaries are too often presented as the mainstream broadband design technique. Here we have shown that multiple *Q* curve transformations although more complex in their derivation have superior bandwidth over the single *Q* matching technique although the single *Q* matching technique is easily demonstrated we recommend that designers consider a multiple *Q* transformation. Furthermore, where device and package parasitics disperse the source impedance counter to a broad band transformation, the use of multiple *Q* curve transformations is perhaps a categorical.

Acknowledgements

The author is indebted to many friends who reviewed this document for accuracy.

Special thanks to John B Call for many broadband network discussions. Special thanks to Kal Shallal for the LDMOS load pull contours, and for the device modeling discussion.

References:

1. "Philip H. Smith: *A Brief Biography*" by Randy Rhea, Noble Publishing 1995.
2. Smith® Chart is a registered trademark and is the property of Analog Instrument Company, New Providence, NJ.
3. Michael Hiebel, Fundamentals of Vector Network Analysis, Rohde & Schwarz 2007, pg. 14.
4. Chris Bowick, *RF Circuit Design,* Newnes imprint of Butterworth-Heinemann, 1982, Ch. 4 - 5.
5. Herbert L. Krauss, Charles W. Bostian, Fredrick H. Raab, *Solid State Radio Engineering,* Zhuyi

Publishing of Taiwan 1980.

6. Donslf W. Dearholt, William R. McSpadden, *Electromagnetic Wave Propagation,* McGraw-Hill Inc. 1973 , Ch. 5.4 - 5.5.

7. Joseph F. White, *High Frequency Techniques / An Introduction to RF and Microwave Engineering,* John Wiley & Sons 2004.

8. Randy Rhea, "Yin-Yang of Matching: Part 2- Practical Matching Techniques," *High Frequency Electronics,* April 2006.

9. *The RF Capacitor Handbook,* American Technical Ceramics Corp. 1994.

10. *1989 ARRL Handbook for the Radio Amateur,* American Radio Relay League, pp 2-27 thru 2-29.

11. Thomas L. Floyd, *Electronics Fundamentals: Circuits, Devices, and Applications,* 2nd ed. McMillan Publishing Co. 1991, Chapters 14.4 - 14.7

12. J. F. White, *High Frequency Techniques / An Introduction to RF and Microwave Engineering,* John Wiley & Sons 2004, pp. 70-71.

13. Dan Moline, *Motorola Impedance Matching Program,* Motorola Inc., April 6, 1992.

14. Agilent Technologies, winSmith 2.0, Noble Publishing 1998.

15. linSmith, John Coppens, 1999-2008, www.jcoppens.com/soft/linsmith.

16. Pederson, Ib F., Smith32, Denmark 2002.

17. Applied Wave Research, Inc. Microwave Office®, El Segundo, CA.

18. Agilent Technologies, Advanced Design System.

19. Load Pull contours courtesy of Khalid Shallal, RFMD.

20. B. Becciolini, *Impedance Matching Networks Applied To R-F Power Transistors,* Motorola AN-721, Motorola Inc., 1974.

Author Information

Anthony Bichler is a design engineer with RFMD in Chandler Arizona. His 25 years of RF experience includes power amplifier design for RFID, cellular handsets, and base stations. Presently, Tony is working on quad-band transmit modules for GSM, PCS, and DCS handsets. Interested readers may contact him at tbichler@rfmd.com

An Improved Design Method For Stepped Line Microwave Filters with Broad Stop Bands

By Piotr Dyderski
Telecommunications Research Institute

The technique described here emphasizes proper setup of initial parameters before applying optimization in the well-known microwave EDA tools

The design problem for filters attenuating signals with frequencies outside the useful (pass) bands can be in many cases reduced to the problem of designing low pass or band-stop filters with sufficiently large bandwidths. It follows from the fact that some elements of complex electronic systems, as for example the radiating elements of antenna arrays, have the characteristics similar to those shown in Figure 1.

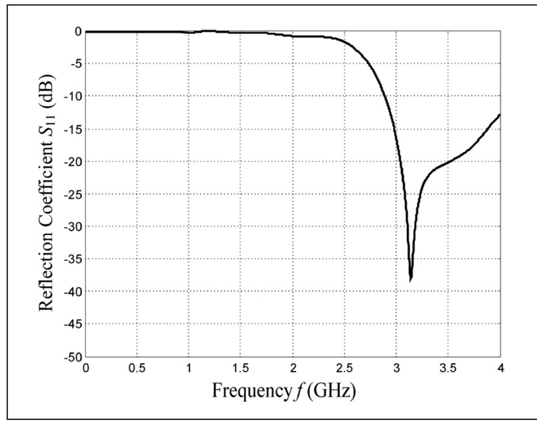

Figure 1 · Reflection coefficient S_{11} of a typical half-wave radiating element with operating frequency band centered at 3.5 GHz.

Among various possible implementations of band-stop filters, those implemented as a cascade connection of transmission line sections—the so-called stepped transmission line band-stop filters [1, 2]—are especially suitable for many applications. These filters are rather simple to manufacture, and their small cross-sections allow you to put them in place of specified sections of the transmission line. Among all analytical design methods, the most general is the one described in [1 - 4]. Its essential feature is the use of R-transformer as a prototype circuit together with the classical Darlington-Riblet method [1 - 5]. Unfortunately, the filters designed according to this last method may be difficult to manufacture in some cases because of the large spread of the characteristic impedances among the line sections. This follows from the fact that corresponding insertion loss function is formed by an appropriate choice of characteristic impedances of sections having equal electrical lengths. Consequently, for a fixed number of sections, the range of characteristic impedances increases when the requirements imposed on the relative stop band of the filter become more restrictive.

Therefore, the aim of this paper is to present the new approach that makes possible the design of band-stop filters with required insertion loss function (including filters with broad stop bands), which can be easily implemented in the prescribed technology. It can be obtained by limiting the range of characteristic impedances by application of optimization methods with constraints. Due to the fact that both characteristic impedances and electrical lengths of the sections are variables during the optimization process, this method belongs to the class of amplitude-phase methods.

The optimization process starts with an initial approximation found by means of an appropriate analytical method [1 - 4]. Naturally, the efficiency of the optimization strategy strongly depends on the quality of initial approximation. For example, analytical

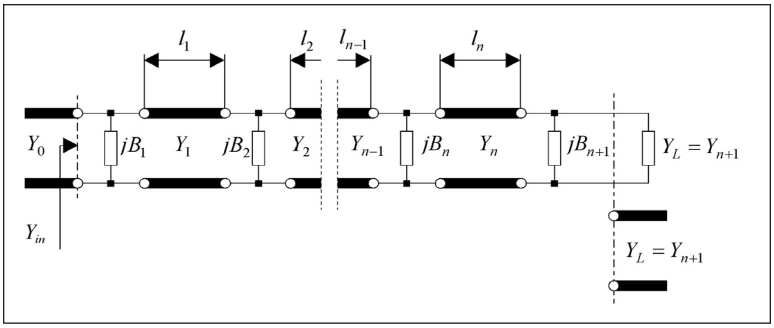

Figure 2 · Electrical scheme of the stepped transmission line band-stop filter.

formulas presented in [3] can be used to obtain filters with a maximum number of sections equal to 20, and their further enhancement would be extremely cumbersome. In the case of filters that require a large stop band, the initial approximation obtained in this way is unsuitable for the optimization process. For this reason, the original approach called "splining the insertion loss frequency response" has been proposed by the author.

In order to confirm the usefulness of the presented algorithm, three coaxial line filters have been designed, manufactured and tested. For one of the filters, the splining procedure was used for the insertion loss frequency response. Additionally, the influence of coaxial line step discontinuities has been investigated on the filter response.

Design Algorithm for Noncommensurate Band-Stop Filters

Let us consider the design of stepped transmission line band-stop filters with the electrical scheme shown in Figure 2.

The lumped-element susceptances B_i ($i = 1, 2, ..., n + 1$) of the electrical scheme (see Fig. 2) represent discontinuities appearing in places of step changes of the line geometry. These susceptances can have capacitive ($B_i > 0$) or inductive ($B_i < 0$) character, depending on the kind of discontinuity. In general, the electrical equivalent scheme of the discontinuity is more complicated and the T or π two-port representation can be used [6], [7].

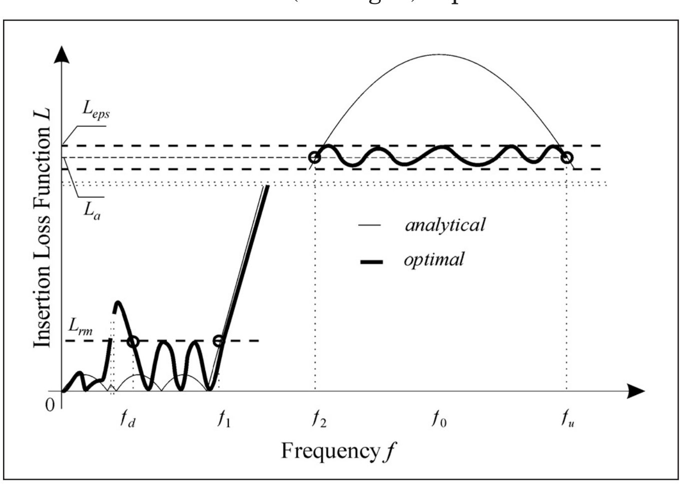

Figure 3 · Example of the insertion loss function *L* of the optimal and analytically designed filters.

It is assumed that optimal insertion loss function of the filter, similar to that shown in Figure 3, should be obtained as a result of the design process, which can be divided into two main stages. During the first stage, taking the R-transformer prototype circuit, the filter being initial approximation for the optimization process is found [1 - 3]. Depending on the assumed filter parameters (insertion loss response and range of characteristic impedances of its particular sections), this stage can be reduced to the design of a filter for which the R-transformer serves as the prototype. As an additional procedure, splining the insertion loss frequency response can be performed in this stage, as described later. The second stage of the design process is the optimization procedure for the filter structure.

Design of the Band-Stop Filters Based on the *R*-transformer Prototype Circuit

Let us assume that the output parameters defining insertion loss function in the prescribed frequency range are given (see Fig. 3), as well as the required characteristic impedance range of particular filter sections, determined by $Z_{\min}$ and $Z_{\max}$. According to the relations given in [1 - 3], a minimum number of filter sections $n_{\min}$ can be found, for which the requirements imposed on the insertion loss response are satisfied. Next, for a given number of filter sections $n \geq n_{\min}$, characteristic impedances of particular sections should be found [1 - 3]. It should be pointed out here that it is possible to design the filter satisfying all imposed requirements and containing smaller or greater number of sections $n \geq n_{\min}$. Reduction of the number of sections leads to the larger spread of characteristic impedances. Initial approximation for the optimization process should be taken in the form of a filter with such number of sections n, that the range of characteristic impedances found analytically $\langle Z_{\min A}; Z_{\max A}\rangle$ is related to the required impedance range $\langle Z_{\min}; Z_{\max}\rangle$ by the following inequalities

$$\begin{cases} Z_{\min A} \geq Z_{\min} - 20, \ (\Omega) \\ Z_{\max A} \leq Z_{\max} + 35, \ (\Omega) \end{cases} \tag{1}$$

where the numbers 20 and 35 appearing in formula (1) determine the tolerance margin assumed by the author of this paper. In case, when these conditions cannot be satisfied, and when the initial approximation found analyti-

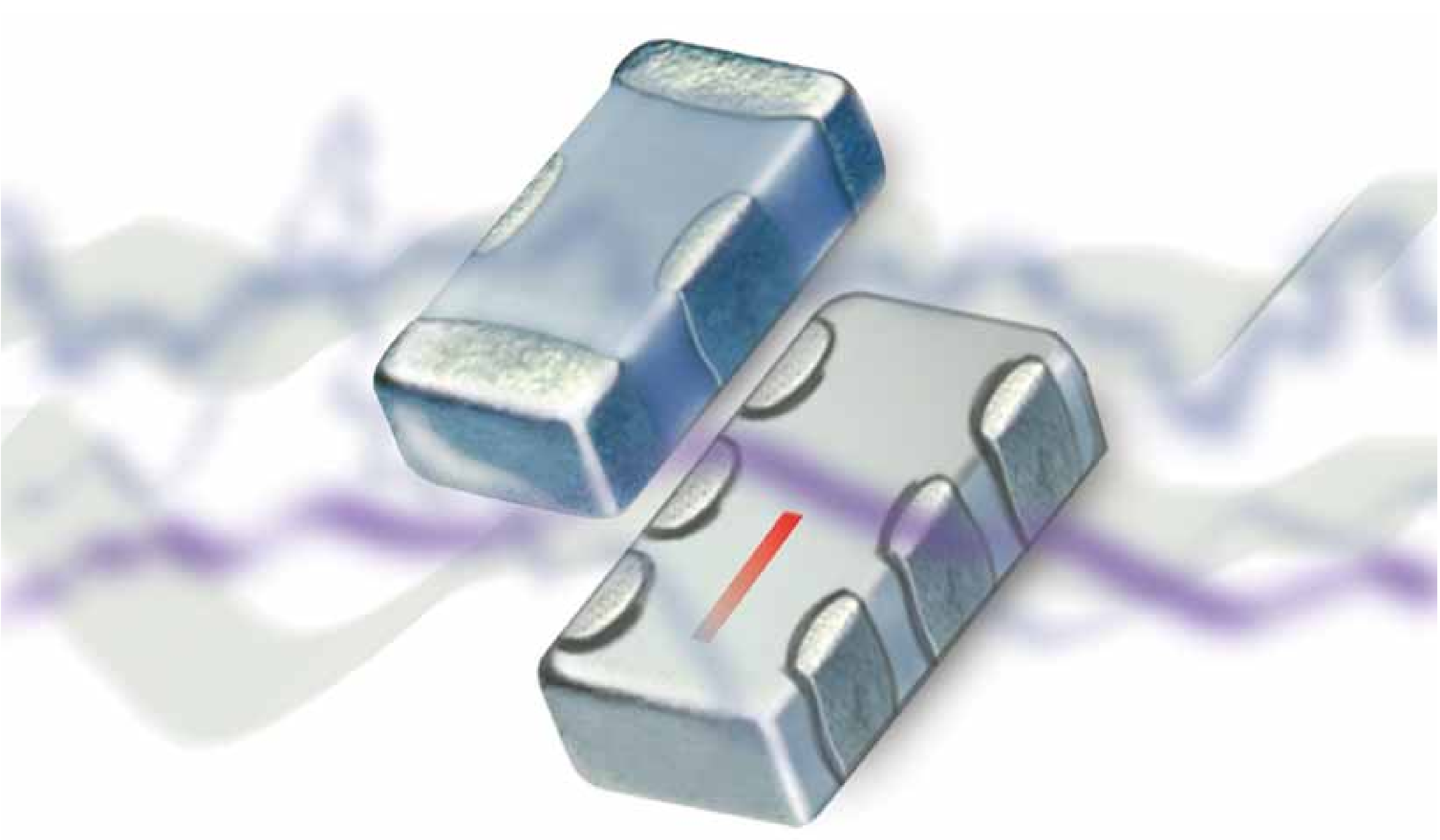

cally lies too far from the optimum, this approximation can be found using the procedure of splining the insertion loss frequency response, which is described in later.

Optimization Procedure for the Filter Structure

Let us assume that characteristic impedances and electrical lengths of particular filter sections have been found during the initial approximation stage of the design process. Input admittance $Y_{in} = G_{in} + jB_{in}$ of the filter shown in Figure 2 can be determined by multiple use of the standard impedance transformation equation, namely (see Fig. 4a)

$$Y_{in} = Y_k \frac{Y_L + jY_k tg(\beta_f l)}{Y_k + jY_L tg(\beta_f l)} \tag{2}$$

where $Y_{in} = G_{in} + jB_{in}$, $Y_L = G_L + jB_L$, $\beta_f = 2\pi/\lambda_f$, and λ_f is the line wavelength. For lossless TEM line section with dielectrical constant ε_r we have

$$\beta_f = \frac{2\pi}{\lambda_f} = \frac{2\pi f}{c\sqrt{\varepsilon_r}}.$$

Equation (2) written for the circuit of Figure 4b takes the following form

$$Y_{in} = Y_k \frac{Y_L + j\left[B + Y_k tg(\beta_f l)\right]}{Y_k - Btg(\beta_f l) + jY_L tg(\beta_f l)} \tag{3}$$

This complex equation can be easily separated into the real and imaginary parts, allowing all calculations to be made using operations on real numbers only. The input reflection coefficient Γ is related to the input admittance through the following simple formulas (see Fig. 2):

$$\Gamma(f) = \frac{Y_0 - Y_{in}(f)}{Y_0 + Y_{in}(f)} = \frac{\left[Y_0 - G_{in}(f)\right] - jB_{in}(f)}{\left[Y_0 + G_{in}(f)\right] + jB_{in}(f)}$$
$$|\Gamma(f)|^2 = \frac{\left[Y_0 - G_{in}(f)\right]^2 + B_{in}^{\ 2}(f)}{\left[Y_0 + G_{in}(f)\right]^2 + B_{in}^{\ 2}(f)} \tag{4}$$

The insertion loss function $L(f)$ of the filter is related to the reflection coefficient $\Gamma(f)$ as follows

$$L(f) = \frac{1}{|S_{21}(f)|} = \frac{1}{1 - |\Gamma(f)|^2} \tag{5}$$

where $S_{21}(f)$ is the coefficient of scattering matrix **S**.

In order to perform the optimization process (obtaining optimal insertion loss response, see Fig. 3) the following objective function should be applied

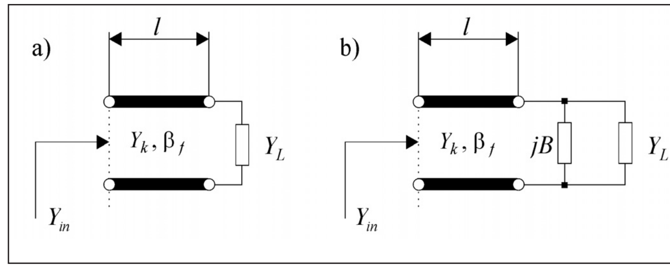

Figure 4 · Illustration of the impedance (admittance) transformation equation with (a) and without (b) the influence of discontinuities.

$$OF(f_i;\mathbf{p}) = \begin{cases} W(f_i)\cdot L(f_i;\mathbf{p}) & f_i \in \langle f_d; f_1\rangle \\ W(f_i)\cdot |L(f_i;\mathbf{p}) - L_a| & f_i \in \langle f_2; f_u\rangle \end{cases} \tag{6}$$

where $W(f_i)$ is the weighting function

$$W(f_i) = \begin{cases} \dfrac{L_{eps} - L_a}{L_{rm}} & f_i \in \langle f_d; f_1\rangle \\ 1 & f_i \in \langle f_2; f_u\rangle \end{cases} \tag{7}$$

Parameter L_a is the nominal value of insertion loss in the stop band, $(L_{eps} - L_a)$ is the maximum loss deviation in the stop band, and L_{rm} is maximum reflection loss in the pass band (see Fig. 3). In the general case of amplitude-phase synthesis, the vector of parameters "**p**" (variables during the optimization process) is composed of $\mathbf{p} \equiv [Z_1,\dots,Z_n,l_1,\dots,l_n]$. The set of admissible solutions Φ determines the values of characteristic impedances and geometrical lengths of the sections

$$\begin{aligned} &Z_{\min} \le Z_i \le Z_{\max} \\ &l_i \ge l_{\min} \quad i \in [1:n] \end{aligned} \tag{8}$$

and the requirements imposed on the range of characteristic impedances of particular sections are tightly involved with the line geometry.

The objective function $OF_p(f_i;\mathbf{p})$ satisfying the above requirements takes the form

$$OF_p(f_i;\mathbf{p}) = OF(f_i;\mathbf{p}) + P(\mathbf{p};t_1,t_2) \tag{9}$$

where $P(\mathbf{p}; t_1, t_2)$ is the penalty component defined as follows

$$P(\mathbf{p};t_1,t_2) = \exp\left[\sum_{j=1}^{n} t_1\left(Z_{\min} - Z_j\right)\right] +$$

$$+\exp\left[\sum_{j=1}^{n} t_1\left(Z_j - Z_{\max}\right)\right] + \exp\left[\sum_{j=1}^{n} t_2\left(l_{\min} - l_j\right)\right] \quad (10)$$

Positive weighting coefficients t_1, t_2 are gradually incremented during consecutive iterations. Finally, the optimization problem can be written as

$$\min_{\mathbf{p}\in\Phi} \max_{i\in[1:N]} OF_p\left(f_1;\mathbf{p}\right) \quad (11)$$

Problem (11) can be solved by means of the ε-steepest descent methods [8, 9]. The essence of these methods and their application to the stepped transmission line band-stop filter design was discussed extensively in [3, 10].

Application of the Optimization Procedure to the Band-Stop Filters Implemented with Coaxial Line

Let us consider the band-stop filter design using the coaxial line technology. (Experimental examples of these filters will be described in the next section.) Cross- and longitudinal-sections of the step change of coaxial line inner conductor diameter [11] are shown in Figures 5a and 5b, respectively. The equivalent circuit at reference plane T is shown in Figure 5c.

The following equality holds for the plane T of the step change of the line transversal dimensions [11]

$$\frac{Y_0'}{Y_0} = \frac{\ln\left(\frac{c}{a}\right)}{\ln\left(\frac{c}{b}\right)} \quad (12)$$

The normalized susceptance B/Y_0 can be calculated from the formulas given in [11]. For this purpose it is necessary to solve the following nonlinear equation

$$J_0(\chi)N_0\left(\frac{\chi c}{a}\right) - N_0(\chi)J_0\left(\frac{\chi c}{a}\right) = 0 \quad (13)$$

The first, nonvanishing root of this equation can be evaluated from the approximate relation [12, 13]

$$\chi_{01} \cong \sqrt{\frac{\pi^2}{(g-1)^2} - \frac{1}{(g+1)^2}} \quad (14)$$

where $g = c/a$ and $Z_m(g\chi) = J_m(g\chi)N_m(\chi) - N_m(g\chi)J_m(\chi)$ is the combination of Bessel-Neumann function of the order m.

The step changes of the coaxial line inner conductor diameter presented in Figure 6 are approximately equivalent. Equivalent circuit for the step change of outer conductor dimensions of the coaxial line is given in [11].

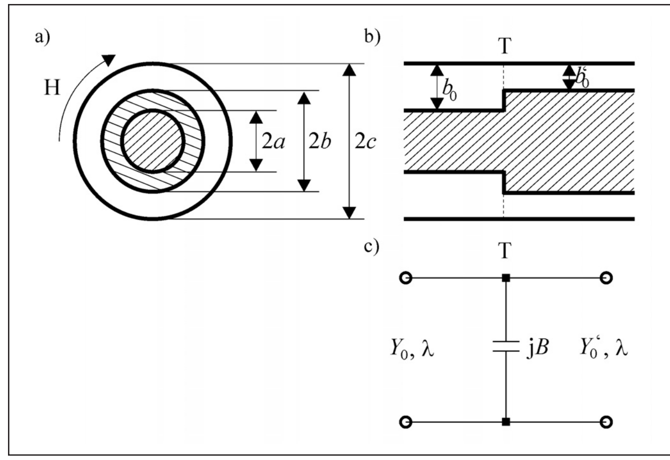

Figure 5 · Cross-section (a), longitudinal section (b) and equivalent circuit (c) of the step change of outer conductor diameter of the coaxial line.

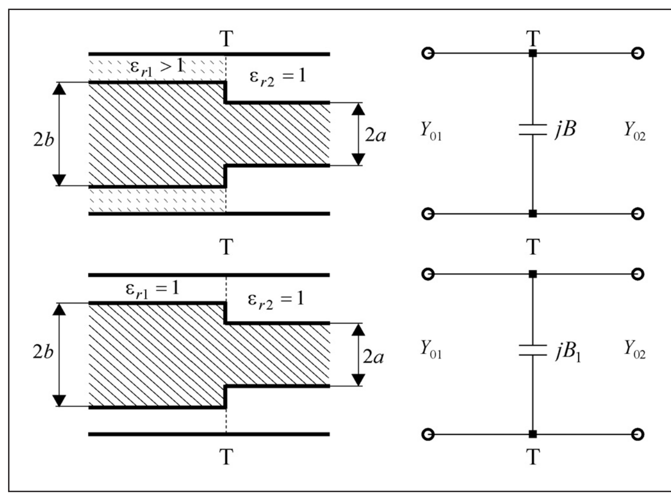

Figure 6 · Equivalent circuits for step dimension changes of coaxial line inner conductor ($B \cong B_1$).

Equivalent circuits of geometry changes for different kinds of lines can be found in many publications, as for example in [7].

It is recommended to perform the filter design first without taking into account the effect of discontinuities. Next for a chosen structure (layout of the dielectric supports) this process should be continued up to the end, using the method in which presence of discontinuities is assumed.

Procedure of Splining the Insertion Loss Frequency Response

Standard microwave band-stop filters incorporating commensurate sections of transmission lines have as a rule the periodically repeated stop bands, situated around the odd harmonics of frequency f_0, which is the center frequency of the first stop band. (This is strictly true for the TEM line. In case of the dispertion lines it refers to the wavelength λ, see for example [14].) It means that pass bands separate consecutive stop bands of the filter (see Fig. 7). (Similar situation of the pass bands repetition occurs in case of the band-pass filters [14].) The procedure of splining the insertion loss frequency response uses the property that in the pass band, where the reflection loss is small, input impedance of the filter is approximately equal to the terminal impedance $Z_{in} \approx Z_L$ ($Y_{in} \approx Y_L$), see Figure 2. It is then possible to connect together the filters having appropriate frequency shift of insertion loss functions, without introducing significant deformation of their characteristics [15]. The initial approximation obtained by use of the spline procedure has the characteristic impedance distribution, which is closer to the optimum and provides excess reduction of the insertion loss in the middle of the stop band (see Fig. 3).

Figure 7 illustrates periodicity of the insertion loss function of an analytically designed band-stop filter with commensurate sections having $\lambda_0/4$ length at the stop band center frequency f_0. The second filter of the cascade structure should be designed to have the central part of its stop band at $2f_0$, that is its stop band should be situated between the first and the second stop band of the first filter. Due to the finite slope of insertion loss responses, the stop band width of the second cascaded filter should be reduced in order to minimize the overlapping effect. It can be assumed that the insertion loss responses of cascaded filters should "intersect" in the middle of the nominal value of the loss assumed in the stop band (in dB scale), see Figure 8. Analogical procedures can be applied in case of greater number of cascaded filters (see Fig. 9).

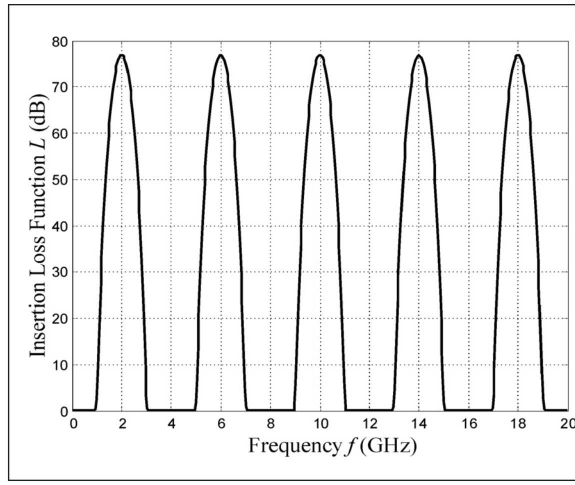

Figure 7 · Illustration of periodical repetition of stop bands for analytically designed stepped transmission line band-stop filter with commensurate sections.

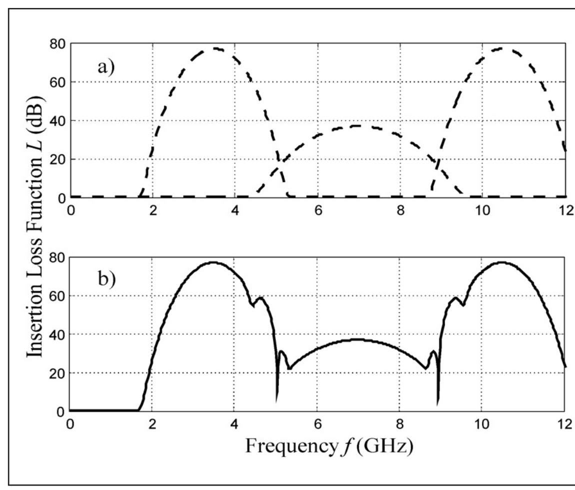

Figure 8 · Insertion loss functions of two cascaded filters (a) and cascade connection of the filters (b).

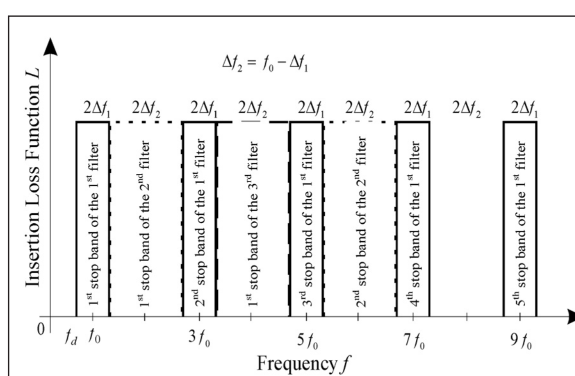

Figure 9 · Stop bands of three cascaded filters.

Example of Application of the Splining Procedure for the Insertion Loss Frequency Responses in Order to Obtain Initial Approximation for the Optimization Process

Let us consider the design of band-stop filter with stopband frequency response described by means of the following parameters: f_d = 1.20 GHz, f_1 = 1.45 GHz, f_2 = 2.0 GHz, f_u = 12 GHz, and also S_{11} < –23 dB over the whole pass band and the minimum value of the reflection losses in the stop band equal to 20 dB (see Fig. 3). The admissible characteristic impedance range of particular filter sections is limited by Z_{min} = 25 Ω and Z_{max} = 90 Ω. The characteristic impedance range for the band-stop filter designed using *R*-transformer with 20 sections is given by $Z_{min\,A}$ = 10 Ω and $Z_{max\,A}$ = 240 Ω. As condition (1) is not satisfied, the procedure of splining the insertion loss frequency response should be applied in order to obtain better initial approximation for the optimization process.

Let us now assume that the band-stop filter composed of two filters (having 18 and 14 sections, respectively) was designed on the base of the *R*-transformer prototype with nominal loss 25 dB in the stop band. The insertion loss functions of the cascaded filters are presented in Figure 8a. Figure 8b shows the insertion loss of two filters in cascade. Significantly higher loss excess in the stop band of the first cascaded filter is the consequence of its much larger relative stop bandwidth. The range of characteristic impedances of the particular sections of the initial approximation is 20.9 Ω ≤ Z_i ≤

119.4 Ω. The filter designed in this manner satisfies condition (1) and can be used as a good approximation for the next optimization stage.

Experimental Results

In order to confirm the usefulness of the design method presented in this paper, three coaxial band-stop filters have been constructed and tested. Two of them, designated Filter I and Filter II, were designed assuming presence of discontinuities appearing in places where there is a step change of line geometry. The third filter, Filter III, was designed by means of the splining procedure, applied to the insertion loss frequency responses, without influence of discontinuities. Characteristics of the filters obtained experimentally were compared with theoretical curves, and the influence of discontinuities on the characteristics of the designed filters was considered.

Filter I

The first filter was designed assuming the following parameters: f_d = 3.1 GHz, f_1 = 3.6 GHz, f_2 = 4.55 GHz and f_u = 10 GHz (see Fig. 3) with the admissible characteristic impedance range given by Z_{min} = 20 Ω and Z_{max} = 100 Ω. It was assumed that S_{11} < –23 dB in the pass band with the loss in the stop at least 40 dB. The filter was implemented in the coaxial line technology, with the diameter of the outer conductor equal to 10 mm, and terminated with 50 Ω type N connectors.

During the first design stage, parameters of the band-stop filter having 20-sections were evaluated using R-transformer prototype. Characteristic impedances of this initial approximation are limited to the range determined by $Z_{\min A}$ = 22.7 Ω and $Z_{\max A}$ = 110.2 Ω, satisfying condition (1). In the next stage, the filter was optimized, taking into account the influence of discontinuities. During the optimization process, the characteristic impedance of the last section resulted in a value of 50 Ω. Thus, the filter is composed of 19 sections. Parameters of the filter obtained after the optimization process are given in Table 1 and construction of the filter is shown in Figure 10.

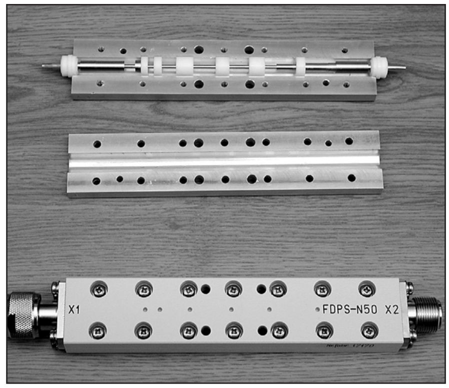

Figure 10 · Construction outline of Filter I.

Figure 11 and Figure 12 show the experimental and theoretical S_{11} and S_{21} responses of the filter. Theoretical characteristics were computed assuming the influence of discontinuities, according to the model introduced in this paper. It should be pointed out that there is a very good agreement between these curves in the whole analyzed frequency range. In spite of the potential for higher, parasitic modes, their influence on filter responses was not observed.

For evaluation of the influence of discontinuities on the filter response, experimental and theoretical curves were compared (with no discontinuity influence taken into account), see Figure 13. It was observed that there is some degradation of the resulting theoretical S_{11} response in the pass band. It was also found that theoretical responses are shifted towards higher frequencies, and the theoreti-

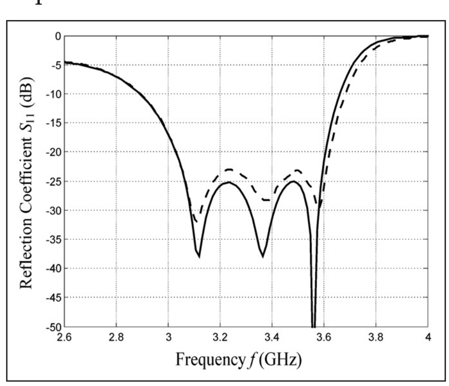

Figure 11 · Theoretical (solid line) and experimental (dashed line) S_{11} responses of Filter I.

Section No. i	Z_{0i} (Ω)	Inner conductor diameter d_i (mm)	Dielectric constant ε_r	Section length l_i (mm)
1	37.1	5.39	1	7.39
2	38.2	5.29	1	13.74
3	91.9	2.16	1	5.41
4	31.3	5.93	1	2.81
5	20.0	6.22	2.06	3.04
6	100.0	1.89	1	3.06
7	20.0	6.22	2.06	3.60
8	100.0	1.89	1	6.92
9	20.0	6.22	2.06	7.98
10	100.0	1.89	1	10.88
11	20.0	6.22	2.06	6.52
12	97.8	1.96	1	9.46
13	20.0	6.22	2.06	7.27
14	100.0	1.89	1	6.09
15	67.2	3.27	1	9.43
16	20.0	6.22	2.06	4.35
17	52.2	4.19	1	11.79
18	48.2	4.48	1	3.57
19	30.8	5.98	1	15.59
			$\sum l_i$ =	138.90

Table 1 · Electrical and construction parameters of Filter I.

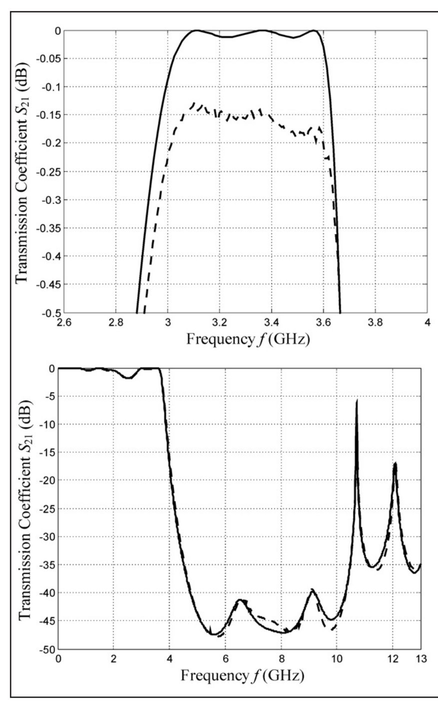

Figure 12 · Theoretical (solid line) and experimental (dashed line) S_{21} responses of Filter I.

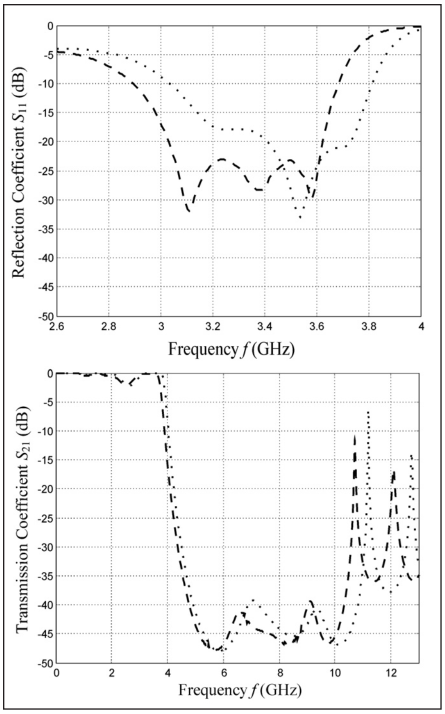

Figure 13 · Comparison of experimental (dashed line) and theoretical (dotted line) S_{11} and S_{21} responses of Filter I obtained assuming the lack of discontinuities.

cal stop band is wider than the experimental one. This means that the filter designed primarily without considering the discontinuities should be shortened (each section) by 1 or 2 percent, in order to obtain a response close to the theoretical curves.

Filter II

The second filter was designed to meet the following requirements: f_d = 1.15 GHz, f_1 = 1.5 GHz, f_2 = 2.1 GHz and f_u = 6 GHz (see Fig. 3) with the characteristic impedance range of particular sections given by Z_{min} = 25 Ω and Z_{max} = 90 Ω. It was assumed that $S_{11} < -23$ dB in the pass band with the stop band loss at least 30 dB. The filter was implemented in coaxial line technology, with the diameter of outer conductor equal to 16 mm, and terminated with standard 7/16 connectors (VSWR < 1.01 in the pass band and VSWR < 1.15 in the stop band was obtained).

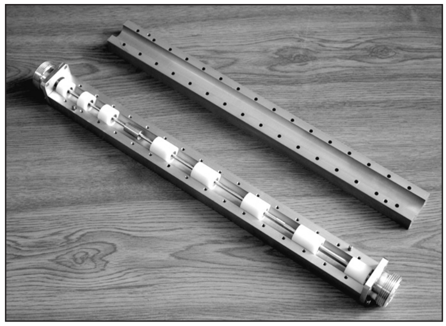

Figure 14 · Construction outline of Filter II.

Section No. i	Z_{0i} (Ω)	Inner conductor diameter d_i (mm)	Dielectric constant ε_r	Section length l_i (mm)
1	27.0	8.42	2.03	9.57
2	81.6	4.10	1	15.37
3	26.0	8.63	2.03	9.23
4	90.0	3.57	1	15.42
5	25.0	8.83	2.03	11.91
6	87.0	3.75	1	14.58
7	34.7	8.97	1	15.91
8	90.0	3.57	1	16.32
9	25.0	8.83	2.03	19.49
10	87.1	3.74	1	24.62
11	26.0	8.63	2.03	20.72
12	86.3	3.79	1	30.71
13	26.8	8.47	2.03	19.71
14	70.2	4.97	1	30.86
15	26.9	8.44	2.03	22.40
16	63.2	5.58	1	26.98
17	34.0	7.13	2.03	17.41
			$\sum l_i$ =	321.21

Table 2 · Electrical and construction parameters of Filter II.

In the first design stage, parameters of a band-stop filter having 18-sections and designed on the basis of the R-transformer prototype were found. Characteristic impedances of this initial approximation are in the range limited by $Z_{\min A}$ = 18.4 Ω and $Z_{\max A}$ = 135.9 Ω, and satisfy condition (1). In the second stage, parameters of the filter were optimized assuming presence of discontinuities. During the optimization process the impedance of the last section attained 50 Ω and a filter having 17 sections was finally obtained. Table II shows the filter parameters after optimization, and its construction is shown in Figure 14.

Figure 15 and Figure 16 show the experimental and theoretical S_{11} and S_{21} curves of the filter. The influence of discontinuities was taken into account in case of theoretical characteristics. It should be pointed out that there is a very good agreement between theoretical and experimental responses in the whole analyzed frequency range. It confirms very high practical value of the method described in this paper. As in the case of Filter I, substantial influence of parasitic modes on the responses of the filter was not observed.

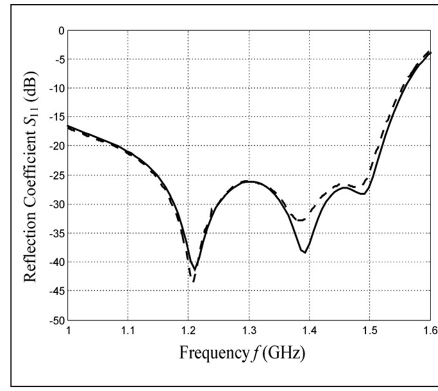

Figure 15 · Theoretical (solid line) and experimental (dashed line) S_{11} responses of Filter II.

In order to evaluate the influence of discontinuities on the response of the filter, experimental and theoretical characteristics of Filter II were compared (neglecting the influence of discontinuities), see Figure 17.

It was observed that theoretical characteristics obtained in this way are shifted towards greater frequencies. The theoretical stop band of the filter is greater than the same band found experimentally. Degradation of S_{11} curves in the pass band was not observed. It is the result of smaller influence of discontinuities in the pass band of Filter II, which follows from the fact that the characteristic impedance range of Filter II is narrower than the respective range for Filter I. In the case of Filter II, the diameter of the coaxial line outer conductor in the pass band is also smaller with respect to the wavelength λ.

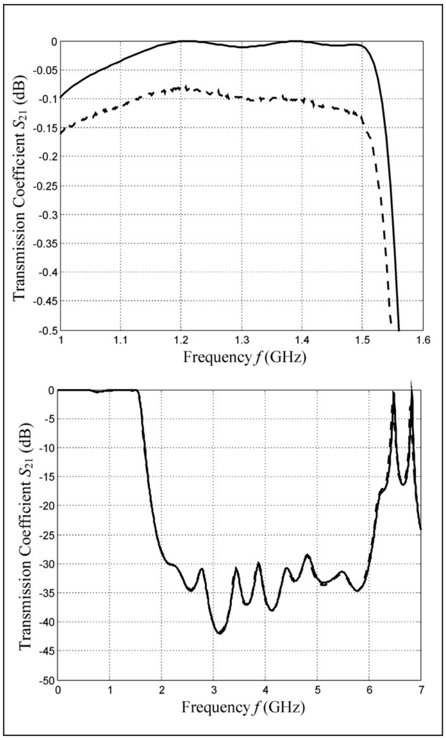

Figure 16 · Theoretical (solid line) and experimental (dashed line) S_{21} responses of Filter II.

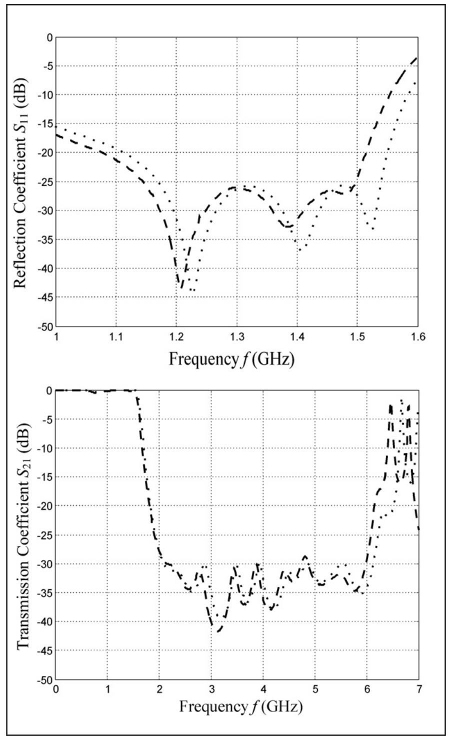

Figure 17 · Comparison of experimental (dashed line) and theoretical (dotted line) S_{11} and S_{21} responses of Filter II obtained assuming the lack of discontinuities.

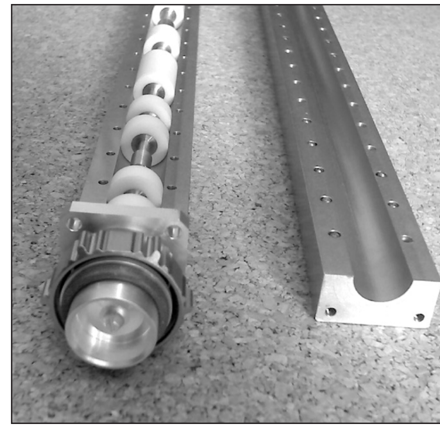

Figure 18 · Construction outline of Filter III.

Sec. No. i	Component filter sect. No. j	Z_{0i} (Ω)	Inner conduct. diam. d_i (mm)	Diel. const. ε_r	Sec. length l_i (mm)	Sec. length l_i (ε_r=1) (mm)
1	1	46.	5.33	2.03	14.55	20.73
2	2	67.	5.15	1	21.19	21.19
3	3	46.	5.33	2.03	14.84	21.14
4	4	73.	4.68	1	21.07	21.07
5	5	57.	6.18	1	21.13	21.13
6	6	75.	4.52	1	21.02	21.02
7	7	39.	6.30	2.03	14.87	21.19
8	8	82.	4.07	1	21.16	21.16
9	9	39.	6.30	2.03	14.84	21.14
10	10	58.	6.07	1	21.21	21.21
11	11	39.	6.30	2.03	14.80	21.09
12	12	83.	3.95	1	21.18	21.18
13	13	25.	8.80	2.03	14.84	21.14
14	14	88.	3.66	1	21.15	21.15
15	15	37.	8.63	1	21.18	21.18
16	16	25.	8.80	2.03	14.81	21.10
17	17	73.	4.66	1	21.11	21.11
18	18	25.	8.80	2.03	14.91	21.24
19	1	25.	8.80	2.03	7.35	10.47
20	2	25.	8.80	2.03	7.42	10.57
21	3	86.	3.80	1	10.65	10.65
22	4	69.	4.98	1	10.59	10.59
23	5	25.	8.80	2.03	7.37	10.50
24	6	53.	6.51	1	10.09	10.09
25	7	25.	8.80	2.03	7.87	11.21
26	8	87.	3.72	1	10.43	10.43
27	9	51.	6.74	1	10.28	10.28
28	10	86.	3.81	1	11.02	11.02
29	11	30.	7.72	2.03	7.22	10.29
30	12	67.	5.20	1	10.28	10.28
31	13	30.	7.72	2.03	7.80	11.11
32	14	73.	4.66	1	10.25	10.25
				$\sum l_i$ =	458.4	

Table 3 · Electrical and construction parameters of Filter III.

Making use of the above conclusions it can be assumed that in some cases the filter designed without taking the discontinuities into account can have characteristics satisfying the requirements only after shortening the filter by 1 or 2 percent (equal shortening of each section).

Filter III

The third filter was designed assuming that the pass and stop bands are determined by the following frequencies: f_d = 1.20 GHz, f_1 = 1.45 GHz, f_2 = 2 GHz and f_u = 12 GHz (see Fig. 3). The characteristic impedance range of particular sections was limited by Z_{min} = 25 Ω and Z_{max} = 90 Ω. It was assumed that S_{11} < –23 dB in the pass band and the insertion loss in the stop band should not be less than 20 dB. This filter was implemented using coaxial line technology with the outer diameter equal to 16 mm and terminated in the same manner as Filter II.

Previously, the way to obtain the initial approximation for the optimization process was described. Table III shows parameters of the filter obtained using the optimization procedure, in which the lack of discontinuities was assumed. Construction outline of Filter III is shown in Figure 18.

Figure 19 and Figure 20 show the experimental and theoretical curves of S_{11} and S_{21} of Filter III. Divergence between these curves is small in the low frequency region and is growing with frequency. It is the opinion of the author that the parasitic modes (near the upper limit of the analyzed frequency range) and the growing influence of discontinuities, which were not taken into account during the design stage, are the cause of these divergences. Theoretical stop band of the filter is narrower in comparison with the measured result. As in the case of Filter II, degradation of S_{11} in the pass band was not observed.

As the design process was, in the case of Filter III, limited mainly to the amplitude synthesis (reducing the characteristic impedances of each

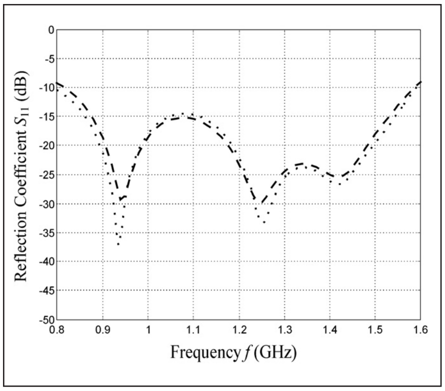

Figure 19 · Theoretical (dashed line) and experimental (dotted line) S_{11} responses of Filter III.

section to the prescribed limits). Table 3, col. 7, shows that the theoretical characteristics of the filter has a periodic form, as confirmed by the measurement in Figure 21.

The group delay of Filter II with a little ripple slightly above the pass band (1.15-1.5 GHz) is presented in Figure 22 as an example of typical group delay for filters under consideration.

Conclusions

In this article, useful method of band-stop filter design has been presented, in which construction constraints, formulated by means of the characteristic impedance range of its particular sections, are taken into account. The insertion loss frequency response of the designed filters is close to the equal-ripple in both the pass- and stop-band.

In order to confirm the usefulness of this method, the three coaxial band-stop filters were designed, manufactured and tested. One of the filters was designed by means of the original spline procedure applied to the insertion loss frequency responses. As it follows from the comparison of theoretical and experimental characteristics, proposed spline procedure makes possible the design of band-stop filters with relatively broad stop bands.

It was also found that there is a

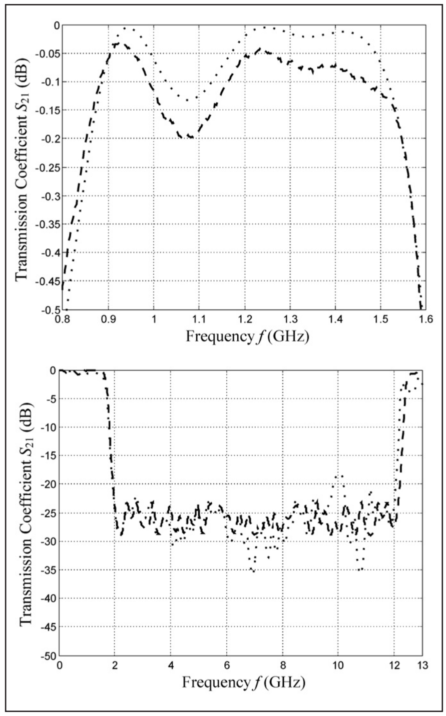

Figure 20 · Theoretical (dashed line) and experimental (dotted line) S_{21} responses of Filter III (theoretical characteristics without the influence of discontinuities).

very good synchronization between experimental and theoretical responses (determined in presence of discontinuities) in the wide frequency range. The observed divergences are very small and remain constant in function of frequency. In case of neglecting the discontinuities during the design process, theoretical characteristics differ from the experimental as follows:

(a) The real curve is shifted towards lower frequencies, with respect to the theoretical characteristic.
(b) The measured stop band of the filter is narrower than the theoretical one.
(c) In some cases the measured S_{11} characteristic in the pass band is a deformed version of the theoretical one.

All discrepancies mentioned above are proportional to the range of characteristic impedances of particular sections of the filter and to the transversal dimensions of the filter, in relation to the wavelength λ (for example, the diameter of the outer conductor of the coaxial line).

It can be also assumed that in certain cases the filter can be designed without taking into account the influence of discontinuities. In this case it would be recommended to shorten equally each filter section by one or two percent for partial compensation of discontinuities.

All of the analyzed filters introduce a pass-band loss, which was found to be not greater than 0.2 dB. Group delay of all tested filters is nearly constant in the pass band with a little ripple above.

References

1. S. Rosloniec, *Algorithms for computer aided design of linear microwave circuits.* Boston: Artech House, 1990, Ch. 4, 5.

2. S. Rosloniec, “About the application of the stepped transmission lines in linear microwave circuit design” (in Polish). Prace Naukowe PW, Elektronika z. 84 (WPW), Warsaw, Poland, 1990.

3. P. Dyderski, “Algorithms for designing of microwave noncommensurate stepped transmission line band-stop filters” (in Polish). M.S. thesis, The Faculty of Electronics and Information Technology, Warsaw University of Technology, Warsaw, Poland, 1999.

4. S. Rosloniec, “Application of the R-transformer to the Design of Microwave Harmonic Filters.” *Archiv fur Elektronic und Ubertragungstechnik* (Electronics and Communication), AEU - Band 41, Heft 4, pp. 251-253, 1987.

5. N. Riblet, “General synthesis of quarter-wave impedance transformers.” *IRE Trans. Microwave Theory and Tech.,* Vol. MTT 5, pp. 36-43, Jan. 1957.

6. C. G. Montgomery, R. H. Dicke,

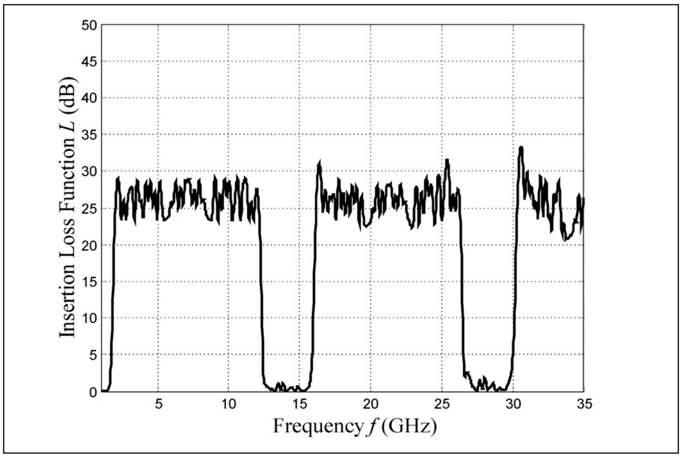

Figure 21 · Illustration of periodicity of the stop bands of Filter III being a cascade of two filters (theoretical characteristics without the influence of discontinuities).

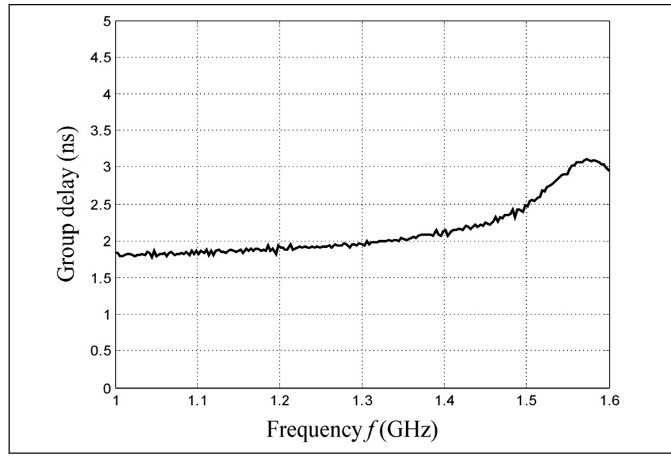

Figure 22 · Group delay for Filter II. This behavior is typical for the type of filters examined.

and E. M. Purcell, *Principles of microwave circuits (*2nd ed.). London/UK: Peter Peregrinus Ltd., 1987, Ch. 4.

7. B. C. Wadell, *Transmission line handbook.* Boston: Artech House, 1991.

8. V. F. Demianov and V. N. Malozemov, *Introduction to minimax.* New York: Wiley, 1974.

9. B. N. Pshenichnyj, *The linearization method for constrained optimization.* Berlin: Springer-Verlag, 1994.

10. P. Dyderski, "Noncommesurate, stepped transmission line band-stop filters" (in Polish). *Proceedings of the Telecommunications Research Institute,* No. 124, pp. 10-17, Warsaw, Poland, 1999.

11. N. Marcuvitz (ed.), *Waveguide handbook* (2nd ed.). London/UK: Peter Peregrinus Ltd., 1986, pp. 310-312.

12. M.A.R. Gunston, "A Simple Formula for Calculating Approximate Values of the First Zeros of a Combination Bessel Function Equation." *IEEE Trans. Microwave Theory and Tech.,* Vol. MTT 11, pp. 93-94, Jan. 1963.

13. J. A. Cochran, "Further Formulas for Calculating Approximate Values of the Zeros of Certain Combinations of Bessel Functions." *IEEE Trans. Microwave Theory and Tech.,* Vol. MTT 11, pp. 546-547, Nov. 1963.

14. G. Matthaei, L. Young, and E.M.T. Jones, *Microwave filters, impedance-matching networks, and coupling structures.* New York: McGraw-Hill Inc., 1964, Ch. 6, 8.

15. S. Rosloniec, Faculty of Electronic, Warsaw University of Technology, Warsaw, Poland, private communication.

Author Information

Piotr Dyderski was born in Przysucha, Poland, on June 22, 1974. He received his M.S. degree in electronic engineering from Warsaw University of Technology, Warsaw, Poland, in 1999. Since 1998 he has been involved with Passive Microwave Devices Dept. of the Telecommunications Research Institute, Warsaw, Poland. His current research interests include computer-aided design of equiphase array antennas and microwave circuits, especially filters and rotary joints for radiolocations and radionavigations systems. He can be reached by e-mail at: Piotr.Dyderski@pit.edu.pl.

MAX Series Frequency Doubler

MITEQ introduces its new frequency doubler, Model MAX2M-0714N01U, which produces an output of +23 dBm from 13,500 to 14,500 MHz with an input harmonic rejection of –20 dBc typical. This doubler requires an input power of 10 dBm typical, +15 VDC at 350 mA and –15 VDC at 10 mA. It is supplied with type “K” female connectors. The MAX2M0714-N01U measures 0.90" × 0.69" × 0.23" without connectors.

MITEQ, Inc.
www.miteq.com

GaAs pHEMT Gain Block

Hittite Microwave Corporation has introduced a new SMT packaged GaAs pHEMT MMIC gain block amplifier that is ideal for broadband and CATV applications from 50 to 960 MHz. The HMC599-ST89E is a GaAs pHEMT based, wide dynamic range gain block MMIC amplifier that is rated from 50 to 960 MHz and delivers 14 dB gain, +39 dBm output IP3, and noise figure as low as 2 dB. Input and output return losses are excellent at 15 dB or better. The HMC599ST89E can be used as a cascadable 75-ohm RF or IF gain stage as well as a PA or LO driver with up to +19 dBm P_{1dB} output power.

Hittite Microwave Corporation
www.hittite.com

Ultra Broadband Fixed Chip Attenuator

EMC Technology introduces a new high frequency, wire bondable chip attenuator, KFA. Designed with the KTVA footprint in mind this component offers a flat attenuation from 16-36 GHz. The KFA chip attenuator can handle 200 mW and is available in 1 dB to 10 dB with an operating temperature from –55 to +150 ºC. The KFA is also available for high-reliability applications under the HRKFA part number with Group A, B and C life testing according to Mil-PRF-55342. This new attenuator is available with gold wire bondable terminals and a platinum silver, solder attachable ground plane in an ultra miniature chip size 0.065" × 0.120" (1.65 × 3.05 mm). The KFA ultra broadband attenuator is available for immediate delivery.

EMC Technology & Florida RF Labs
www.rflabs.com

Digitally Programmable VGA

Linear Technology introduces the LT5554, a broadband digitally programmable gain IF amplifier, featuring a 48 dBm OIP3 at 200 MHz. The amplifier has very low noise, enabling very high dynamic range performance in wireless communication receivers and signal processing systems. Its gain is digitally controlled from 2 to 18 dB by a 7-bit parallel word. The amplifier settles in less than 5 ns from a gain change, producing low glitch noise and supporting very fast and accurate AGC performance. The device comes in a 32-lead, 5 × 5 mm plastic QFN surface mount package. Prices for the LT5554 start at $4.40 each in 1,000-piece quantities. The LT5554 is available immediately from stock.

Linear Technology
www.linear.com

Up/Down Converter Assembly

The Ka-Band up/down converter assembly is a custom designed system. It is operating in an anechoic chamber in order to simulate a radar receiver with realistic target echoes. The system operates at 33.3 to 36.3 GHz RF frequency range and IF of 4.3 to 5.3 GHz. The receiver channel has the gain of greater than 40 dB and noise figure of 5 dB, while the transmitter P_{1dB} varies from +20 dBm to +32 dBm with different channels according to requirements. The LO input is about 13 dBm from 29 GHz to 31 GHz. The assembly is in the standard rack mountable box with the dimension of 19" × 7" × 19".

Ducommun Technologies
www.dt-usa.com

Bias Tee/Diplexer

Mini-Circuits has developed a new Bias Tee/Diplexer (ZABT-2R15G +) that is well suited for Satellite/VSAT (Very Small Aperture Terminal), LNB (Low Noise Block Converter) , and BUC (Block Up Converters) and modems. The ZABT-2R15G+ can be used as a Bias Tee or Diplexer that can inject 10 MHz and DC on a L Band signal. It can also be used in the reverse direction which can

strip off the DC and/or 10 MHz signal. A prime application for this model is in a satellite system where the basic architecture consists of a modem usually in the base or hub. This modem will convert IF signals to L band (950-2150 MHz). The L band will then be moved over a cable to the BUC (Block Up Converter) located usually at the antenna.

Mini-Circuits, Inc.
www.minicircuits.com

GaN HEMT Microwave Transistor

Cree, Inc. announces the sample release of a highly efficient 120-watt GaN HEMT microwave transistor for general-purpose military and industrial applications such as electronic warfare, tactical communications, radar, instrumentation and direct video broadcast applications. This transistor provides outstanding RF power performance over wide instantaneous bandwidths. The new transistor, CGH40120F, consists of a single, unmatched GaN HEMT die providing a minimum of 120 watts of saturated output power at 28 volts, in a small, industry-standard, flanged ceramic-metal package. The CGH40120F complements Cree's broadband GaN HEMT general-purpose microwave transistors now available at power levels of 10W, 25W, 35W, 45W and 90W.

Cree, Inc.
www.cree.com

RF Modules

TriQuint Semiconductor, Inc. announced it is shipping the TRITIUM II PA-Duplexer Module™ family, its latest solution of RF modules for mobile handset manufacturers. The TRITIUM II PA-Duplexer Module™ family supports the CDMA 2000 (EV-DO) protocol with the following bands: PCS, cellular, and AWS. The family includes the TQM663029A, (PCS band) the TQM613029 (cellular band) and the TQM653029 (AWS band). Together with TriQuint's SP3T antenna switch, GPS LNA/filter module and RF filters, the PA-Duplexers provide customers a complete front-end solution for multi-band CDMA handsets. Each 7 × 4 mm PA-Duplexer contains a transmit SAW filter, coupler, duplexer, biasing/regulator circuitry, internal matching and a state-of-the-art high efficiency amplifier. The family is now shipping in high volume and available for purchase.

TriQuint Semiconductor, Inc.
www.triquint.com

Gallium Nitride Broadband Power Amplifier

Aethercomm Model Number SSPA 0.020-0.100-125 is a high power, broadband, Gallium Nitride (GaN) RF amplifier that operates from 20 to 100 MHz. This PA is ideal for broadband military platforms as well as commercial applications because it is robust and offers high power over a multi-octave bandwidth with excellent power added efficiency. It is packaged in a modular housing that is approximately 2.5" × 6.4" × 1.06". It has a typical P_{3dB} of 125 watts at room temperature. Noise figure at room temperature is 10.0 dB maximum. It offers a typical gain of 50 dB with a typical gain flatness of ±1.0 dB. The power and gain flatness across the band is extremely flat for the bandwidth. Input VSWR is 2.0:1 maximum.

Aethercomm
www.aethercomm.com

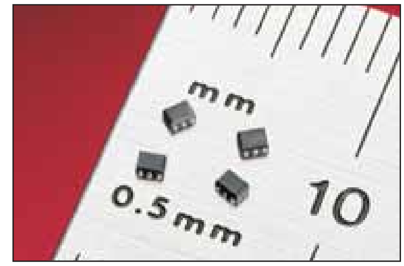

Miniature Twin Transistor Devices

Engineers tasked with shrinking their VCO designs will be especially interested in the new UPA828TD Twin Transistor from NEC. The UPA828TD combines two closely matched silicon NPN chips in a 1.2 × 1.0 × 0.5 mm 6-pin leadless RoHS-compliant package. Ideal for VCO applications, the UPA828TD enables oscillator and buffer amplifier functions to be combined in one miniature device. Its small size and extremely low power consumption make it a great choice for portable, battery-powered products. The chip inside the UPA828TD is NEC's NE687, for which non-linear models can be found on the CEL website. Available now, the UPA828TD is priced at 68¢ in 10k quantities.

California Eastern Laboratories
www.cel.com

Synthesizer and Mixer Family

Analog Devices, Inc. introduced the ADF4350 synthesizer with on-chip VCO and PLL. The ADF4350 integrated synthesizer provides designers with a single, low phase-noise solution supporting a continuous tuning range from 137.5 MHz to 4.4 GHz. ADI also introduced a family of highly integrated active and passive mixers. The active ADL5802 and passive ADL5356, ADL5358 and ADL5360 dual-channel diversity mixers expand ADI's portfolio of main and diversity products and when coupled with the ADF4350 provide a highly integrated two-chip diversity down conversion solution for cellular base stations, satellite communications, and point-to-point microwave radio equipment.

Analog Devices, Inc.
www.analog.com

Solid-State Magnetron Transmitters

A line of high power, solid-state magnetron transmitter upgrade modules that can be used with all major transmitter technologies has been introduced by Diversified Technologies, Inc. The DTI PowerMod™ series high power solid-state magnetron transmitters deliver peak RF powers of 3 to 50 kW and can drive magnetrons across the L to Ka band frequency range. Measuring 10" × 13" × 9", these compact modules provide precise RF control to within <0.1% and 50 ns rise/fall, adjustable from pulse-to-pulse, and support pulse repetition frequencies up to 400 kHz. DTI PowerMod™ magnetron transmitters are priced from $30,000.00 to $200,000.00, depending upon radar system requirements.

Diversified Technologies, Inc.
www.divtecs.com

RF MEMS Switch

Omron Electronic Components LLC has announced the release of the 2SMES-01 high frequency mechanical relay utilizing its expertise in MEMS (Micro Electro Mechanical Systems) technology. Developed to meet the needs of the automated test equipment market, this product has exceptional high frequency characteristics at 10 GHz (50Ω) typical: 30 dB isolation, 1 dB insertion loss, and 10 dB return loss. The relay is comprised of two SPST-NO silicon chips, packaged together for SPDT or DPST-NO operation in a compact enclosure measuring 5.2 × 3.0 × 1.8 mm. Driven by an electrostatic drive system, it is rated for 100 million operations at 0.5 mA at 0.5 VDC resistive load, and has been tested over 1 Billion cycles. Additionally its power consumption is extremely low at 10 µW max. Parts are currently available for order, with prototype quantities being delivered in about 3-4 weeks.

Omron Electronic Components
Tel: 847-882-2288
www.components.omron.com

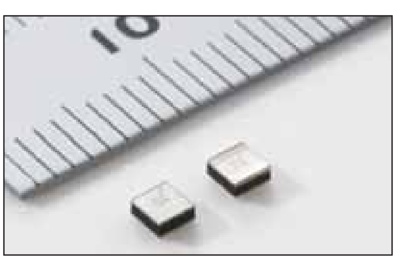

Small Isolator

Murata Electronics North America introduced the smallest isolator on the market. The CEG23 series measures only 2.0 × 2.0 × 1.0 mm—representing a 56 percent reduction in size from current Murata isolators. The dramatically compact dimension makes this high performance isolator ideal for multi-band, mobile phones. The CEG23 series isolator includes LGA terminals, which contribute to the reduction of mounting space and adds freedom in the RF circuit layout. In addition, Murata reduced characteristics such as dispersion, insertion loss and variation within the bandwidth by using a new electrode construction, improving production processes and introducing a new integrated circuit board. This series also inherits the two-port circuit technology from current models to maintain excellent matching with the power amplifier. Murata's CEG series is available for the sample price of $1.50.

Murata Electronics North America
www.murata-northamerica.com

GPS RF Front End Module

Avago Technologies announced a highly integrated GPS low noise amplifier (LNA) with high performance levels. The ALM-1712 effectively integrates a sophisticated GPS LNA and two FBAR filters. This results in a complete, compact and high-performance GPS RF front end module that simplifies the design of a wide range of GPS applications. The ALM-1712 is housed in a 4.5 × 2.2 × 1.0 mm MCOB package, reducing PCB space by more 50% when compared to a discreet-only solution. The integration of FBAR filtering enables the ALM-1712 to reach more than 85 dBc of cell/PCS-band rejection levels. Additionally, the ALM-1712 effectively leverages Avago's 0.5 µm GaAs enhancement-mode pHEMT process to deliver a 1.7 dB noise figure, 13.5 dB gain, and +5 dBm IIP3 (input third order intercept point) at typical operating condition of 2.7V and 8 mA. Pricing for the ALM-1712 begins at $1.81 in the 10,000 piece quantity range.

Avago Technologies
www.avagotechwireless.com

High-Speed Threshold Detector

Planar Monolithics Industries Model No: TD-30T-914-DX is a high-speed threshold detector designed to operate over the 9 to 14 GHz frequency range, with an adjustable threshold level of –18 dBm to +5 dBm, and a typical VSWR of 2.0:1 (2.5:1 maximum). This unit comes in a very small size with a field removable GPO connector on the input and a solder pin on the output.

Planar Monolithics Industries
www.planarmonolithics.com

Proprietary RF Modules

Laird Technologies, Inc. announced a new range of proprietary RF modules. Laird Technologies'

LT2510 is a fifth generation 2.4 GHz FHSS module that sets the standard for industrial RF communication. Embedded with Laird Technologies' robust server-client protocol, the LT2510 permits each module to communicate with any other in-range module for true peer-to-peer operation. "Out of range" modules can be reached via a meshing topology. The configuration and test software enables OEMs to structure and optimize networks to suit their application. The SMT package is well-suited for space-constrained designs and is available in pick-and-place packaging for volume manufacturing.

Laird Technologies, Inc.
www.lairdtech.com/wireless

Thermoelectric Evaluation Kit

Nextreme Thermal Solutions announced the availability of the eTEG Thermoelectric Power Generation Evaluation Kit. The kit provides customers with an easy to use first evaluation solution for assessment of Nextreme's power generation/energy harvesting technology. The evaluation kit includes a thick film heater as the heat source, an embedded eTEG UPF40 power generator module, a heat sink/fan assembly and thermocouples for temperature measurement. The kit provides the full thermal path from heat source to heat sink and requires only a power supply for the heater and a volt meter to measure the voltage generated by the eTEG across a load resistor. The eTEG Evaluation Kit is available for $295 and encouraged for first time evaluations.

Nextreme Thermal Solutions
www.nextreme.com

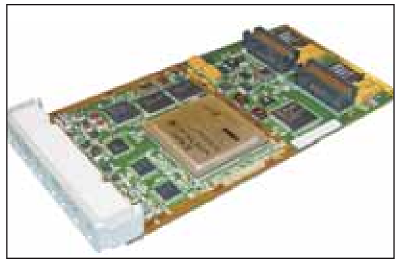

COTS Digital Receivers

Mercury Computer Systems, Inc. announced availability of its initial offering of the new Echotek® Series family of high-performance, Virtex™-5-based digital receivers. The new Echotek Series DCM-V5-XMC digital receiver features the latest in A/D and D/A technology, allowing for high-speed/high-resolution data conversion while still preserving the quality of the original signal. It implements either a Virtex-5 SX95T or LX155T FPGA, which can be programmed by the end user for customer-specific application features. The Echotek Series DCM-V5-XMC digital receiver is the first of a line of Virtex-5 based digital receivers that is planned for release by Mercury within the next calendar year.

Mercury Computer Systems, Inc.
www.mc.com/dcmv5

Isolators/Circulators

MECA expands our connectorized isolators and circulators for high frequency X and Ku band (8.0 - 18.0 GHz) applications. Featuring SMA-Female connectors and average power ratings of 2 watts. Other specifications include 0.4 dB insertion loss, 1.30:1 VSWR and 18 dB isolation across the entire band. Available from stock to 4 weeks ARO. Made in USA with a 36-month warranty.

MECA Electronics
www.e-MECA.com

Frequency Synthesizers

EM Research introduces the ZLX Series frequency synthesizer, which is a drop-in replacement for several of the industry's standard PLOs and synthesizers. The ZLX can be custom-designed to operate fixed or programmable from less than 800 MHz to over 3.8 GHz, and is housed in a standard commercial surfacemount package, 0.6" × 0.6" × 0.14". The ZLX offers extremely low phase noise, (<–106 dBc/Hz at 10 kHz, F_{out} = 3.1 GHz), and low power consumption, (<100 mW at +3.3 VDC).

EM Research, Inc.
www.emresearch.com

3.65 GHz WiMAX Solution

Vecima Networks Inc. announced the launch of its FCC-certified 3.65 GHz VistaMAX base and subscriber stations, the latest addition to Vecima's VistaMAX family of WiMAX compliant products. Based on the IEEE 802.16-2004 standard, the FCC certified 3.65 GHz VistaMAX products, including both base and subscriber stations, offers U.S. operators the opportunity to reap the benefits of WiMAX while operating in a lightly licensed piece of spectrum. The 3.65 GHz VistaMAX is based upon the same platform as Vecima's 3.5 GHz VistaMAX, which has been successfully deployed in 25 different countries. In order to allow U.S. operators to test Vecima's equipment in their own environment, Vecima has designed two cost-effective 3.65 GHz WiMAX starter kits. For a limited time Vecima is offering qualified U.S. Wireless Internet Service Providers the opportunity to evaluate the equipment for a 30-day period.

Vecima Networks, Inc.
www.vecima.com

Advertiser Index

Find Our Advertisers' Web Sites using *HFeLink*™

1. Go to our company information Web site: www.HFeLink.com
   (from www.highfrequencyelectronics.com, just click on the *HFeLink* reminder on home page)
2. Companies in our current issue are listed, or you can choose one of our recent issues
3. Find the company you want to know more about ... and just click!
4. The Web site of each company you choose will open in a new browser window

Or... You Can Browse Through Our Online Edition and Simply Click on Their Ad!

Advertisers — Reach our *Active* and *Interested* Readership

Contact one of our advertising professionals today:

ADVERTISING SALES — EAST COAST
Gary Rhodes
Tel: 631-274-9530
Fax: 631-667-2871
E-mail: grhodes@highfrequencyelectronics.com

ADVERTISING SALES — WEST
Tim Burkhard
Tel: 707-544-9977
Fax: 707-544-9375
E-mail: tim@highfrequencyelectronics.com

ADVERTISING SALES — CENTRAL
Keith Neighbour
Tel: 773-275-4020
Fax: 773-275-3438
E-mail: keith@highfrequencyelectronics.com

PUBLISHER — OTHER REGIONS & INTERNATIONAL
Scott Spencer
Tel: 603-472-8261
Fax: 603-471-0716
E-mail: scott@highfrequencyelectronics.com

Advertising and media information is available online at www.highfrequencyelectronics.com

DESIGN NOTES

Two Wires, Many Uses

In this column, we'll discuss an RF transformer building block that can be used in many ways. It is a simple set of two windings on a magnetic core. Using such a core accomplishes two things:

- Increases the mutual coupling to near unity for applications requiring magnetic coupling between windings
- Provides sufficient reactance to effectively isolate the windings from end-to-end, for transmission line transformer type applications

Also, the two wires are closely spaced—either parallel bonded wires or a twisted pair. This enhances the mutual coupling and establishes a low impedance for the pair as a transmission line.

This one component can be used for several functions, as described in the diagrams of Figure 1. Two or more of these can be combined in various forms to make more complex subsystems, such as the 4-way power combiner/divider of Figure 2.

Readers wishing to experiment can build a transformer using 8 turns of a twisted pair comprising two #26 enameled wires, wound on a 0.5-inch diameter ferrite toroid core. Operation in the HF range allows operation at low enough frequencies that parasitics are small and performance is easily measured with a spectrum analyzer or oscilloscope. The following core materials can be used over the approximate frequency ranges noted. Other manufacturers' equivalent materials are also appropriate (e.g. from TDK, Ceramic Magnetics, Ferroxcube and others):

~10-100 MHz:	Fair-Rite 61 material (μ_i = 125)
~3-50 MHz:	Fair Rite 43 material (μ_i = 850)
~0.5-15 MHz:	Fair-Rite 77 material (μ_i = 2000), or 73 material (μ_i = 2500)

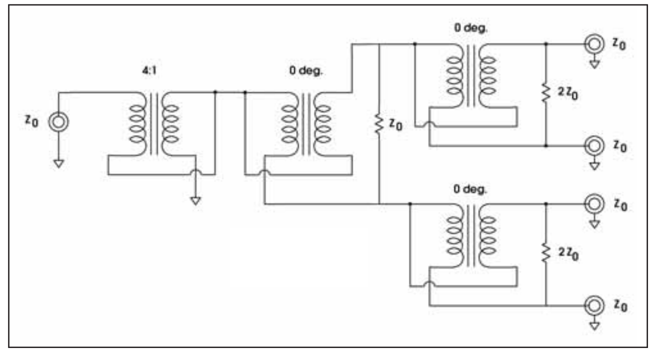

Figure 2 · 4-way 0° combiner/divider.

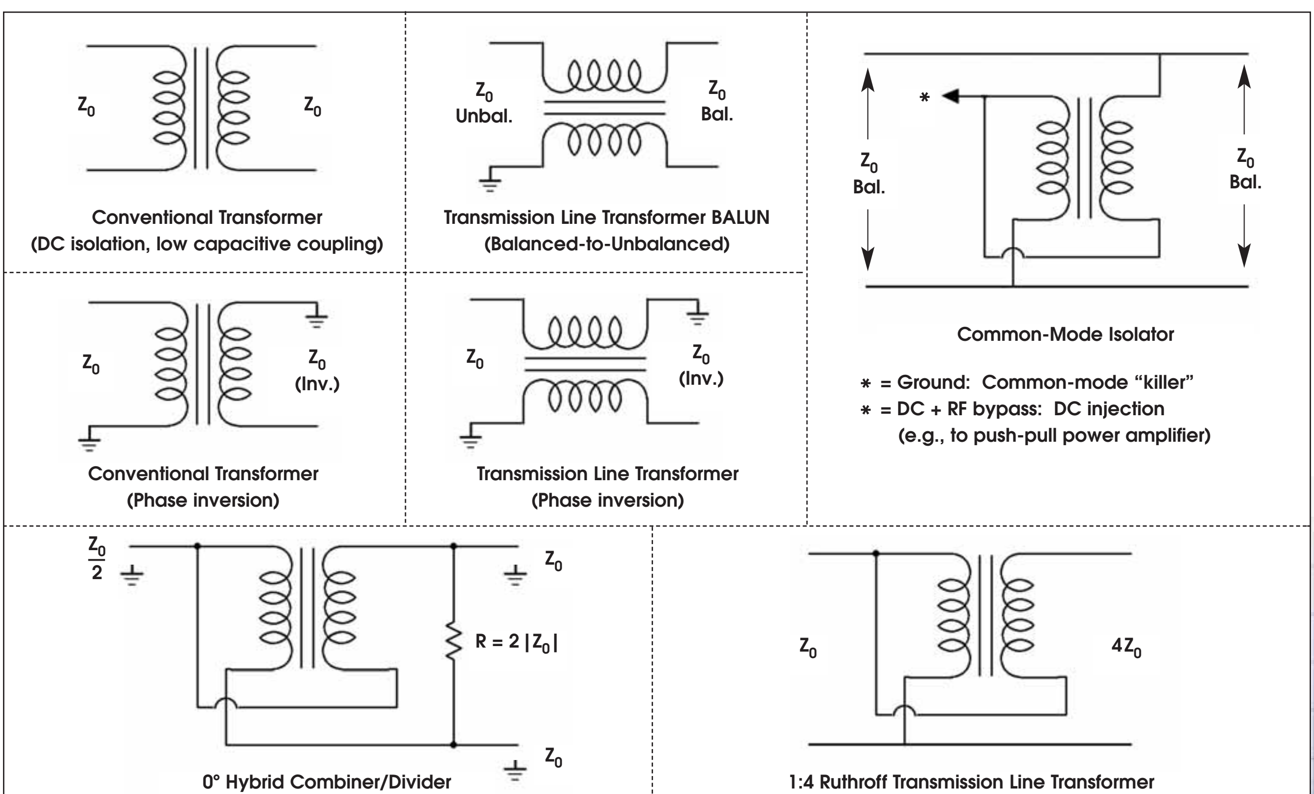

Figure 1 · Various 2-wire transformer configurations.

MILLIMETER WAVE

COMPONENTS

AMPLIFIERS • MIXERS • MULTIPLIERS

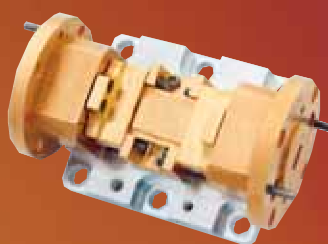

AMPLIFIERS

Model Number	Frequency (GHz)	Gain (dB, Min.)	Gain Flatness (±dB, Max.)	Noise Figure (dB, Max.)	In/Out VSWR (Max.)	Output Power at 1dB Comp. (dBm, Typ.)
JSW4-18002600-20-5A	18-26	34	1.5	2.0	2.0:1/2.0:1	5
JSW4-26004000-28-5A	26-40	25	2.5	2.8	2.2:1/2.0:1	5
JSW4-18004000-35-5A	18-40	21	2.5	3.5	2.5:1/2.5:1	5
JSW4-33005000-45-5A	33-50	21	2.5	4.5	2.5:1/2.5:1	5
JSW5-40006000-55-0A	40-60	18	2.5	5.5	2.75:1/2.75:1	0

Higher output power options available.

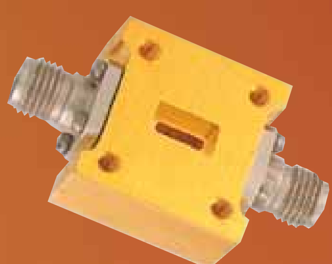

MIXER/CONVERTER PRODUCTS

Model Number	Frequency (GHz)			Conversion Gain/Loss (dB, Typ.)	Noise Figure (dB, Typ.)	Image Rejection (dB, Typ.)	LO-RF Isolation (dB, Typ.)
	RF	LO	IF				
LNB-1826-30	18-26	Internal	2-10	42	2.5	25	45
LNB-2640-40	26-40	Internal	2-16	42	3.5	25	45
IR1826N17*	18-26	18-26	DC-0.5	11	9.5	25	25
IR2640N17*	26-40	26-40	DC-0.5	11	9.5	25	25
SBW3337LG2	33-37	33-37	DC-4	-7.5	8	N/A	25
TB0440LW1	4-40	4-42	.5-20	-10	10.5	N/A	20
DB0440LW1	4-40	4-40	DC-2	-9	9.5	N/A	25
SBE0440LW1	4-40	2-20	DC-1.5	-10	10.5	N/A	20

* For IF frequency options, please contact MITEQ.

MULTIPLIERS

Model Number	Frequency (GHz)		Input Level (dBm, Min.)	Output Power (dBm, Min.)	Fundamental Feed Through Level (dBc, Min.)	DC current @+15VDC (mA, Nom.)
	Input	Output				
MAX2M260400	13-20	26-40	10	10	18	160
MAX2M200380	10-19	20-38	10	10	18	200
MAX2M300500	15-25	30-50	10	10	18	160
MAX4M400480	10-12	40-48	10	10	18	250
MAX3M300300	10	30	10	10	60	160
MAX2M360500	18-25	36-50	10	10	18	160
MAX2M200400	10-20	20-40	10	10	18	160
TD0040LA2	2-20	4-40	10	-3	30	N/A

Higher output power options available.

MITEQ also offers custom designs to meet your specific requirements. For additional information or technical support, please contact our Sales Department at (631) 439-9220 or e-mail components@miteq.com

nqa. ISO 9001 Registered ANAB ACCREDITED

3 YEAR WARRANTY

MITEQ

100 Davids Drive • Hauppauge, NY 11788
TEL.: (631) 436-7400 • FAX: (631) 436-7430
www.miteq.com